A Theoretical Study on the Stability and Reactivity of Doubly Bonded Group 4B Species

Takako Kudo
Department of Chemistry
Faculty of Education
Yokohama National University

1985

Preface

The formation of multiple p_π - p_π bonds is a well-known property of the first-row elements such as carbon, nitrogen, and oxygen. In contrast, their heavier atom congeners especially in the group 4B are reluctant to form stable multiple bonds. In view of the fact that carbon-carbon or carbon-oxygen multiply bonded compounds play a central role in organic chemistry, the corresponding unsaturated analogues containing the heavier group 4B elements such as silicon and germanium have always attracted the considerable interest of experimental and theoretical chemists. However, most of the attempts to synthesize and isolate such compounds have failed except few examples such as sterically protected $(Me_3Si)_2Si=C(OSiMe_3)C_{10}H_{15}$, $Mes_2Si=SiMes_2$, and $Ar_2Ge=GeAr_2$ (Ar=2,6-diethylphenyl) by very bulky substituents.

The primary aim of this thesis is to investigate the nature and properties of p_π - p_π bonding of the group 4B elements Si and Ge by using ab initio molecular orbital theory and to disclose the factors govering the thermodynamic and kinetic stability. The present theoretical work would be rewarding if it could open up a new area of the chemistry of multiply bonded group 4B compounds.

This thesis consists of three parts. Part I is concerned with the silicon analogues of ethenes, silicon-carbon (silaethenes or silenes) and silicon-silicon (disilenes) doubly bonded compounds. The mechanistic aspects of reactions of silaethene ($H_2Si=CH_2$) and the possible interconversion of divalent and doubly bonded species

in silaethene and disilene ($H_2Si=SiH_2$) are examined in this part. Part II involves mainly the studies for the possible existence and stabilization of the formaldehyde analogues, silanone ($H_2Si=O$) and silanethione ($H_2Si=S$). In the last part are investigated the stabilities and reactivities of germanium-containing doubly bonded compounds, germaethene ($H_2Ge=CH_2$) and digermene ($H_2Ge=GeH_2$) in comparison with those of the corresponding silicon analogues. Each part is a collection of the author's publication in the following journals.

Part I : J. Chem. Soc., Chem. Commun. 1984, 1392. ibid 1984, 141. "The Proceedings of the Applied Quantum Chemistry Symposium"; Smith V. H. et al. Eds.; D. Reidel Publishing: Dordrecht, Netherland, 1985; pp 000. Organometallics, 1984, 3, 1320.

Part II : J. Phys. Chem. 1984, 88, 2833. J. Organomet. Chem. 1983, 253, C23. J. Am. Chem. Soc. 1985, 89, 0000. ibid. to be published.

Part III : Chem. Phys. Lett. 1981, 84, 375. Organometallics 1984, 3, 324. J. Mol. Struct. THEOCHEM 1983, 103, 35.

A theoretical challenge to the topics was a great pleasure to the author throughout the studies from 1981 to 1985. She is very grateful to Associate Professor Shigeru Nagase for his continuing guidance and encouragement through profound discussions. She also

thanks Mr. Keiji Ito and the members of the Nagase Laboratory for their helpful discussions. Finally, she would like to thank her parents for their warm encouragement.

Takako Kudo

May, 1985

Contents

Page

Part I Silicon-Carbon and Silicon-Silicon Double Bonds

Chapter 1 Silaethene to Silylene Isomerization····· 2
Chapter 2 Effects of Methyl Substitution on the Silaethene to Silylene Isomerization····· 11
Chapter 3 Mechanistic Aspects of the Reactions of Silaethene with Polar Reagents and the Factors Governing the Reactivity····· 19
Chapter 4 Disilene to Silylene Isomerization····· 32

Part II Silicon-Oxygen and Silicon-Sulfur Double Bonds

Chapter 1 The Possible Existence of Silanone. The Thermodynamic and Kinetic Stability····· 42
Chapter 2 Effects of Fluorine Substitution on the Thermodynamic Stability of Silanone····· 81
Chapter 3 The Dimerization of Silanone and the Properties of the Polymeric Products $(H_2SiO)_n$ (n = 2, 3, and 4)····· 90
Chapter 4 The Thermodynamic and Kinetic Stability of Silanethione. The Ground, Excited, and Protonated States····· 127

Part III Germanium-Carbon and Germanium-Germanium Double Bonds

Chapter 1 The Relative Stability of Germaethene and Its Isomers····· 172

Chapter 2 Barrier Heights for the Germaethene to Germylene Isomerization and for the Reaction with Water..... 189
Chapter 3 Comparison in the Properties of Digermene with Ethene, Silaethene, Disilene, and Germaethene..... 198

PART I

SILICON - CARBON AND SILICON - SILICON DOUBLE BONDS

CHAPTER 1

Silaethene to Silylene Isomerization

Ab initio calculations including polarization functions and electron correlation show that the silaethene - silylene interconversions via 1,2-hydrogen, 1,2-methyl, and 1,2-silyl shifts proceed only at high temperatures.

Recent years have seen dramatic developments in silene chemistry[1]. Nevertheless, the possible interconversions of silenes and the isomeric silanediyls have been the subject of intensive discussion[2]. Several examples via the 1,2-hydrogen shift were reported in the last few years[3-5]. However, the calculated barrier heights (ca.40 kcal/mol)[6,7] and the further experimental studies[8-11] have led to the conclusion that the unimolecular interconversion via the 1,2-hydrogen shift are very unlikely to proceed at room temperature.

In contrast, it has recently been found from both experimental[12] and theoretical[13] sides that the 1,2-silyl shift in silylsilanediyls to disilenes proceeds rapidly at room temperature while the 1,2-methyl shift does not occur readily. This finding urged interest in the ab initio calculations of the transition states and barrier heights for the 1,2-silyl and 1,2-methyl group shifts in the interconversions of silenes(1) and methylsilanediyls(2).

$$\underset{1}{RHSi{=}CH_2} \rightleftharpoons \underset{2}{H\ddot{S}i\text{-}CH_2R} \quad , \quad R = SiH_3 \text{ or } CH_3$$

All calculations were for closed-shell singlets. Geometries were fully optimized at the Hartree-Fock(HF) level with three basis sets (3-21G, 6-31G, and 6-31G*)[14] by using the energy gradient method. The optimized geometries at the HF/6-31G* level are shown in Figures 1 and 2. Electron correlation was incorporated at the HF/6-31G* geometries through second- and

third-order Møller-Plesset perturbation (MP2 and MP3) theories,[15] with core-like orbitals held doubly occupied. The results are summarized in Table 1. For comparison, our previous results[7] for R=H are also given in this Table.

As Table 1 shows, the barriers for the 1,2-methyl and 1,2-hydrogen shifts are too sizable (40-55 kcal/mol) to be surmountable at room temperature. On the other hand, the barriers for the 1,2-silyl shift are much smaller. At the HF/6-31G level the 1,2-silyl shift barriers are 32.1($\underset{\sim}{1} \rightarrow \underset{\sim}{2}$) and 39.3($\underset{\sim}{2} \rightarrow \underset{\sim}{1}$) kcal/mol. Upon addition of polarization functions on Si and C, these barriers decrease to 30.1 and 34.8 kcal/mol, respectively. Electron correlation at MP3/6-31G* level lowers the HF/6-31G* barriers by 3.9($\underset{\sim}{1} \rightarrow \underset{\sim}{2}$) and 10($\underset{\sim}{2} \rightarrow \underset{\sim}{1}$) kcal/mol. Here, it is instructive to note that the MP3/6-31G* barriers of 26.2($\underset{\sim}{1} \rightarrow \underset{\sim}{2}$) and 24.8($\underset{\sim}{2} \rightarrow \underset{\sim}{1}$) kcal/mol are considerably larger than that of 8.5 kcal/mol calculated for the isomerization of $(SiH_3)HSi{=}SiH_2$ to $H\ddot{S}i\text{-}SiH_2(SiH_3)$[13]. This indicates that silyl groups are much less mobile in silenes and methylsilanediyls than in disilenes and silylsilanediyls.

Although calculations at more sophisticated levels of theory may reduce the size of the barriers, the interconversions of silenes and silanediyls are unlikely to proceed rapidly at room temperature. In fact, all the examples observed up to now are restricted to the high-temperature experiments; $(Me_3Si)MeSi{=}CH_2 \rightarrow Me\ddot{S}i\text{-}CH_2(Me_3Si)$ (840°C)[16,11a] and $Me_3Si\text{-}\ddot{S}i\text{-}CH(SiMe_3)_2 \rightarrow (Me_3Si)_2Si{=}CHSiMe_3$ (450°C)[17].

A thing which has not yet been discussed is the effect of substituents on the ease of the 1,2-shiftings. For this purpose, the barriers for the 1,2-hydrogen shifts $RHSi{=}CH_2 \rightarrow RSi{-}CH_3$ were calculated and compared with R = H, CH_3, and SiH_3. At the MP3/6-31G* level the barriers were 42.2(R=H), 43.5($R{=}CH_3$), and 42.8($R{=}SiH_3$) kcal/mol, there being no significant difference. This suggests that substituents have little effect on the magnitude of the barriers.

The authors are grateful to Profs. Ando and Sekiguchi for interesting discussions. All calculations were carried out at the Computer Center of the Institute for Molecular Science by using an IMS version of the GAUSSIAN 80 series of programs[18].

References

1 For recent comprehensive reviews, see L.E. Gusel'nikov and N.S. Nametkin, Chem. Rev., 1979, 79, 529; B. Coleman and M. Jones, Rev. Chem. Intermed., 1981, 4, 297; G. Bertrand, G. Trinquier, and P. Mazerolles, J. Organomet. Chem. Library, 1981, 12, 1.

2 H.F. Schaefer, Acc. Chem. Res., 1982, 15, 283.

3 R.T. Conlin and D.L. Wood, J. Am. Chem. Soc., 1981, 103, 1843.

4 T.J. Drahnak, J. Michl, and R. West, J. Am. Chem. Soc., 1981, 103, 1845.

5 H.P. Reisenauer, G. Mihm, and G. Maier, Angew. Chem., Int. Ed. Engl., 1982, 21, 854.

6 J.D. Goddard, Y. Yoshioka, H.F. Schaefer, J. Am. Chem. Soc., 1980, 102, 7644; Y. Yoshioka and H.F. Schaefer, J. Am. Chem. Soc., 1981, 103, 7366.

7 S. Nagase and T. Kudo, J. Chem. Soc., Chem. Commun., 1984, 141.

8 R.T. Conlin and R.S. Gill, J. Am. Chem. Soc., 1983, 105, 618. See also R.T. Conlin and Y.-W. Kwak, Organometallics, 1984, 3, 918.

9 C.A. Arrington, R. West, and J. Michl, J. Am. Chem. Soc., 1983, 105, 6176.

10 I.M.T. Davidson, S. Ijadi-Maghsoodi, T.J. Barton, and N. Tillman, J. Chem. Soc., Chem. Commun., 1984, 478.

11 See also (a) T.J. Barton, S.A. Burns, and G.T. Burns, Organometallics, 1982, 1, 210; (b) R. Walsh, J. Chem. Soc.,

Chem. Commun., 1982, 1415.

12 H. Sakurai, H. Sakaba, and Y. Nakadaira, J. Am. Chem. Soc., 1982, 104, 6156; H. Sakurai, Y. Nakadaira, and H. Sakaba, Organometallics, 1983, 2, 1484.

13 S. Nagase and T. Kudo, Organometallics, 1984, 3, 1320.

14 M.S. Gordon, J.S. Binkley, J.A. Pople, W.J. Pietro, and W.J. Hehre, J. Am. Chem. Soc., 1982, 104, 2797; M.M. Francl, W.J. Pietro, W.J. Hehre, J.S. Binkley, M.S. Gordon, D.J. DeFrees, and J.A. Pople, J. Chem. Phys., 1982, 77, 3654.

15 J.A. Pople, J.S. Binkley, and R. Seeger, Int. J. Quantum Chem., Quantum Chem. Symp., 1976, 10, 1.

16 T.J. Barton, and S.A. Jacobi, J. Am. Chem. Soc., 1980, 102, 7979.

17 A. Sekiguchi and W. Ando, Tetrahedron Lett., 1983, 24, 2791.

18 J.S. Binkley, R.A. Whiteside, R. Krishnan, R. Seeger, D.J. DeFrees, H.B. Schlegel, S. Topiol, L.R. Kahn, and J.A. Pople, QCPE, 1981, 10, 406.

Table 1. Barrier Heights for the interconversions of $RHSi{=}CH_2$ (1) and $H\ddot{S}i\text{-}CH_2R$ (2) in kcal/mol calculated at several levels of theory.

levels of theory	R=SiH_3		R=CH_3		R=H[a]	
	1 → 2	2 → 1	1 → 2	2 → 1	1 → 2	2 → 1
HF/3-21G	29.0	43.1	52.4	51.9	42.9	57.8
HF/6-31G	32.0	39.3	53.2	53.7	43.4	57.5
HF/6-31G*	30.1	34.8	55.9	50.5	43.5	49.3
MP2/6-31G*	26.4	23.5	55.5	42.6	44.5	42.5
MP3/6-31G*	26.2	24.8	54.7	44.4	42.2	43.0

a Taken from ref.7.

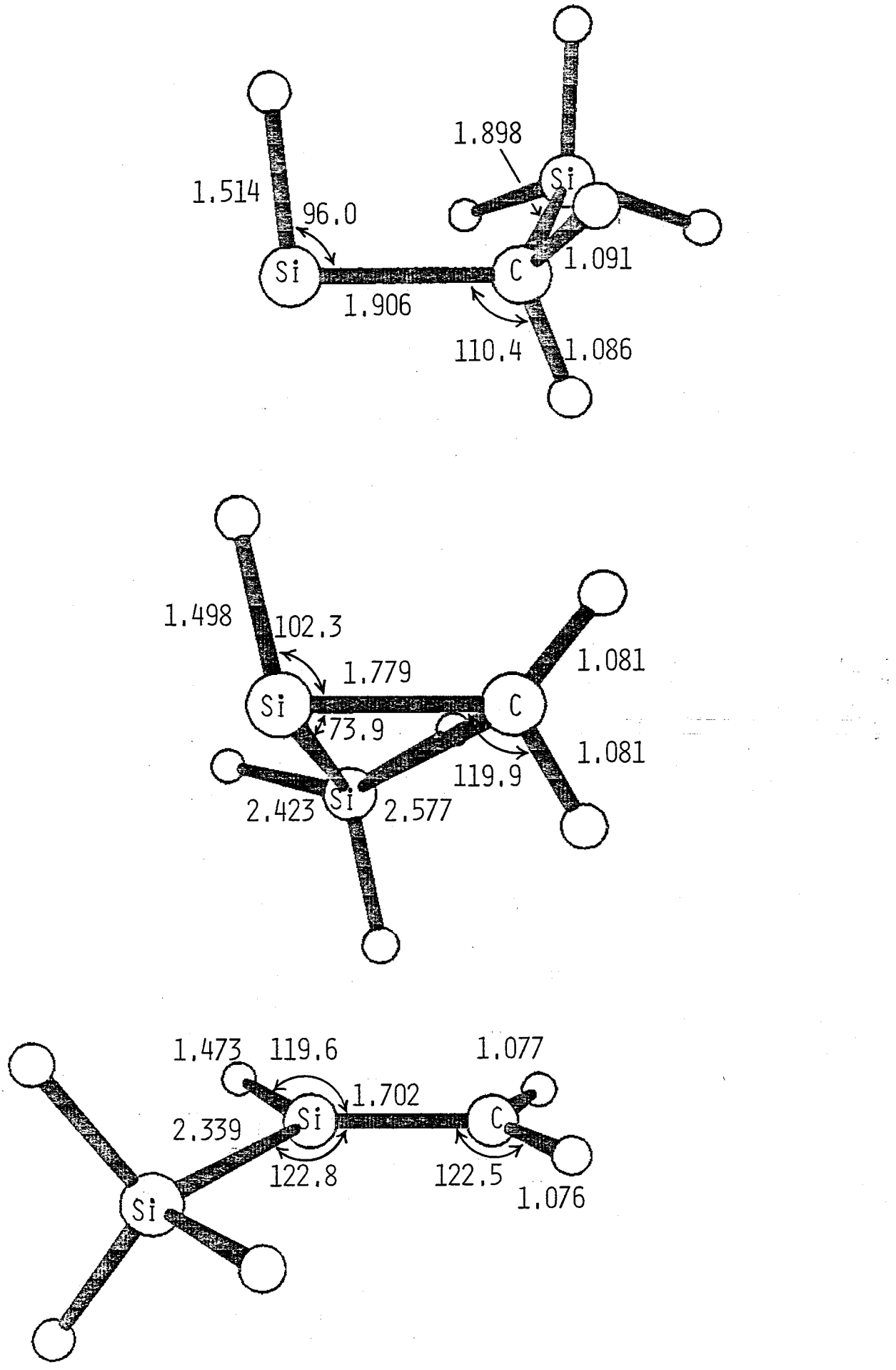

Figure 1. The HF/6-31G* optimized geometries of $(SiH_3)HSi{=}CH_2$, $H\ddot{S}i\text{-}CH_2(SiH_3)$, and the transition state (middle) connecting them in angstroms and degrees.

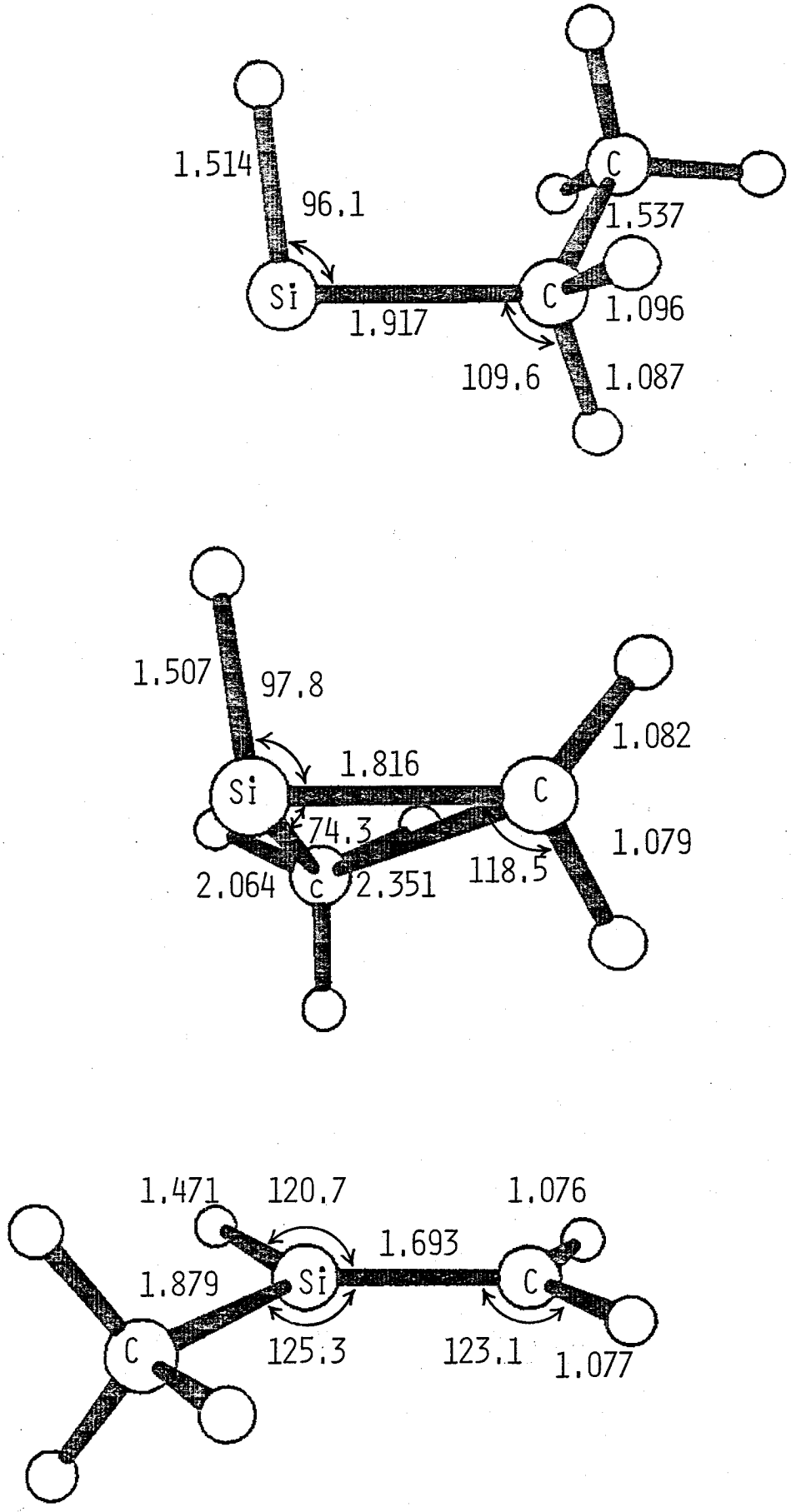

Figure 2. The HF/6-31G* optimized geometries of $(CH_3)HSi{=}CH_2$, $H\ddot{S}i\text{-}CH_2(CH_3)$, and the transition state (middle) connecting them in angstroms and degrees.

CHAPTER 2

Effects of Methyl Substitution on the Silaethene to Silylene Isomerization

Through ab initio calculations including electron correlation, it is found that both $H_2Si{=}CH_2$ to $H\ddot{S}i\text{-}CH_3$ and $MeSiH{=}CH_2$ to $Me\ddot{S}i\text{-}CH_3$ isomerizations are almost thermoneutral and proceed with a sizable barrier of ~40 kcal/mol; there exists no significant effect of methyl substitution.

Despite a great deal of recent developments in silaethene chemistry[1], there have been apparent discrepancies between theory and experiment in barrier height and heat of reaction for the following isomerizations (via 1,2-hydrogen shift),

$$H_2Si{=}CH_2 \rightarrow H\ddot{S}i\text{-}CH_3 \qquad (1)$$

$$MeSiH{=}CH_2 \rightarrow Me\ddot{S}i\text{-}CH_3 \qquad (2)$$

A theoretical study by Goddard, Yoshioka, and Schaefer[2] predicted the barrier for reaction (1) to be 41.0 kcal/mol. In contrast, experimental studies by Conlin and Wood[3], and Drahnak, Michl, and West[4] suggested evidence that reaction (2) proceeds rapidly. Among the experimental data, the Conlin and Wood observation might be interpretted in terms of a reasonable high temperature process[5]. However, the apparent observation of reaction (2) at 100 K[4] means that its barrier should be less than 5 kcal/mol. Thus, Yoshioka and Schaefer[6] recalculated the barrier for reaction (1) at a higher level of theory, but again obtained a sizable barrier of 40.6 kcal/mol. Since the calculations refer to strictly reaction (1), of course, there remains the possibility that the presence of the methyl group in reaction (2) is responsible for the discrepancy between theory and experiment.

It has been calculated[2,8-9] at high levels of theory† that

---

†The necessities of polarization functions and correlation energy correction are well established to calculate correctly the heat of reaction.

reaction (1) is approximately thermoneutral[10]. In contrast, a recent ion cyclotron resonance study by Pau, Pietro, and Hehre[11] showed evidence that $MeSiH{=}CH_2$ is 28 kcal/mol more stable than $\ddot{M}eSi\text{-}CH_3$, i.e., reaction (2) is highly endothermic. If this result is indeed true[12], it may provide indirect support for a significant barrier between $MeSiH{=}CH_2$ and $\ddot{M}eSi\text{-}CH_3$. However, the sizable energy difference favoring $MeSiH{=}CH_2$ over $\ddot{M}eSi\text{-}CH_3$ is not compatible with the near degeneracy in energy of $H_2Si{=}CH_2$ and $H\ddot{S}i\text{-}CH_3$,[2,8-9] unless the additional methyl group has a dramatic effect.

In light of these apparent conflicts, what is now of urgent need is to pursue the effects of methyl substitution. Thus, ab initio calculations were performed at several levels of theory to provide insight into the difference between reactions (1) and (2). All geometries were fully optimized at the Hartree-Fock(HF) level with three basis sets (3-21G, 6-31G, and 6-31G*)[13], by using the analytic energy gradient technique. Electron correlation was incorporated at the 6-31G* HF optimized geometries through third-order Møller-Plesset perturbation(MP3)[14] and configuration interaction(CI) theories. In the correlation calculations, all single(S) and double(D) excitations were included, with the restriction that excitations from core-like orbitals (1s,2s,2p for Si and 1s for C) were excluded. The final CI energies (denoted by CISDQ) were obtained by adding the Davidson correction[15] to

allow for unlinked quadruple(Q) excitations.

In Figure 1 are shown the transition states for reactions (1) and (2). It is noteworthy that the two transition state structures are very similar. Probably reflecting the structural similarity, the magnitude of the barrier height for reaction (2) differs little from that for reaction (1), as given in Table I. The barriers for reactions (1) and (2) are both sizable, the latter barrier being rather slightly larger than the former at all levels of theory. Obviously, the present findings exclude the favorable and dramatic effect of methyl substitution on the isomerization barrier height. Moreover, Table I reveals that at all levels of theory the energy difference between $H_2Si{=}CH_2$ and $H\ddot{S}i\text{-}CH_3$ is comparable to that between $MeSiH{=}CH_2$ and $Me\ddot{S}i\text{-}CH_3$, and at high levels[†] reactions (1) and (2) are almost thermoneutral (or slightly exothermic), in disagreement with the experimental work by Pau, Pietro, and Hehre[1].

The present communication confirms that the additional methyl group in reaction (2) can provide no significant difference between reactions (1) and (2). Further experimental work or alternative interpretations seem to be required.

References

1 H.F. Schaefer, Acc. Chem. Res., 1982, 15, 283.

2 J.D. Goddard, Y. Yoshioka, and H.F. Schaefer, J. Am. Chem. Soc., 1980, 102, 7644.

3 R.T. Conlin, and D.L. Wood, J. Am. Chem. Soc., 1981, 103, 1843. For an argument on the reliable precursor of $MeSiH=CH_2$, see T.J. Barton, S.A. Burns, and G.T. Burns, Organometallics, 1982, 1, 210.

4 T.J. Drahnak, J. Michl, and R. West, J. Am. Chem. Soc., 1981, 103, 1845. Also see H.P. Reisenauer, G. Mihm, and G. Maier, Angew. Chem., Int. Ed. Engl., 1982, 21, 854.

5 R. Walsh, J. Chem. Soc., Chem. Commun., 1982, 1415; R.T. Conlin, and R.S. Gill, J. Am. Chem. Soc., 1983, 105, 618.

6 Y. Yoshioka, and H.F. Schaefer, J. Am. Chem. Soc., 1981, 103, 7366.

7 M.S. Gordon, Chem. Phys. Lett., 1978, 54, 9.

8 G. Trinquier, and J.-P. Malrieu, J. Am. Chem. Soc., 1981, 103, 6313.

9 H.J. Köhler, and H. Lischka, J. Am. Chem. Soc., 1982, 104, 5884.

10 For a thermochemical estimation, see R. Walsh, Acc. Chem. Res., 1981, 14, 246.

11 C.F. Pau, W.J. Pietro, and W.J. Hehre, J. Am. Chem. Soc., 1983, 105, 16.

12 For a theoretical example at the HF level against the result, see M.S. Gordon, J. Am. Chem. Soc., 1982, 104, 4352.

13 M.S. Gordon, J.S. Binkley, J.A. Pople, W.J. Pietro, and W.J. Hehre, J. Am. Chem. Soc., 1982, 104, 2797; M.M. Francl, W.J. Pietro, W.J. Hehre, J.S. Binkley, M.S. Gordon, D.J. DeFrees, and J.A. Pople, J. Chem. Phys., 1982, 77, 3654.

14 J.A. Pople, J.S. Binkley, and R. Seeger, Int. J. Quantum Chem., Quantum Chem. Symp. 1976, 10, 1.

15 S.R. Langhoff, and E.R. Davidson, Int. J. Quantum Chem. 1974, 8, 61; E.R. Davidson, and D.W. Silver, Chem. Phys. Lett., 1977, 52, 403.

Table I. Barrier Heights and Heats of Reaction for the Isomerizations (1) and (2) in kcal/mol Calculated at Several Levels of Theory[1].

levels of thory	barrier height (1)	barrier height (2)	heat of reaction (1)	heat of reaction (2)
HF//3-21G	42.9	45.5	-14.9	-15.7
HF//6-31G	43.4	46.0	-14.1	-14.8
HF//6-31G*	43.5	47.4	-5.8	-5.1
MP3/6-31G*	42.2	43.5	-0.8	-1.9
CISD/6-31G*	41.6	44.9	-3.8	-2.7
CISDQ/6-31G*	39.3	41.4	-3.4	-2.0

[1] Correlation calculations were carried out at the 6-31G* HF optimized geometries.

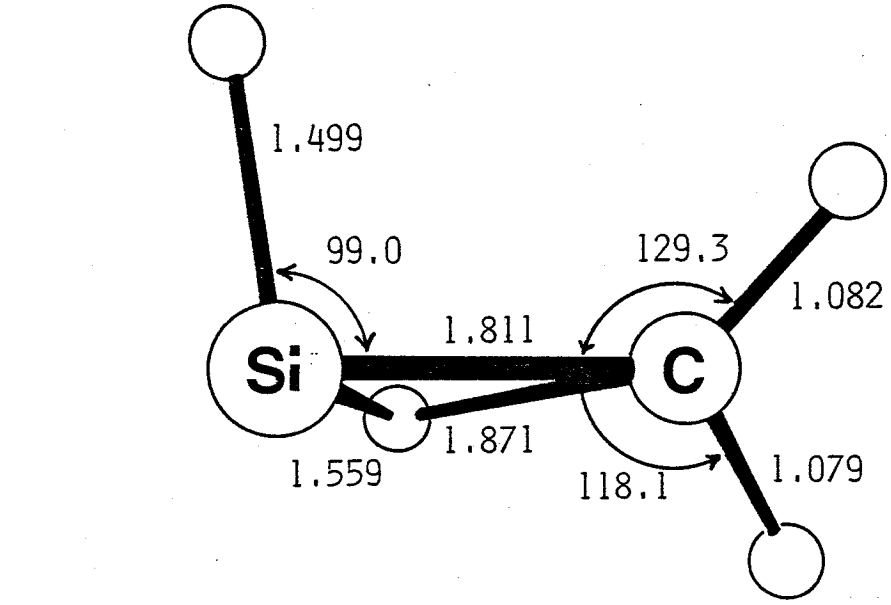

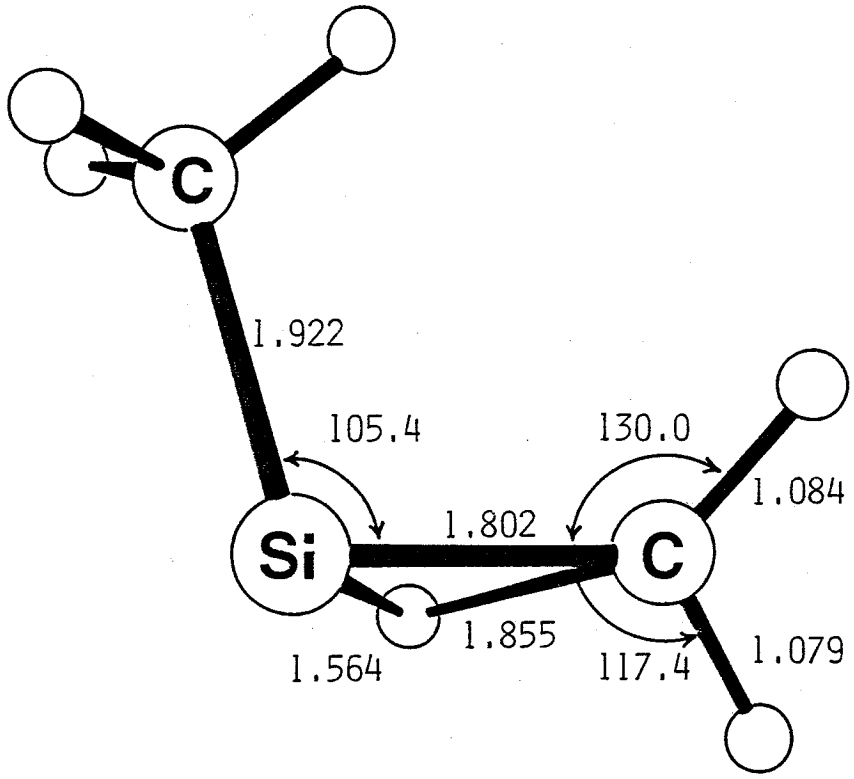

Figure 1. Transition state geometries for the isomerizations (1) and (2) in angstroms and degrees, obtained at the 6-31G* HF level.

CHAPTER 3

Mechanistic Aspects
of
the Reactions of Silaethene with Polar Reagents
and
the Factors Geoverning the Reactivity

In an attempt to provide theoretical insight into the mechanistic aspects of the reactions of silaethenes, the additions of HCl and H_2O are investigated through ab initio molecular orbital calculations. Silaethene is found to be much more reactive toward HCl and H_2O than ethene. Also examined are the effects of substituents (Me, F, and OH) on the reactivity of silaethene. It is suggested that the charge factor plays a more important role in controlling the reactivity than the frontier factor.

Although in recent years much progress has been made in the generation and characterization of silicon-carbon doubly bonded intermediates[1], relatively little is known about their reactivities. In an attempt to provide theoretical insight into the mechanistic aspects of the reactions of silaethene ($H_2Si{=}CH_2$), we considered the addition of HCl as an example of electrophilic reactions and the addition of water as an example of nucleophilic reactions. Our purposes are to disclose the factors governing the reactivity of silaethene and to control them by the electronic effects of relatively small substituents.

Stationary points on potential energy surfaces were located at the Hartree-Fock (HF) level with the 3-21G[2] and 6-31G*[3] basis sets using the analytical gradient technique. Following the full optimization of stational point structures, additional single point calculations were carried out with electron correlation incorporated through third-order Møller-Plesset perturbation (MP3)[4] theory with the 6-31G* basis set. In the MP3 calculations, all single and double excitations were included, with the restriction that excitations from core-like orbitals (1s, 2s, 2p for Si and 1s for C) were excluded.

Results and Discussion

Mechanistic Aspects. The feature of the potential energy surfaces for the additions of HCl and H_2O to silaethene is schematically summarized in Figure 1. All these reactions initiate

the formation of a weak complex in a relatively early stage of the reactions. The intermediate complex is transformed via a transition state to the product. The reactions are all exothermic. To simplify discussion, we here concentrate mainly on the magnitude of the overall barrier (ΔE) in Figure 1.

Figure 2 compares the transition structures for the HCl additions to ethene and silaethene.

$$H_2C{=}CH_2 + HCl \longrightarrow H_2ClC\text{-}CH_3 \qquad (1)$$

$$H_2Si{=}CH_2 + HCl \longrightarrow H_2ClSi\text{-}CH_3 \qquad (2)$$

Reaction (1) involves a four-center-like transition state with C_s symmetry. This is no surprising. In reaction (2), however, two points are noteworthy. First, reaction (2) proceeds via a two-center-like transition state with C_s symmetry, differing substantially from reaction (1). Second, it has been assumed in the experimental work by Wiberg[5] that the Cl atom (carring negative charge) of HCl first attacks the Si atom (carring positive charge) of $H_2Si{=}CH_2$ in a nucleophilic way. That is, $H_2Si{=}CH_2$ and HCl were supposed to act as a Lewis acid and base, respectively. According to the present calculations, however, it is found that reaction (2) proceeds through the interaction between the H atom (carring positive charge) of HCl and the C atom (carring negative charge) of $H_2Si{=}CH_2$. The electrophilic addition of HCl is also confirmed by the Mulliken population analysis at

the transition state.

Figure 3 shows the transition structures for the water additions to ethene and silaethene.

$$H_2C{=}CH_2 + H_2O \longrightarrow H_2COH\text{-}CH_3 \qquad (3)$$

$$H_2Si{=}CH_2 + H_2O \longrightarrow H_2SiOH\text{-}CH_3 \qquad (4)$$

These transition structures have C_s symmetry and are very similar to each other. In the transition structures the H_2O moiety is oriented in a manner that one of the lone pairs has a favorable nucleophilic interaction with the π^*-orbital of ethene or silaethene.

Table I summarizes the overall barrier heights and heats of reaction calculated for reactions (1)-(4). The reactions of silaethene are much more exothermic than the reactions of ethene. As the large difference in exothermicity shows, the barriers for reactions (2) and (4) are much smaller than those for reactions (1) and (3), indicative of the high reactivities of the silicon-carbon double bond toward HCl and H_2O. It appears that the high reactivities make difficult the experimental detection of the important species. As Table I shows, silaethene is more reactive toward H_2O than toward HCl.

What factors are responsible for the high reactivities of the silicon-carbon double bonds ? In this respect, the following points are noteworthy. First, the double bond in silaethene

($H_2Si^{+.52\ -.55}{=\!=}CH_2$) is more strongly polarized than that in ethene ($H_2C^{-.25\ -.25}{=\!=}CH_2$). Second, the frontier orbital π (-8.5 eV) and π^* (2.5 eV) energy levels of silaethene are considerably higher and lower, respectively, than the π (-10.2 eV) and π^* (5.0 eV) levels of ethene. These suggest that the reactions of silaethene are "frontier-controlled" as well as "charge-controlled".

The Effects of Substituents. We are now in a position to reduce the high reactivities by introducing relatively small substituents. For this purpose, we first considered the reaction of $Me_2Si=CH_2$ with HCl. As Table II shows, the calculated barrier of 5.2 kcal/mol is considerably smaller than that for the reaction of $H_2Si=CH_2$, and it is in reasonable agreement with the activation energy of 2.4 $\pm$ 1.7 kcal/mol observed recently by Davidson et al.[6]. The higher reactivity of $Me_2Si=CH_2$ over $H_2Si=CH_2$ is not surprising since the methyl-substituted silaethene has the higher-lying π orbital level and more strongly polarized double bond, as shown in Figure 4.

Next, we considered the reaction of $F_2Si=CH_2$, because the frontier π level is considerably lower than that of $Me_2Si=CH_2$ (See Figure 4). As expected, the barrier for the electrophilic HCl addition to $F_2Si=CH_2$ was calculated to be twice larger than that for the corresponding addition to $Me_2Si=CH_2$. However, the barrier for the reaction of $F_2Si=CH_2$ is still smaller than that for the reaction of $H_2Si=CH_2$ (Table II). Furthermore, the reaction of $F_2Si=CH_2$ with H_2O was found to proceed with no overall barrier. As

obvious from Figure 4, these are ascribable to the fact that in $F_2Si{=}CH_2$ the silicon and carbon atoms are much more positively and negatively charged, respectively.

The finding prompts us to attach electron-donating substituents to the carbon end of the Si=C bond so that the charge separation decreases or the polarity reverses significantly. To see if such substitution is valid[7], we chose $H_2Si{=}CHOH$ which is polarized in a way that the silicon atom is much less positively charged and the carbon is slightly negatively charged. As Table II shows, the barrier for the reaction of $H_2Si{=}CHOH$ with H_2O increases drastically to 17.6 kcal/mol, $H_2Si{=}CHOH$ being significantly less reactive than $H_2Si{=}CH_2$. This suggests that the charge factor is more important in controlling the reactivities than the frontier factor[8]. In other words, the high reactivities of silaethenes can be deduced to a considerable extent by the substituents which decrease the charge separation in the silicon-carbon double bond.

References

1 For recent comprehensive reviews, see : Gusel'nikov, L. E.; Nametkin, N. S. Chem. Rev. 1979, 79, 529. Coleman, B.; Jones, M. Rev. Chem. Intermed. 1981, 4, 297. Bertrand, G.; Trinquier, G.; Mazerolles, P. J. Organomet. Chem. Library 1981, 12, 1. Schaefer, H. F. Acc. Chem. Res. 1982, 15, 283.

2 Gordon, M. S.; Binkley, J. S.; Pople, J. A.; Pietro, W. J. ; Hehre, W. J. J. Am. Chem. Soc. 1982, 104, 2797.

3 Francl, M. M.; Pietro, W. J.; Hehre, W. J.; Binkley, J. S. ; Gordon, M. S.; DeFrees, D. J.; Pople, J. A. J. Chem. Phys. 1982, 77, 3654.

4 Pople, J. A.; Binkley, J. S.; Seeger, R. Int. J. Quantum Chem., Quantum Chem. Symp. 1976, 10, 1.

5 Wiberg, N. J. Organomet. Chem. 1984, 273, 141.

6 Davidson, I. M. T.; Dean, C. E.; Lawrence, F. T. J. Chem. Soc., Chem. Commun. 1981, 52.

7 For the validity for preventing dimerization, see : Morokuma, K. IMS Ann. Rev. 1984, 13.

8 For the similar conclusion based on frontier orbital theory, see : Apeloig, Y.; Karni, M. J. Am. Chem. Soc. 1984, 106, 6676.

Table I MP3/6-31G*//6-31G* calculations (kcal/mol).

reaction	barrier	heat of reaction
$H_2C{=}CH_2 + HCl$	46.5	-27.8
$H_2Si{=}CH_2 + HCl$	13.8	-80.1
$H_2C{=}CH_2 + H_2O$	64.0	-11.8
$H_2Si{=}CH_2 + H_2O$	8.4	-77.0

Table II Comparison of the barriers (kcal/mol) for the HCl and H_2O additions to substitued silaethenes at the HF/6-31G*//3-21G level.

	$H_2Si=CH_2$	$Me_2Si=CH_2$	$F_2Si=CH_2$	$H_2Si=CH(OH)$
HCl	19.2	5.2	10.1	
H_2O	10.7		no barrier	17.6

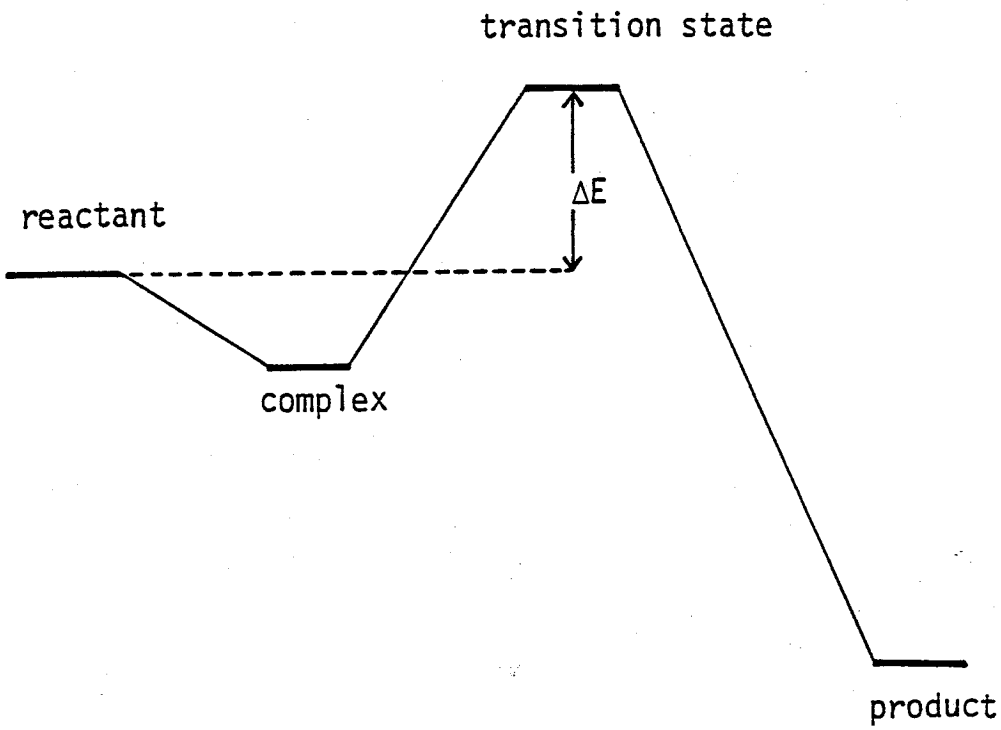

Figure 1. Schematic description of the energy profiles for the reactions of silicon-carbon doubly bonded compounds.

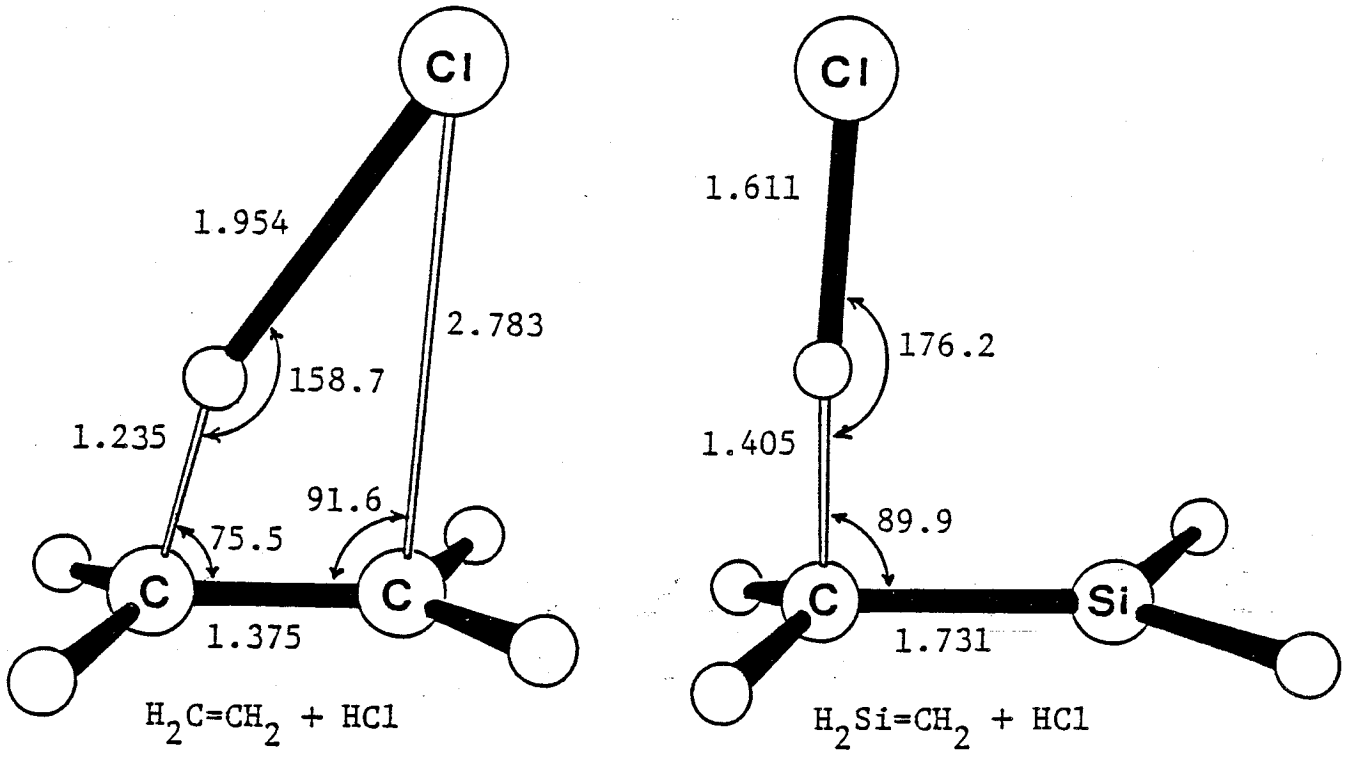

Figure 2. HF/6-31G* transition structures for reactions (1) and (2) in angstroms and degrees.

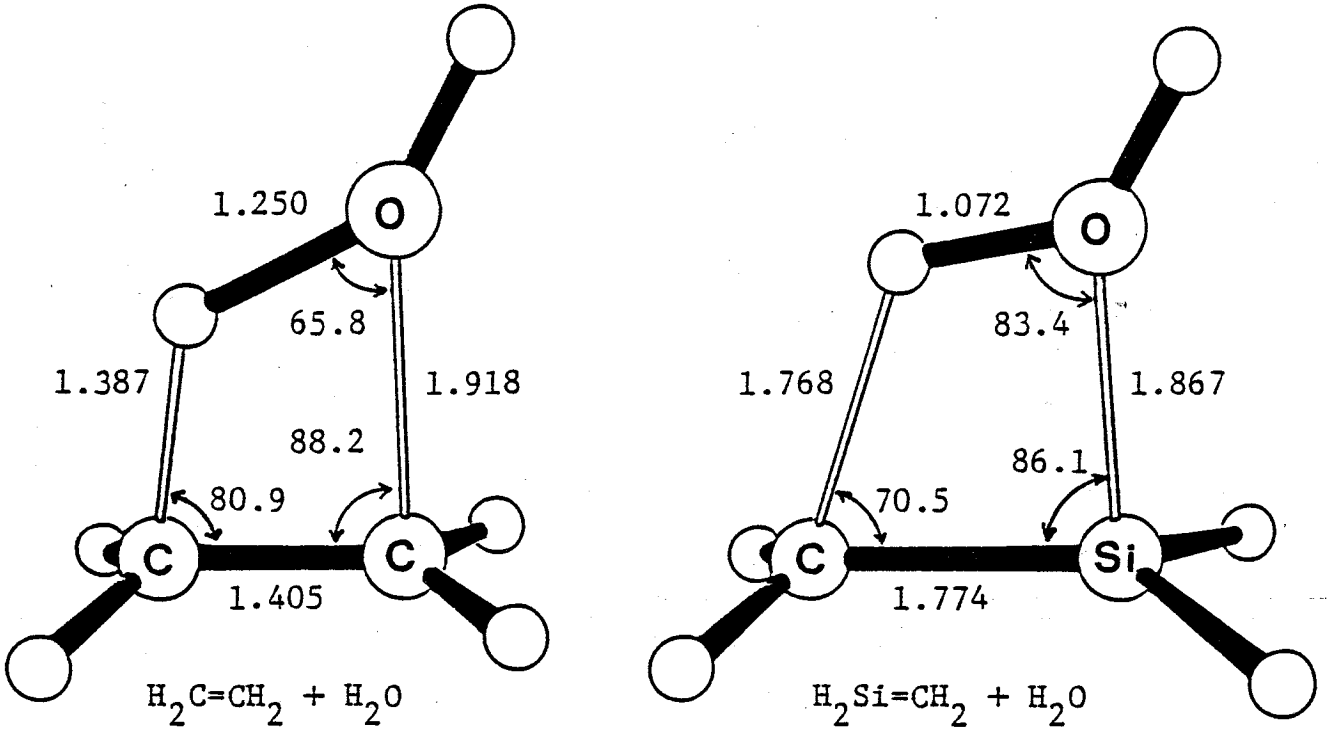

Figure 3. HF/6-31G* transition structures for reactions (3) and (4) in angstroms and degrees.

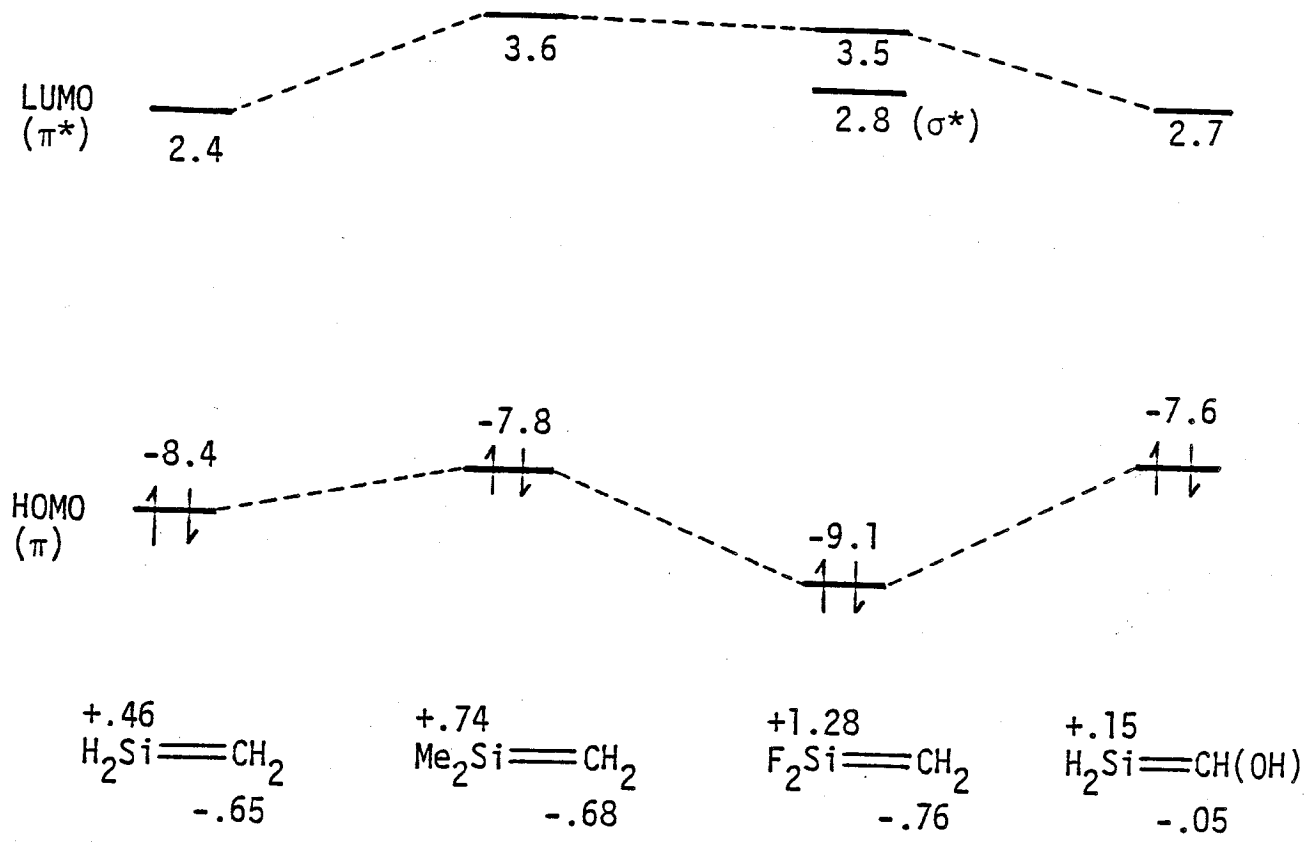

Figure 4. Net atomic charge densities and frontier orbital π and π* energies (eV) at the HF/6-31G*//3-21G level.

CHAPTER 4

Disilene to Silylene Isomerization

Transition states and barrier heights for the title reactions via 1,2-silyl and 1,2-methyl shifts are investigated through ab initio calculations. The 1,2-silyl shift in silylenes to disilenes is found to proceed at room temperature, this being in agreement with the recent experiment. Also discussed are the structures of disilenes.

There is considerable current interest in the possible interconversion of divalent and doubly bonded silicon compounds. Several examples of the silylene-silene isomerizations (via 1,2-hydrogen[1] and 1,2-silyl[2] shifts) have been documented in the last few years. However, the unimolecular reactions are likely to proceed only at high temparature, as the calculated barrier heights[3] as well as the further experimental studies[4] reveal. In contrast, recently Sakurai and co-workers[5] have found that a silylene, $\ddot{\text{M}}\text{eSiSiMe}_2(\text{SiMe}_3)$(1), isomerizes rapidly to a disilene, $(\text{SiMe}_3)\text{MeSi=SiMe}_2$(2): this is the first example at room temparature. We report here the ab initio calculations of the transition states and barrier heights for the following interconversion reactions.[6]

$$\ddot{\text{H}}\text{SiSiH}_2(\text{SiH}_3) \rightleftharpoons (\text{SiH}_3)\text{HSi=SiH}_2$$
$$\underset{\sim}{3} \qquad\qquad \underset{\sim}{4}$$

$$\ddot{\text{H}}\text{SiSiH}_2(\text{CH}_3) \rightleftharpoons (\text{CH}_3)\text{HSi=SiH}_2$$
$$\underset{\sim}{5} \qquad\qquad \underset{\sim}{6}$$

All calculations were for closed-shell singlets. Geometries were fully optimized at the Hartree-Fock level with the 6-31G[7] energy gradient method. Energies were improved with the larger 6-31G* basis set[7] using third-order Møller-Plesset perturbation theory[8].

The ORTEP drawings of optimized geometries of $\underset{\sim}{3}$, $\underset{\sim}{4}$, and the transition state connecting them are shown in Fig.1. In the notation of $\text{H}^{\text{a}}\ddot{\text{S}}\text{i}^{\text{a}}\text{Si}^{\text{b}}\text{H}_2(\text{SiH}_3)$ and $(\text{SiH}_3)\text{H}^{\text{a}}\text{Si}^{\text{a}}\text{=Si}^{\text{b}}\text{H}_2$, the silyl

group shifts diagonally across the Si^aSi^b bond to accomplish the interconversion. In the transition state the shifting group is positioned almost under the Si^aSi^b bond, as characterized by the $SiSi^aSi^bH^a$ dihedral angle of 95.6°, but away from the perpendicular bisector of the Si^aSi^b bond in the way that the Si atom in the silyl group is 0.383 Å nearer to Si^a than to Si^b. The $SiSi^a$ distance of 2.608 Å is only 0.254 Å longer than the value (2.354 Å) in 4 while the $SiSi^b$ distance of 2.991 Å is 0.606 Å longer than the value (2.385 Å) in 3. As also seen in several of the remaining geometrical parameters except for the $H^aSi^aSi^b$ angle, the transition state is closer to 4 rather than to 3.

Nevertheless, the transition state for the 1,2-silyl shift lies 18.2 kcal/mol above 4 and 8.5 kcal/mol above 3. The barrier for reaction 4 → 3 is 2.14 times larger than that for the reverse reaction. Correction for zero-point vibrational energies[9] can reduce the barriers only very slightly to 17.2(4 → 3) and 8.4(3 → 4) kcal/mol. Most interesting is the small barrier[10] for the 1,2-silyl shift in 3 to 4 which is likely to be surmountable at room temperature with a considerable rate.[11] This finding is comparable to the apparent observation of the rapid isomerization of 1 to 2 at room temperature. In contrast, the barrier for 4 → 3 is somewhat too large for the reaction to occur at room temperature,[11] suggesting that disilenes are kinetically more stable to isomerization than silylenes. In fact, the isomerization of 2 back to 1 was not observed at 15 ± 2 °C by Sakurai et al., though found to proceed at an elevated temperature (300 °C).[5]

There is the possibility that via 1,2-methyl shift 1 isomerizes to 2. To theoretically check this, we have undertaken reaction 5 → 6. As Fig.2 shows, the feature of the geometrical changes in the 1,2-methyl shift is essentially the same as that in Fig.1. However, the calculated barrier for 5 → 6 is as large as 27.8 kcal/mol, and excludes the methyl-shift mechanism in the formation of 2 from 1 at room temparature. As the sizable barrier (34.7 kcal/mol) for 6 → 5 also suggests, methyl groups are much more reluctant to migrate in disilenes and silylenes than are silyl groups.[12] Several years ago, Barton and co-workers[13] claimed that tetramethyldisilene isomerized rapidly to trimethylsilylmethylsilylene. This is not surprising in the high-temparature experiment (700 °C). However, they could find no evidence for the reverse 1,2-methyl shift under the condition : this may conflict with our expectation that its barrier is rather smaller.

Finally, the structures of disilenes are worth mentioning. The equilibrium structures of 4 and 6 are in Cs symmetry with a planar disilene framework, as shown in Figs. 1 and 2. These differ significantly from the equilibrium structure of $H_2Si{=}SiH_2$ since the parent compound has been predicted to adopt a trans-bent C_{2h} form (not a planar D_{2h} form).[14] At this point, it is interesting to note that the two silicon atoms and four attached carbons in 1,2-di-tert-butyl-1,2-dimesithyldisilene are recently found to be coplanar by the X-ray crystal study,[15a] while the silicon atoms in tetramesityldisilene are moderately anti-pyramidalized.[15] It seems that the planarity of disilene frameworks is sensitive to substitution.

References and Notes

(1) (a) Conlin, R.T.; Gaspar, P.P. J. Am. Chem. Soc. 1976, 98, 868. (b) Conlin, R.T.; Wood, D.L. J. Am. Chem. Soc. 1981, 103, 1843. (c) Drahnak, T.J.; Michl, J.; West, R. J. Am. Chem. Soc. 1981, 103, 1845. (d) Reisenauer, H.P.; Mihm, G.; Maier, G. Angew. Chem.,Int. Ed. Engl. 1982, 21, 854. See also, (e) Barton, T.J.; Burns, S.A.; Burns, G.T. Organometallics, 1982, 1, 210.

(2) (a) Barton, T.J.; Jacobi, S.A. J. Am. Chem. Soc. 1980, 102, 7979. (b) Sekiguchi, A.; Ando, W. Tetrahedron Lett. 1983, 24, 2791.

(3) The barriers (ca.41 kcal/mol) for $H\ddot{S}iCH_3 \rightleftharpoons H_2Si{=}CH_2$: (a) Goddard, J.D.; Yoshioka, Y.; Schaefer, H.F. J. Am. Chem. Soc. 1980, 102, 7644. (b) Yoshioka, Y.; Schaefer, H.F. J. Am. Chem. Soc. 1981, 103, 7366. The barriers (39-43 kcal/mol) for $CH_3\ddot{S}iCH_3 \rightleftharpoons (CH_3)HSi{=}CH_2$: (c) Nagase, S.; Kudo, T. J. Chem. Soc., Chem. Commun. 1984, 141. The barriers (26-27 kcal/mol) for $H\ddot{S}iCH_2(SiH_3) \rightleftharpoons (SiH_3)HSi{=}CH_2$: (d) Nagase, S.; Kudo, T., to be published. It is to be noted that the barriers for silylenes → silenes are all calculated to be almost equal to those for the reverse reactions. For a germylene-germene isomerization, see (e) Nagase, S.; Kudo, T. Organometallics, 1984, 3, 324.

(4) (a) Conlin, R.T.; Gill, R.S. J. Am. Chem. Soc. 1983, 105, 618. (b) Arrington, C.A.; West, R.; Michl, J. J. Am. Chem. Soc. 1983, 105, 6176.: These authors interpreted that the facile isomerization observed at 100 K is catalyzed rather than unimolecular.

(5) (a) Sakurai, H.; Nakadaira, Y.; Sakaba, H. Organometallics, 1983, 2, 1484. (b) Sakurai, H.; Sakaba, H.; Nakadaira, Y. J. Am. Chem. Soc. 1982, 104, 6156.

(6) For the parent disilene-silylene isomerization, see Krogh-Jespersen, K. Chem. Phys. Lett. 1982, 93, 327.

(7) Francl, M.M.; Pietro, W.J.; Hehre, W.J.; Binkley, J.S.; Gordon, M.S.; DeFrees, D.J.; Pople, J.A. J. Chem. Phys. 1982, 77, 3654.

(8) (a) Pople, J.A.; Binkley, J.S.; Seeger, R. Int. J. Quantum Chem., Quantum Chem. Symp. 1976, 10, 1. (b) The calculations were carried out with all orbitals included except the corelike orbitals (1s,2s, and 2p for Si and 1s for C in character).

(9) Because of the size of the reaction system, harmonic vibrational frequencies at the 3-21G level were used to compute zero-point energies : 31.5 (3), 32.2 (4), and 31.3 (transition state) kcal/mol.

(10) Since it is likely that calculations at higher levels will reduce the size of the barrier, the present value may be an upper limit to the experimental one.

(11) On the basis of the structures, energies, and frequencies obtained from the present ab initio calculations, the enthalpy and entropy of activation for reaction 3 → 4 are evaluated to be 7.8 kcal/mol and -5.1 e.u., respectively, at room temperature, while those for 4 → 3 are 16.8 kcal/mol and -3.6 e.u.. Within the framework of conventional transition state theory, the evaluated thermodynamic quantities allow us to estimate the rate constants on the order of 8.6×10^{5}(3 → 4) and 4.7×10^{-1}(4 → 3) $sec.^{-1}$ at high pressures.

(12) In addition, note that silyl groups are much more mobile in disilenes and silylenes than in silenes and silylenes.[3d]

(13) Wulff, W.D.; Goure, W.F.; Barton, T.J. J. Am. Chem. Soc. 1978, 100, 6236.

(14) (a) Snyder, L.C.; Wasserman, Z.R. J. Am. Chem. Soc. 1979, 101, 5222. (b) Poirier, R.A.; Goddard, J.D. Chem. Phys. Lett. 1981, 80, 37. (c) Krogh-Jespersen, K. J. Phys. Chem. 1982, 86, 1492. (d) Lischka, H.; Köhler, H.-J. Chem. Phys. Lett. 1982, 85, 467; J. Am. Chem. Soc. 1982, 104, 5889. For a trans-bent digermene, see Trinquier, G.; Malrieu, J.-P. Rivière, P. J. Am. Chem. Soc. 1982, 104, 4529, and Nagase, S.; Kudo, T. J. Mol. Struct., THEOCHEM, 1983, 103, 35.

(15) (a) Fink, M.J.; Michalczyk, M.J.; Haller, K.J.; Michl, J.; West, R. in press (private communication by Prof. West). (b) Fink, M.J.; Michalczyk, M.J.; Haller, K.J.; Michl, J.; West, R. J. Chem. Soc., Chem. Commun. 1983, 1010.

(16) Binkley, J.S.; Whiteside, R.A.; Krishnan, R.; Seeger, R.; DeFrees, D.J.; Schlegel, H.B.; Topiol, S.; Kahn, L.R.; Pople, J.A. QCPE 1981, 10, 406.

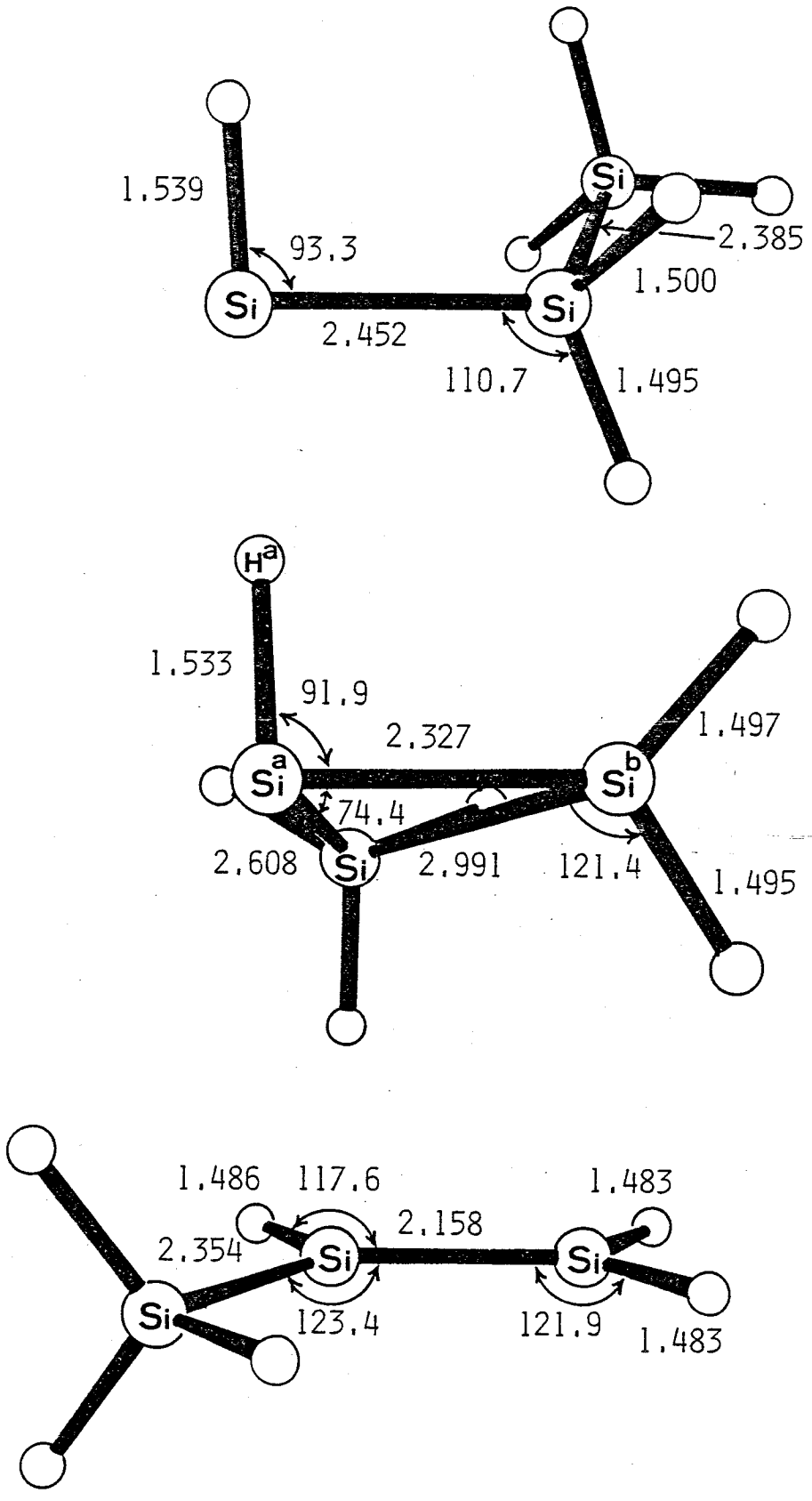

Figure 1. ORTEP drawings of the optimized geometries of 3 (top), 4 (bottom), and the transition state for the 1,2-silyl group shift, in angstroms and degrees.

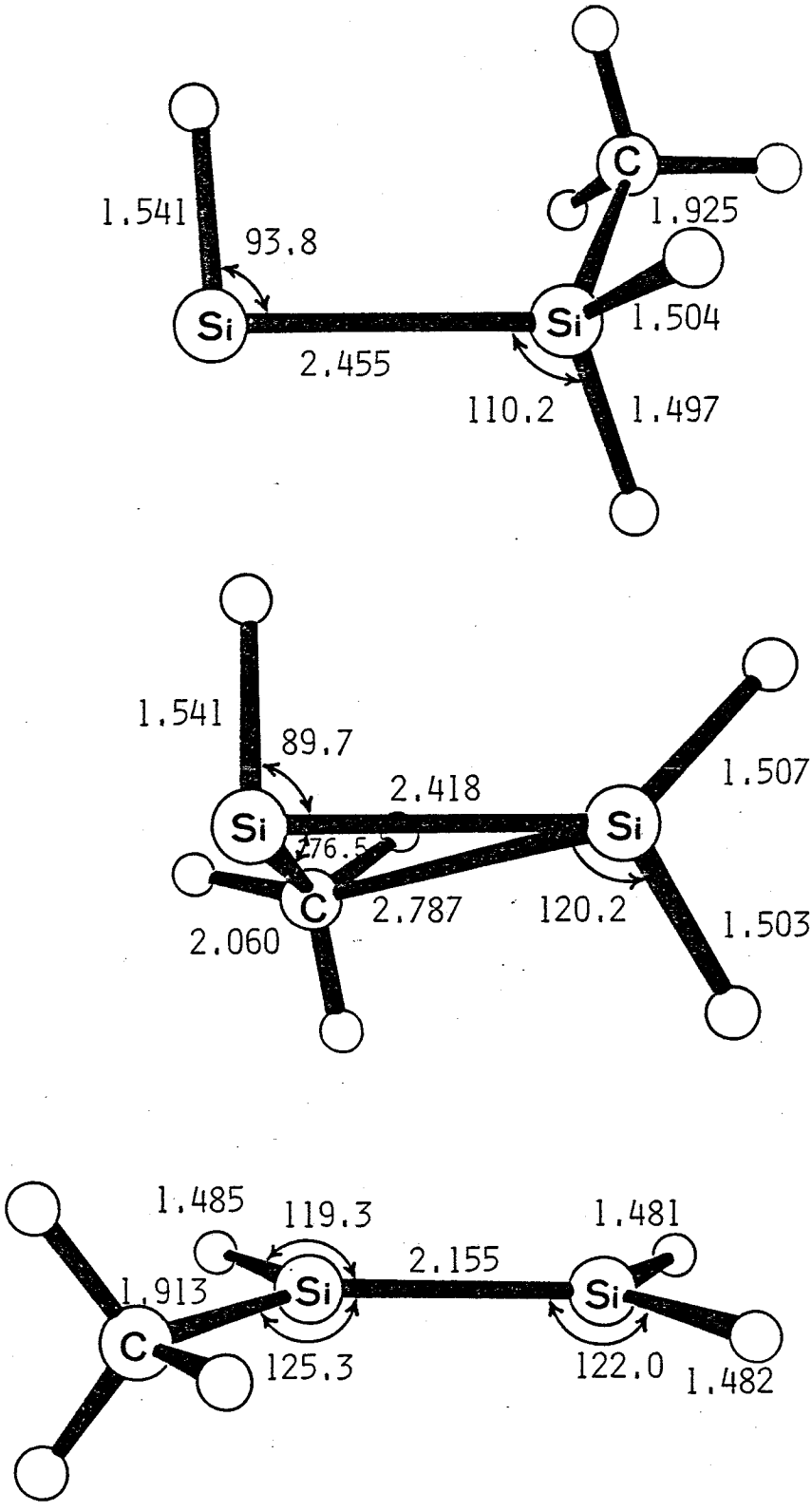

Figure 2. ORTEP drawings of the optimized geometries of 5 (top), 6 (bottom), and the transition state for the 1,2-methyl group shift, in angstroms and degrees.

Part II

Silicon - Oxygen and Silicon - Sulfur Double Bonds

CHAPTER 1

The Possible Existence of Silanone

The Thermodynamic and Kinetic Stability

In light of increasing current interest in the possible existence of silicon-oxygen doubly bonded compounds, the lowest singlet potential energy surface of the parent unsubstituted silanone, $H_2Si{=}O$, was investigated by means of ab initio calculations including polarization functions and electron correlation. Although not highly stable in a thermodynamic sense, silanone itself is certainly the existing species and found to be kinetically stable to unimolecular reactions such as $H_2SiO \rightarrow H_2 + SiO$, $H_2SiO \rightarrow H + HSiO$, and $H_2SiO \rightarrow HSiOH$. Of these pathways leading to the destruction of silanone, the lowest energy route is the 1,2-hydrogen shift forming the slightly more stable hydroxysilylene, but the barrier height is calculated to be as large as 63.9 (60.8 after zero point correction) kcal/mol. The bimolecular reaction of silanone with water was also examined and found to proceed with no overall barrier, indicating the very high reactivity of the silicon-oxygen double bond toward polar reagents. All these results were compared with those calculated at the same level of theory for the corresponding unimolecular and bimolecular reactions of formaldehyde.

Introduction

For many years the possible existence of π-bonded silicon intermediates has been attracting a great deal of attention in organosilicon chemistry[1]. Now that the isolation and characterization of compounds containing silicon-carbon[2] or silicon-silicon[3] double bonds are well under way, it is natural that current interest is directed toward the preparation of silicon-oxygen doubly bonded compounds, silanones. Several schemes for the generation and trapping of silanones have been devised, which involve the pyrolysis or photolysis of silylperoxide[4], cyclosiloxane[5], polysilane[6], silaoxetane[7] and disilaoxetane[8]. Despite the active experimental approaches, most of the experimental evidence for the transient existence is rather indirect. In view of the situation, theoretical information on the thermodynamic and kinetic stability should be helpful for further developments in silanone chemistry, but little effort along this line has been made[9,10].

In a continuation of our studies on π-bonded group 4B compounds[11], we report here a theoretical analysis of lowest singlet potential energy surface of the parent compound, $H_2Si{=}O$, through ab initio calculations including polarization functions and electron correlation. Unimolecular reactions pertinent to the stability of $H_2Si{=}O$ are shown in Scheme I.

Scheme I

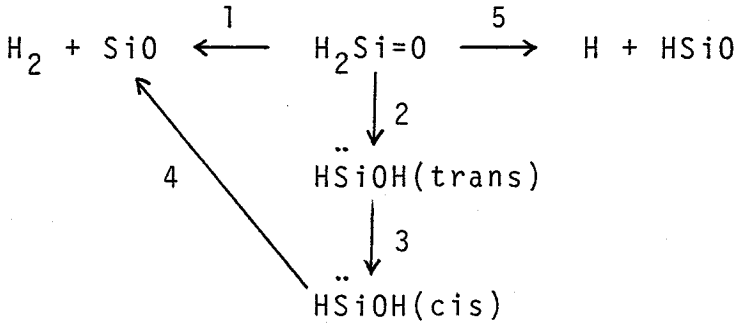

Of the species in Scheme I, hydroxysilylene $\ddot{H}SiOH$ is recently observed in the matrix isolation studies of reaction of silicon with water[12]. Very little information is currently available on the mechanistic details of reactions 1-5[13]. In contrast, the corresponding reactions of formaldehyde have been emerging as a prototype for fundamental molecular photochemistry and photolysis, and subject to a number of theoretical studies[14-18]. A great deal has been learned concerning the reactions of formaldehyde. Comparison of properties of $H_2Si=O$ and $H_2C=O$ at the same level of theory is expected to provide insight into the characteristic of the silicon-oxygen double bond, and particularly emphasized throughout the present work.

Also examined was the reactivity of silanone toward polar reagents. The reaction considered as a typical example is the addition of water:

$$H_2O + H_2Si=O \rightarrow HOSiH_2\text{-}OH$$

The feature of potential energy surface for the addition was compared with that for the reaction of formaldehyde with water, at the same level of theory.

To this end, it is shown that in several respects silanone differs remarkably from formaldehyde. Nevertheless, silanone is found to be the existing species that is highly reactive toward polar reagents.

Computational Details

In this work, stationary points on potential energy surfaces were located at the Hartree-Fock(HF) level with the 6-31G* basis set[19] using the analytical gradient technique. They were then characterized by checking the number of negative eigenvalues of the force constant matrix constructed by numerical differentiation of energy gradients; zero for equilibrium structures and one for transition structures. The harmonic vibrational frequencies obtained at the HF/6-31G* level were used to compute zero-point vibrational energies.

Following the full optimization of stational point structures, additional single-point calcualtions were carried out with electron correlation incorporated through configuration interaction(CI) or second- and third-order Møller-Plesset perturbation (MP2 and MP3)[20] theories, using the 6-31G* or the larger 6-31G** basis sets[19]. In the CI and MP calculations, all singly(S) and doubly(D) excited configurations relative to the respective HF reference configuration were included, with the restriction that core-like orbitals(1s,2s, and 2p for Si, 1s for O and C in character) were excluded. The final CI energies were obtained by using the Davidson formula[21] to allow for unlinked cluster quadruple correction(QC), these being denoted by CI(S+D+QC).

For silanone and trans-hydroxysilylene only, a more advanced theoretical prediction of the equilibrium structures was carried out at the MP2 level with the 6-31G* basis set.

Results and Discussion

Silanone and its isomers

Structures. Figure 1 shows the equilibrium structures of the H_2SiO species and silanol calculated at the HF/6-31G* level. In light of previous theoretical studies of the H_2CO species[14-18], it is not surprising that silanone has a C_{2v} symmetry structure and its 1,2-hydrogen shifted isomers hydroxysilylenes are planar in trans and cis forms. The Si-O double bond length of silanone is calculated to be 0.149 Å shorter than the Si-O single bond length of silanol. The shortening is somewhat smaller as compared with that of 0.215 Å[22] calculated at the same level from methanol to formaldehyde, but indicates a certain strength of p_π- p_π bonding between Si and O.

For the structure of silanone no experimental values are available for comparison, but one can quote the CEPA-PNO values of SiO=1.507 Å, SiH=1.471 Å, and ∠HSiH=110.0° obtained by Jaquet et al.[9]. Our results agree very well(to within 0.009 Å and 1.1°) with the CEPA-PNO results.

For the structure of trans-hydroxysilylene the following values have been proposed through the infrared spectrum study by Ismail et al[12].; SiO=1.591 ± 0.100 Å, SiH=1.521 ± 0.030 Å, OH=0.958 ± 0.005 Å, ∠HSiO=96.6 ± 4.0°, and ∠HOSi=114.5 ± 6°. Of these proposed values, only the HOSi bond angle was calculated by using the Teller-Redlich product rule while the other values were all estimated from available data of similar molecules. Nevertheless, the proposed geometrical parameters are all close to our calculated ones, except that the proposed Si-O single bond length seems to be somewhat underestimated.

Applying the Teller-Redlich product rule, Ismail et al[12]. also determined the HOSi angle in cis-hydroxysilylene. The value of 113° thus determined was comparable to (or slightly smaller than) the corresponding value of 114.5° for the trans isomer. In contrast, our calculated results shows that the HOSi angle is 4.6° larger in the cis form than in trans form. It seems more reasonable to adopt the view that on going from the trans to the cis form the HOSi angle opens up to relieve steric repulsion between the hydrogens. In fact, such opening up is also seen for the HOC angle in hydroxycarbene (HCOH) on going from the trans to the cis form[15-16].

The optimized structures of silanone and trans-hydroxysilylene at the MP2/6-31G* level are shown in Fig.2. Apparently, the effects of electron correlation are relatively small. Electron correlation typically increases the HF/6-31G* bond lengths by 0.01-0.05 Å and changes the bond angles by 0.3-3.3°. As for the Si-O double bond length of silanone, the MP2/6-31G* value is 0.038 Å larger than the CEPA-PNO value. This may reflect the general overcorrection of multiple bond lengths at the MP2 level[22].

Fig.3 shows the HF/6-31G* transition structures for the reactions 1-4 in Scheme I. In Fig.3, structures A, B, C and D are true transition states in the sense of the force constant matrices having single negative eigenvalue(see Table I). A and B are the transition states for molecular dissociations (reactions 1 and 4) leading to H_2 + SiO. Both are planar with C_s symmetry. C and D are the transition states for 1,2-hydrogen shift (reaction 2) and trans to cis isomerization

(reaction 3), which are both nonplanar.

The 1,2-hydrogen shift of silanone may be worth describing in more detail because the corresponding reaction of formaldehyde is calculated to proceed via a planar transition state[15-16]. With the C_s symmetry constraint of planarity, we searched for stationary points associated with the 1,2-hydrogen shift of silanone. As a consequence, a stationary point was indeed found whose structure (E in Fig.3) is very similar to C except for its planarity. However, the stationary point E was calculated to be 0.4 kcal/mol more unstable than C and to have two negative eigenvalues. One of the negative eigenvalues was associated with out-of-plane motion, excluding the planar transition state for the 1,2-hydrogen shift of silanone unlike the reaction of formaldehyde.

It may also be interesting to mention the trans to cis isomerization of hydroxysilylene from a technical point of view. As structure D in Fig.3 shows, the isomerization involves a rotational transition state with the dihedral angle of $\angle HOSiH=94.1^\circ$ (the dihedral angle is defined to be zero for HSiOH(cis) and 180° for HSiOH(trans)). A planar structure (F in Fig.3), in which the HOSi group is almost linear, is the stationary point which corresponds to inversion at the oxygen center. However, F was found to be 1.1 kcal/mol more unstable than D and to have two negative eigenvalues. That is, F is a maximum with respect to inversion and rotation. The slight advantage of D over F was unchanged by introduction of electron correlation. When d-type polarization functions were

omitted, however, F was slightly preferred to D and identified as the transition state for the isomerization. This result means that polarization functions play an important role in locating the rotational transition state. In contrast, the isomerization of formaldehyde was calculated to prefer the rotational to the inversion transition state, regardless of polarization functions.

Vibrational Frequencies. Table I summarizes the HF/6-31G* harmonic vibrational frequencies and the associated zero-point energeis for equilibrium and transition structures. Since the silanone structure is likely to be observed in the near future, our discussion focuses on the theoretical prediction of its infrared spectrum.

It is now well known that frequencies calculated at the HF level are generally overestimated[23]. For a set of 36 one- and two-heavy atom molecules, for example Hehre et al.[24] reported that HF/6-31G* frequencies are on the average 1.126 times as large as experimental (anharmonic) frequencies[25] and that the errors are relatively constant allowing systematic corrections to be made. In view of this fact, the predicted frequencies ($\nu_{calc}/1.126$) for silanone are presented in Table II. The Si=O stretching mode is expected to be actually observed near 1203 cm^{-1} and to be ~600 cm^{-1} lower than the C-O stretching mode in formaldehyde. In an experimental attempt to assign absorption peaks, information on the isotopic frequency shifts is often useful. Thus, the predicted shifts upon deuteration and oxygen-18 substitution are also given in Table II. The Si=O stretching frequency is predicted to be shifted in the following

way; 1195 cm^{-1} for HDSiO, 1187 cm^{-1} for D_2SiO, 1162 cm^{-1} for $H_2Si^{18}O$, 1153 cm^{-1} for $HDSi^{18}O$, and 1146 cm^{-1} for $D_2Si^{18}O$. The isotopic shifts are relatively small compared with those of the remaining vibrational modes in silanone.

Recently, the infrared spectrum of hydroxysilylene was observed[12]. In Table III, the observed frequencies are compared with our predicted ones ($\nu_{calc}/1.126$). It is interesting to notice a good agreement between them.

Energies. The total energies of the H_2SiO species were calculated at several levels of theory, using the HF/6-31G* structures. These results are listed in Table IV. The relative energies are given in Table V. The energy profile at the CI(S+C+QC)/6-31G** level is schematically shown in Fig.4. The energy values with zero-point correction are also given in this figure.

Pople et al[16a]. calculated the corresponding energy profile of the H_2CO species at the MP4/6-31G** level using both MP2/6-31G* and HF/6-31G* structures[26]. In order to facilitate comparison, nevertheless, our CI(S+D+QC)/6-31G** values based on the HF/6-31G* structures by Pople et al. are shown in Fig.4. At this point, it may be of value to make a brief comparison of CI and MP relative energies. As Table VI shows, CI(S+D+QC) values agree very well (to within 0.7 kcal/mol) with MP4 values, indicating that the effect of unlinked clusters can be corrected with Davidson formula[21]. In addition, CI(S+D) values are in reasonable agreement with MP3 values, except for the discrepancy of 1.5 kcal/mol in the relative energy of the isolated molecules H_2 + CO. A portion of the discrepancy may be

ascribable to the size-inconsistency problem inherent in singly and doubly excited CI.

Fig.4 reveals several interesting similarities and differences between the energy profiles of silanone and formaldehyde. To simplify the following discussion we emphasize the vibrationally corrected values in Fig.4 which may correspond to experimental values at 0 K.

The first point to be noted in Fig.4 is that the enrgy difference between $H_2Si=O$ and HSiOH(trans) is as small as 2.4 kcal/mol, which is in distinct contrast to the much larger energy difference (53.9 kcal/mol) favoring $H_2C=O$ over HCOH(trans). As calculated for $H_2Si=CH_2$[27] and $H_2Si=SiH_2$[28], the small energy difference between the double bonded and the divalent species is a general feature of silicon compounds, and indicates that silicon is reluctant to form doubly bonded compounds.

To assess the stability of the silicon-oxygen double bond, the energies released upon the addition of H_2 to $H_2Si=O$ and $H_2C=O$ were calculated at the same level of theory. As Table VII shows, the hydrogenation energy of silanone is twice as large as that of formaldehyde. This result suggests that the Si=O bond is considerably less stable in a thermodynamic sense than the C=O bond.

In the interest in isolating the silanone structure, more important is the magnitude of energy barrier between silanone and the more stable trans-hydroxysilylene. The barrier is 26.1 kcal/mol smaller as compared with that between $H_2C=O$ and HCOH(trans), but still as large as 60.8 kcal/mol. This finding suggests that silanone is kinetically stable to 1,2-hydrogen shift. Here, one may suspect

that there still remain two possible pathways for the unimolecular destruction of silanone, i.e., the molecular and radical dissociations which lead to H_2 + SiO and H + HSiO, respectively. As Fig.4 shows, the former reaction must proceed with a sizable barrier of 85.8 kcal/mol while the energy required for the latter reaction was expected to be more than 85 kcal/mol[29]. These results confirm that silanone is sufficiently stable in a kinetic sense despite its thermodynamic instability. In addtion, one should note that the relative stability of silanone and hydroxysilylene can be dramatically reversed when hydrogens were replaced by substituents such as fluorine, as demonstrated in our recent theoretical study[10].

As for the divalent species $H\ddot{S}iOH$ and $H\ddot{C}OH$, both are calculated to be more stable in the trans form than in the cis form. In either case the enrgy difference in favor of the trans form is rather small (0.3 kcal/mol for HSiOH and 4.7 kcal/mol for HCOH). As already discussed, the trans to cis isomerizations of the divalent species prefer rotation to inversion. The rotational barriers calculated for HSiOH and HCOH are 9.3 and 28.0 kcal/mol, respectively. It is noteworthy that the latter value is quite sizable and three times as large as the former. The large barrier for the isomerization of HCOH was explained by Goddard and Schaefer[15a] in terms of π bonding between C and O. The view that the CO bond contains some double bond character comes from the fact that its bond length increases by $\sim$0.04 Å at the rotationary transition state in which the CH and OH bonds are nearly orthogonal. To the extent that Goddard and Schaefer's view is valid, there is no appreciable change in the

SiO bond length on rotation about the SiO bond of HSiOH (see Figs. 1 and 3). Furthermore, it is interesting to note that the shortening of ~0.1 Å is seen in the CO bond length on going from H_3COH to HCOH while the SiO bond length is essentially constant from H_3SiOH to HSiOH. Thus, it is not surprising that the rotational barrier for hydroxysilylene is calculated to be small. These results are compatible with the experimental observation in the low temperature matrix isolation study[12]; upon warming up slightly cis-hydroxysilylene converts to the more stable trans isomer.

We return to the 1,2-hydrogen shift and molecular dissociation of silanone and speculate on the possible formation of H_2 and SiO. Although, as pointed out, the energies required for the two reactions are both sizable (60.8 and 85.8 kcal/mol), the former parthway leading to HSiOH(trans) is available at a lower energy than is the latter to H_2 + SiO. As Fig.4 shows, the reactions subsequent to the more facile 1,2-hydrogen shift are HSiOH(trans) → HSiOH(cis) → H_2 + SiO. The transition states for the subsequent reactions lie in energy considerably below that for the 1,2-hydrogen shift. This suggests that when the 1,2-hydrogen shift occurs it is likely to be followed by generation of H_2 and SiO via the transiency of hydroxysilylene. In contrast, the 1,2-hydrogen shift and molecular dissociation of formaldehyde seem to compete with each other since the barriers for those reactions are comparable.[30] Even if the 1,2-hydrogen shift takes place, a considerable, additional energy is required to surmount the barrier for HCOH(cis) → H_2 + CO.

In case of formaldehyde it appears that H_2 and CO are directly formed by the molecular dissociation.

Reaction of silanone with water

As demonstrated, silanone is certainly the existing species at an energy minimum separated by sizable barriers from its isomers. We are now in a position to provide insight into the reactivity toward reagents such as water.

In Fig.5 are shown the ORTEP drawings of an intermediate complex, the product silanediol, and the transition state connecting them, which were located at the HF/6-31G* level for the reaction of silanone with water. The geometrical parameters and total energies calculated are summarized in Table VIII. Because of the size of the reaction system, electron correlation was incorporated through the MP3/6-31G* scheme. In this regard, it is advisable to refer to MP and CI relative energies in Tavle VI. For comparison, the reaction of formaldehyde with water was also calculated at the same level of theory[31]. These results are summarized in Fig.6 and Table IX.

As Fig.6 and Table IX show, water approaches with an angle of $\angle O1CO2=89.4^{\circ}$ and complexes formaldehyde at large intermolecular separations (C-O2=2.911 Å and O1-H3=2.643 Å). Both reactants undergo no significant changes in their structures. In the C_s symmetry-like complex formed, the H_2O moiety is almost coplanar with the C-O1 carbonyl bond. With the progression of approach of the H_2O moiety (i.e., the large decreases of ~1.3 Å in the C-O2 and O1-H3 distances), the complex reaches a four-center-like transition state which leads to the product methanediol. At the transition state, atoms O2, C, O1,

and H3 form an essentially planar four-membered ring with a dihedral angle of ∠H301C02=-0.1°. As a dihedral angle of ∠H402C01=106.1° shows, however, the non-reacting hydrogen H4 of the H_2O moiety now lies out of the planar ring in a fashion that one of lone pairs of H_2O is oriented for maximum nuclophilic interaction with the carbonyl π* orbital. On passing through the C_1 symmetry transition state, the dihedral angle H402C01 decreases from 106.1 to 60.3° while the dihedral angle H301C02 increases from -0.1 to 60.3°, these leading to the product methanediol with C_2 symmetry.

In contrast, Fig.5 and Table VIII reveals that water complexes silanone at much closer separation distances (for instance, Si-02= 2.006 Å) with a larger approaching angle of ∠01Si02=98.4°. Reflecting the closer separation, several significant structural changes are seen in both reactants. Among them, it is interesting to note that the reacting hydrogen H3 of the H_2O moiety lies approximately in the 01-Si-02 plane, as characterized by the dihedral angle of ∠H301Si02= 1.7°. However, the remaining hydrogen H4 of the H_2O moiety lies strongly below the 01-Si-02 plane (∠H402Si01=112.3°). That is, even for the structure of complex, C_1 symmetry is calculated to be already preferred slightly (2.7 kcal/mol at the MP3/6-31G* level) over C_s symmetry for stronger nucleophilic interaction between water and silanone. The C_1 symmetry complex is transformed to a four-center-like transition state by approximately clockwise rotations of the H_2O moiety about 02 and Si in the 01-Si-02 plane, as characterized by the following representative changes. On going from the complex to transition state, the Si02H3 and 01Si02 angles decrease by 22.5°

(from 99.7 to 77.2) and 14.7° (from 98.4 to 83.7), respectively, while the SiO2 distance changes only by 0.159 Å (from 2.006 to 1.847). The transition state with C_1 symmetry is converted to the product silanediol in C_2 symmetry via a process similar to that described for the $H_2O + H_2C{=}O$ reaction.

In Fig.7 are schematically shown the energy profiles calculated at the MP3/6-31G* level. Obviously, the energy profile for the $H_2O + H_2Si{=}O$ reaction differs markedly from that for the $H_2O + H_2C{=}O$ reaction. Silanone complexes water with a stabilization energy of 21.1 kcal/mol much more strongly than does formaldehyde with a stabilization of 3.7 kcal/mol. The $H_2O + H_2SiO$ complex proceeds across a small barrier of 4.8 kcal/mol, through the transition state which resembles the complex in structure, to the silanediol product. In contrast, the $H_2O + H_2CO$ complex must surmount a much larger barrier of 42.8 kcal/mol to reach the methanediol product. The products silanediol and methanediol are 72.6 and 16.3 kcal/mol more stable, respectively, than the reactants. That is, the $H_2O + H_2Si{=}O$ reaction is calculated to be 56.3 kcal/mol more exothermic than the $H_2O + H_2C{=}O$ reaction. Reflecting the large difference in exothermicity, the former reaction gives rise to the "earlier" transition state than does the latter reaction (Figs.5 and 6).

A most important finding is that the reaction of silanone proceeds without an overall barrier, indicative of the very high reactivity of the silicon-oxygen double bond. The high reactivity seems to be one of reasons why it is not easy to detect experimentally silanones. On the other hand, the reaction of formaldehyde undergoes a sizable

overall barrier of 42.8 kcal/mol. It appears that the following factors are responsible for the great difference in reactivity between silanone and formaldehyde. First, the double bond in silanone ($H_2Si^{+0.94}=O^{-0.68}$) is more strongly polarized than that in formaldehyde ($H_2C^{+0.14}=O^{-0.42}$). The strong dipolar character in the Si=O bond enhances the electrostatic interaction with polar reagents such as water. Second, the frontier orbital π (-12.3 eV) and π^* (1.5 eV) energy levels of silanone are considerably higher and lower, respectively, than the π (-14.7 eV) and π^* (4.0 eV) levels of formaldehyde. Undoubtedly, the lower-lying π^* orbital of silanone makes much more facile the attack of nucleophilic reagents such as water. In addition, silanone is also more reactive toward electrophilic reagents, because of the higher-lying π orbital. In the reactions with nonpolar reagents the frontier orbital interaction (i.e. charge transfer interaction) may be more significant than the electrostatic interaction. Anyhow, it is reasonable to say that in Klopman's terminology[32] the higher reactivity of silanone is "frontier-controlled" as well as "charge-controlled", as emphasized in our recent study on the reactions of silene, germene, and disilene.[11c-11e] Both "frontier" and "charge" factors would play an important role in the future design of a kinetically more stable substituted silanone.

Concluding Remarks

The conclusions from the present calculations on silanone chemistry may be summarized as follows:

(1) Silanone ($H_2Si=O$) lies at a minimum of the potential energy

surface, which is the existing species separated by sizable barriers from its isomers.

(2) The Si=O stretching frequency is predicted to be ~1203 cm^{-1} and its isotopic shifts are relatively small.

(3) Silanone is slightly less stable than its 1,2-hydrogen shifted isomers hydroxysilylenes (trans and cis). The small energy difference reflects that silicon is reluctant to form doubly bonded compounds.

(4) Despite the certain strength of p_π- p_π bonding, the silicon-oxygen double bond is considerably less stable in a thermodynamic sense than the carbon-oxygen double bond.

(5) Of the three pathways considered for the unimolecular destruction of silanone, the lowest energy route is the 1,2-hydrogen shift. However, the calculated barrier height is sizable (60.8 kcal/mol), suggesting that silanone itself is kinetically stable to the unimolecular destruction.

(6) Silanone reacts with water with no overall barrier, indicative ot the very high reactivity of the silicon-oxygen double bond toward polar reagents.

Acknowledgment. All calculations were carried out at the Computer Center of the Institute for Molecular Science, using the IMSPAK (WF10-9)[33] and GAUSSIAN 80 (WF10-25)[34] programs in the IMS Computer Center library program package.

References and Notes

(1) For recent comprehensive reviews, see: (a) Gusel'nikov, L.E.; Nametkin, N.S. Chem. Rev. 1979, 79, 529. (b) Coleman, B.; Jones, M. Rev. Chem. Intermed. 1981, 4, 297. (c) Schaefer, H.F. Acc. Chem. Res. 1982, 15, 283.

(2) (a) Brook, A.G.; Abdesaken, F.; Gutekunst, B.; Gutekunst, G.; Kallury, R.K. J. Chem. Soc., Chem. Commun. 1981, 191. (b) Brook, A.G.; Kallury, R.K.M.R.; Poon, Y.C. Organometallics 1982, 1, 987. (c) Brook, A.G.; Nyburg, S.C.; Abdesaken, F.; Gutekunst, B.; Gutekunst, G.; Kallury, P.K.M.R.; Poon, Y.C.; Chang, Y.-N.; Wong-Ng, W. J. Am. Chem. Soc. 1982, 104,5667.

(3) (a) West, R.; Fink, M.J.; Michl, J. Science(Washington, D.C.) 1981, 214, 1343. (b) Masamune, S.; Hanzawa, Y.; Murakami, S.; Bally, T.; Blount, J.F. J. Am. Chem. Soc. 1982, 104, 1150. (c) Boudjouk, P; Han, B.-H.; Anderson, K.R. J. Am. Chem. Soc. 1982, 104, 4992.

(4) Tomadze, A.V.; Yablokova, N.V.; Yablokov, V.A.; Razuvaev, G.A. J. Organomet. Chem. 1981, 212, 43.

(5) (a) Davidson, I.M.T.; Thompson, J.F. J. Chem. Soc., Chem. Commun. 1971, 251. (b) Davidson, I.M.T.; Thompson, J.F. J. Chem. Soc., Faraday Trans 1 1975, 2260.

(6) (a) Soysa, H.S.D.; Okinoshima, H.; Weber, W.P. J. Organomet. Chem. 1977, 133, C17. (b) Alnaimi, I.S.; Weber, W.P. J. Organomet. Chem. 1983, 241, 171.

(7) (a) Roark, D.N.; Sommer, L.H. J. Chem. Soc., Chem. Commun. 1973, 167. (b) Barton, T.J.; Kilgour, J.A. J. Am. Chem. Soc.

1974, 96, 2278. (c) Golino, C.M.; Bush, R.D.; On, P.; Sommer, L.H. J. Am. Chem. Soc. 1975, 97, 1957. (d) Sekiguchi, A.; Migita, T. J. Am. Chem. Soc. 1975, 97, 7159. (e) Golino, C.M.; Bush, R.D.; Sommer, L.H. J. Am. Chem. Soc. 1975, 97, 7371. (f) Barton, T.J.; Kilgour, J.A. J. Am. Chem. Soc. 1976, 98, 7231. (g) Ishikawa, M.; Fuchikami, T.; Kumada, M. J. Am. Chem. Soc. 1977, 99, 245. (h) Ando, W.; Ikeno, M.; Sekiguchi, A. J. Am. Chem. Soc. 1977, 99, 6447. (i) Barton, T.J.; Hoekman, S.K.; Burns, S.A. Organometallics 1982, 1, 721. (j) Ando, W.; Sekiguchi, A.; Sato, T. J. Am. Chem. Soc. 1982, 104, 6830. (k) Märkl, G.; Horn, M. Tetrahedron Lett. 1983, 24, 1477. (l) Hussmann, G.; Wulff, W.D.; Barton, T.J. J. Am. Chem. Soc. 1983, 105, 1263. (m) Barton, T.J.; Hussmann, G.P. Organometallics 1983, 2, 692.

(8) Fink, M.J.; DeYoung, D.J.; West, R.; Michl, J. J. Am. Chem. Soc. 1983, 105, 1070.

(9) Jaquet, R.; Kutzelnigg, W.; Staemmler, V. Theoret. Chim. Acta (Berl.) 1980, 54, 205.

(10) Kudo, T.; Nagase, S. J. Organomet. Chem., 1983, 253, C23.

(11) (a) Hanamura, M.; Nagase, S.; Morokuma, K. Tetrahedron Lett. 1981, 22, 1813. (b) Kudo, T.; Nagase, S. Chem. Phys. Lett. 1981, 84, 375. (c) Nagase, S.; Kudo, T.; J. Mol. Struct., a special issue of THEOCHEM in honor of Prof. Fukui and his Nobel Prize awarded in chemistry, 1983, 103, 35. (d) Nagase, S.; Kudo, T. J. Chem. Soc., Chem. Commun. 1983, 363. (e) Nagase, S. ; Kudo, T. Organometallics, in press. (f) Nagase, S.; Kudo, T.

J. Chem. Soc., Chem. Commun., in press.

(12) Ismail, Z.K.; Hauge, R.H.; Fredin, L.; Kauffman, J.W.; Margrave, J.L. J. Chem. Phys. 1982, 77, 1617.

(13) For the preliminary calculations, see ref.10.

(14) Jaffe, R.L.; Morokuma, K. J. Chem. Phys. 1976, 64, 4881.

(15) (a) Goddard, J.D.; Schaefer, H.F. J. Chem. Phys. 1979, 70, 5117. (b) Goddard, J.D.; Yamaguchi, Y.; Schaefer, H.F. J. Chem. Phys. 1981, 75, 3459.

(16) (a) Harding, L.B.; Schlegel, H.B.; Krishnan, R.; Pople, J.A. J. Phys. Chem. 1980, 84, 3394. (b) Frisch, M.J.; Krishnan, R.; Pople, J.A. J. Phys. Chem. 1981, 85, 1467.

(17) Adams, G.F.; Bent, G.D.; Bartlett, R.J.; Purvis, G.D. J. Chem. Phys. 1981, 75, 834.

(18) Kemper, M.J.H.; Hoeks, C.H.; Buck, H.M. J. Chem. Phys. 1981, 74, 5744.

(19) (a) Hehre, W.J.; Ditchfield, R.; Pople, J.A. J. Chem. Phys. 1972, 56, 2257. (b) Hariharan, P.C.; Pople, J.A. Theor. Chim. Acta 1973, 28, 213. (c) Francl, M.M.; Pietro, W.J.; Hehre, W.J. ; Binkley, J.S.; Gordon, M.S.; DeFrees, D.J.; Pople, J.A. J. Chem. Phys. 1982, 77, 3654. (d) Olbrich, G. Chem. Phys. Lett. 1980, 73, 110.

(20) Pople, J.A.; Binkley, J.S.; Seeger, R. Int. J. Quantum Chem., Quantum Chem. Symp. 1976, 10, 1.

(21) (a) Langhoff, S.R.; Davidson, E.R. Int. J. Quantum Chem. 1974, 8, 61. (b) Davidson, E.R.; Silver, D.W. Chem. Phys. Lett. 1978, 52, 403.

(22) DeFrees, D.J.; Levi, B.A.; Pollack, S.K.; Hehre, W.J.; Binkley, J.S.; Pople, J.A. J. Am. Chem. Soc. 1979, 101, 4085.

(23) Yamaguchi, Y.; Schaefer, H.F. J. Chem. Phys. 1980, 73, 2310.

(24) Hout, R.F.; Levi, B.A.; Hehre, W.J. J. Comput. Chem. 1982, 3, 234.

(25) A portion of the discrepancy arises from the fact that the calculated frequencies refer to strictly harmonic vibrations, as comparison with experimental harmonic frequencies shows a smaller average deviation[24].

(26) It is noteworthy that the use of HF/6-31G* structures introduces errors of only ~1 kcal/mol in the relative energies.

(27) (a) Gordon, M.S. Chem. Phys. Lett. 1978, 54, 9. Gordon, M.S.; J. Am. Chem. Soc. 1982, 104, 4352. (b) Goddard, J.D.; Yoshioka, Y.; Schaefer, H.F. J. Am. Chem. Soc. 1980, 102, 7644. Yoshioka, Y.; Schaefer, H.F. J. Am. Chem. Soc. 1981, 103, 7366. (c) Trinquier, G.; Malrieu, J.-P. J. Am. Chem. Soc. 1981, 103, 6313. (d) Köhler, H.J.; Lischka, H. J. Am. Chem. Soc. 1982, 104, 5884.

(28) (a) Snyder, L.C.; Wasserman, Z.R. J. Am. Chem. Soc. 1979, 101, 5222. (b) Poirier, R.A.; Goddard, J.D. Chem. Phys. Lett. 1981, 80, 37. (c) Lischka, H.; Köhler, H.J. Chem. Phys. Lett. 1982, 85, 467. (d) Krogh-Jespersen, K. J. Phys. Chem. 1982, 86, 1492. Krogh-Jespersen, K. Chem. Phys. Lett. 1982, 93, 327.

(29) Since the radical dissociation was calculated to be 85 kcal/mol endothermic, we did not locate actually the transition state for the present purpose.

(30) At the highest level of theory, it is calculated by Pople et al.[16b] that the barrier for the molecular dissociation is 1.8 kcal/mol smaller than that for the 1,2-hydrogen shift.

(31) For the calculations at the HF/STO-3G and HF/4-31G levels, see (a) Williams, I.H.; Spangler, D.; Femec, D.A.; Maggiora, G.M.; Schowen, R.L. J. Am. Chem. Soc. 1980, 102, 6619. (b) Williams, I.H.; Maggiora, G.M.; Schowen, R.L. J. Am. Chem. Soc. 1980, 102, 7831.

(32) (a) Klopman, G. J. Am. Chem. Soc. 1968, 90, 223. (b) Klopman, G. "Chemical Reactivity and Reaction Paths"; John Wiley: New York, 1974; PP55-165.

(33) Morokuma, K.; Kato, S.; Kitaura, K.; Ohmine, I.; Sakai, S.; Obara, S. IMS library program NO.372, 1980.

(34) An IMS version of the GAUSSIAN 80 series of programs by Binkley, J.S.; Whiteside, R.A.; Krishnan, R.; Seeger, R.; DeFrees, D.J.; Schlegel, H.B.; Topiol, S.; Kahn, L.R.; Pople, J.A. QCPE 1981, 10, 406.

Table I: HF/6-31G* Vibrational Frequencies(cm^{-1}) and Zero Point Energies(kcal/mol)

	frequencies	zero point
equilibrium structures[a]		
H_2	4643(σ_g)	6.6
SiO	1408(σ)	2.0
HSiO	755(a'), 865(a'), 2156(a')	5.4
H_2SiO	787(b_1), 812(b_2), 1125(a_1), 1356(a_1), 2432(b_1), 2433(a_1)	12.8
HSiOH (cis)	665(a"), 829(a'), 924(a'), 1070(a'), 2109(a'), 4130(a')	13.9
HSiOH (trans)	704(a"), 876(a'), 924(a'), 1052(a'), 2205(a'), 4124(a')	14.1
transition structures[b]		
A	2391i(a'), 634(a"), 700(a'), 1275(a'), 1438(a'), 2387(a')	9.2
B	2540i(a'), 769(a'), 1192(a'), 1282(a"), 1718(a'), 2019(a')	10.0
C	2086i, 318, 867, 1178, 2135, 2267	9.7
D	738i, 479, 921, 964, 2116, 4191	12.4

a For the structures, see Fig.1

b For each of the transition structures, the first frequence is the imaginary reaction coordinate frequency, which is neglected in the zero-point summation. For the structures, see Fig.3

Table II: Predicted Vibrational Frequencies(cm^{-1}) of silanone and its Isotopomers[a]

symmetry and mode	H_2SiO	HDSiO	D_2SiO	$H_2Si^{18}O$	$HDSi^{18}O$	$D_2Si^{18}O$
a_1 SiH_2 s-stretch	2160	2160	1555	2160	2160	1553
a_1 SiO stretch	1203	1195	1187	1162	1153	1146
a_1 SiH_2 scis.	1000	903	720	997	900	718
b_1 SiH_2 a-stretch	2159	1159	1563	2159	1558	1563
b_1 SiH_2 rock	699	581	543	695	577	539
b_2 SiH_2 wag	721	642	552	719	641	551

a Frequencies corrected for a factor of 1.126(see text)

Table III: Comparison between Observed[a] and Calculated[b] Frequencies (cm^{-1}) of trans-Hydroxysilylene.

Vibrational mode	Obs.	Calc.
ν_1(OH)	3650	3662
ν_2(SiH)	1872	1958
ν_3(HSiO)	937	934
ν_4(SiO)	851	819
ν_5(SiOH)	723	778
ν_6(torsion)	659	625

a Taken from Ref.12

b Corrected for a factor of 1.126

Table IV: Total Energies(hartrees) Based on HF/6-31G* Geometries

species	6-31G*	6-31G**		
	HF	HF	CI(S+D)	CI(S+D+QC)
H_2 + SiO	-364.90567	-364.91020	-365.18716	-365.21496
H_2SiO	-364.91440	-364.91754	-365.18699	-365.21097
HSiOH(cis)	-364.92168	-364.93005	-365.19309	-365.21603
HSiOH(trans)	-364.92213	-364.93041	-365.19381	-365.21686
H_3SiOH(stag.)	-366.13040	-366.14191	-366.42743	-366.45124
A	-364.74413	-364.75303	-365.03748	-365.06853
B	-364.81792	-364.83003	-365.10965	-365.13718
C	-364.78491	-364.79050	-365.07773	-365.10909
D	-364.90654	-364.91561	-365.17671	-365.19926

Table V: Relative Energies(kcal/mol) Based on HF/6-31G* Geometries

species	6-31G*	6-31G**		
	HF	HF	CI(S+D)	CI(S+D+QC)
H_2SiO	0.0	0.0	0.0	0.0
H_2 + SiO	5.5	4.6	-0.1	-2.5
HSiOH(cis)	-4.6	-7.9	-3.8	-3.2
HSiOH(trans)	-4.9	-8.1	-4.3	-3.7
A	106.8	103.2	93.8	89.4
B	60.5	54.9	48.5	46.3
C	81.3	79.7	68.6	63.9
D	4.9	1.2	6.5	7.3

Table VI: Comparison of Relative Energies(kcal/mol) from MP/6-31G** and CI/6-31G** Calculations Based on HF/6-31G* Geometries[a]

species	MP3	MP4	CI(S+D)	CI(S+D+QC)
H_2CO	0.0	0.0	0.0	0.0
H_2 + CO	5.2	2.8	3.7	3.4
HCOH(cis)	59.5	59.6	58.8	59.1
HCOH(trans)	54.3	54.4	53.6	54.0
$H_2CO \rightarrow H_2+CO$[b]	98.2	95.5	99.3	95.5
$HCOH(cis) \rightarrow H_2+CO$[b]	—	—	119.8	117.3
$H_2CO \rightarrow HCOH(trans)$[b]	93.6	91.0	93.7	91.3
$HCOH(trans) \rightarrow HCOH(cis)$[b]	85.1	85.5	84.2	84.8

a MP values from Ref.16a. CI values from this work.

b Transition states

Table VII: Comparison of Hydrogenation Energies(kcal/mol) of Silanone and Formaldehyde Based on HF/6-31G* Geometries

	H_2SiO	H_2CO
HF/6-31G**	58.4	28.6
CI(S+D)/6-31G**	51.1	28.6
CI(S+D+QC)/6-31G**	48.1	26.9

Table VIII: Structures and Total Energies Calculated for the Reaction of H_2SiO with H_2O

	complex	transition state	product
bond distances, bond angles, and dihedral angles[a]			
Si01	1.514	1.559	1.642
Si02	2.006	1.847	1.642
SiH1	1.472	1.466	1.468
SiH2	1.478	1.472	1.468
01H3	2.453	1.419	0.947
02H3	0.959	1.119	—
02H4	0.953	0.952	0.947
01Si02	98.4	83.7	112.5
01SiH1	123.8	122.5	111.3
01SiH2	123.7	122.0	104.9
Si01H3	68.5	76.3	118.6
Si02H3	99.7	72.2	—
Si02H4	117.1	120.8	118.6
H1Si0102	-104.3	-105.6	-117.3
H2Si0102	100.8	103.5	121.1
H301Si02	1.7	-1.2	64.6
H402Si01	112.3	109.5	64.5
total energies in hartrees[b]			
HF/6-31G*	-440.95742	-440.94347	-441.04790
MP3/6-31G*[c]	-441.41682	-441.40928	-441.49890

a HF/6-31G* structures in angstroms and degrees. For the numberings of atoms, see Fig.5. b Total energies of reactants are -440.92515 (HF/6-31G*) and -441.38327(MP3/6-31G*). c Calculated at the HF/6-31G* structures.

Table IX: Structures and Total Energies Calculated for the Reaction of H_2CO with H_2O

	complex	transition state	product
bond distances, bond angles, and dihedral angles[a]			
C01	1.187	1.294	1.386
C02	2.911	1.639	1.386
CH1	1.090	1.083	1.083
CH2	1.090	1.087	1.083
O1H3	2.643	1.324	0.949
O2H3	0.948	1.149	—
O2H4	0.947	0.953	0.949
O1C02	89.4	93.3	112.4
O1CH1	122.1	119.6	111.8
O1CH2	122.2	119.5	105.8
C01H3	84.6	77.2	108.8
C02H3	73.5	69.2	—
C02H4	179.5	114.0	108.8
H1C0102	-90.3	-105.7	-118.8
H2C0102	89.7	108.6	122.2
H301C02	-0.1	-0.1	60.3
H402C01	-36.2	106.1	60.3
total energies in hartrees[b]			
HF/6-31G*	-189.88240	-189.79842	-189.90063
MP3/6-31G*[C]	-190.37960	-190.31138	-190.39962

a HF/6-31G* structures in angstroms and degrees. For the numberings of atoms, see Fig.6. b Total energies of reactants are -189.87708 (HF/6-31G*) and -190.37366(MP3/6-31G*). c Calculated at the HF/6-31G* structures.

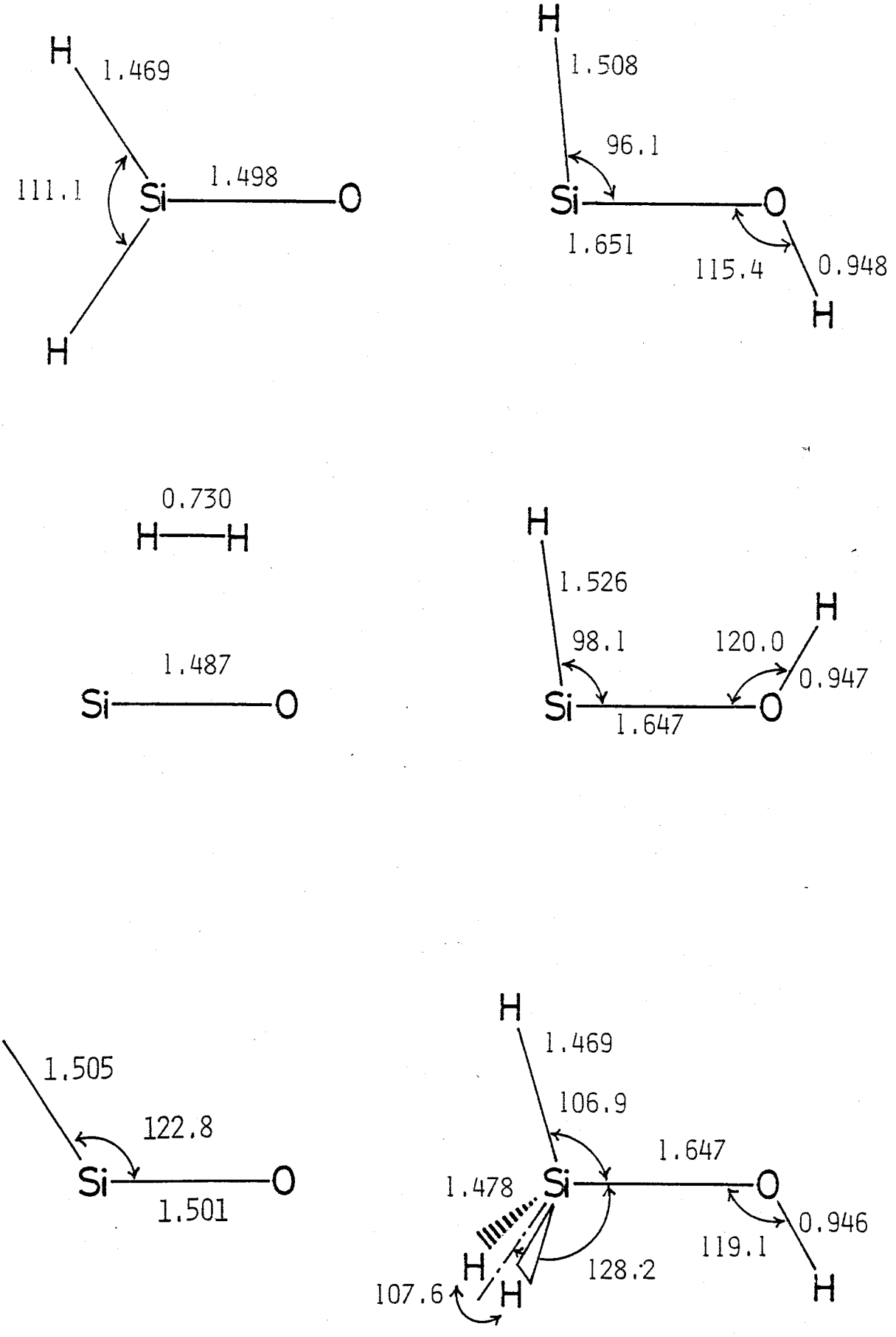

Figure 1. Equilibrium structures in angstroms and degrees calculated at the HF/6-31G*.

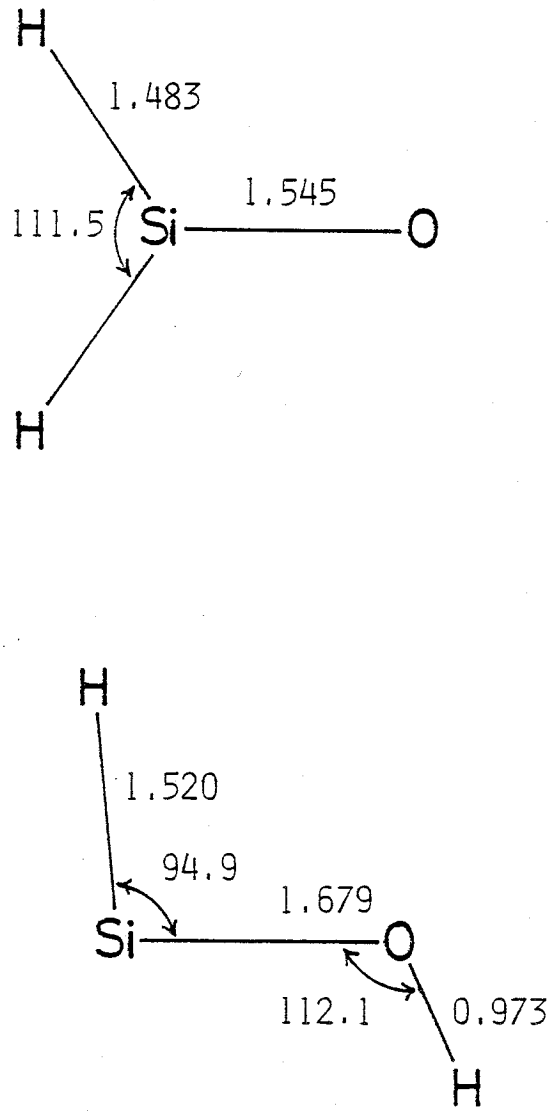

Figure 2. MP2/6-31G* structures of silanone and trans-hydroxysilylene in angstroms and degrees.

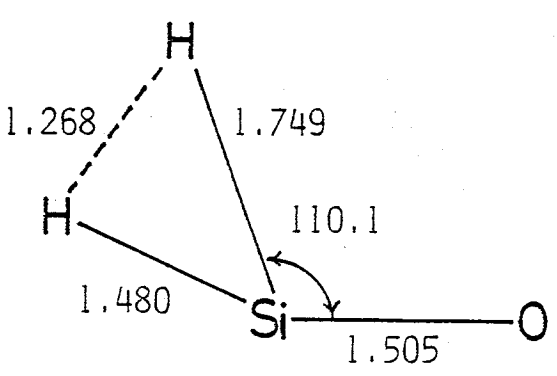

A

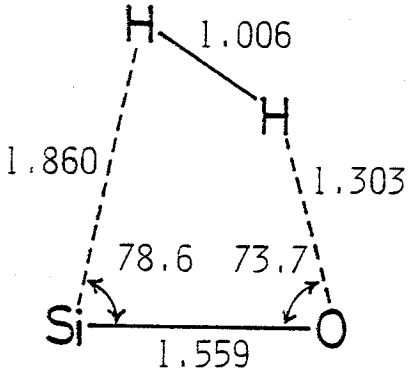

B

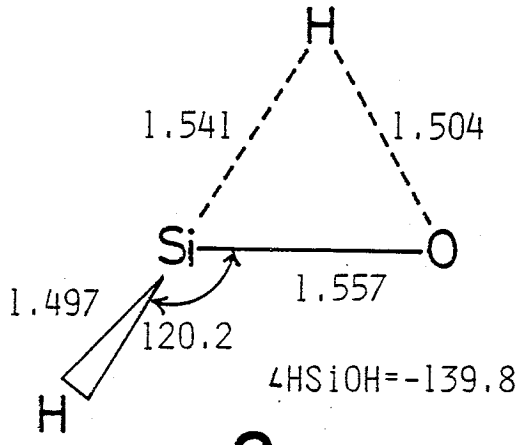

C

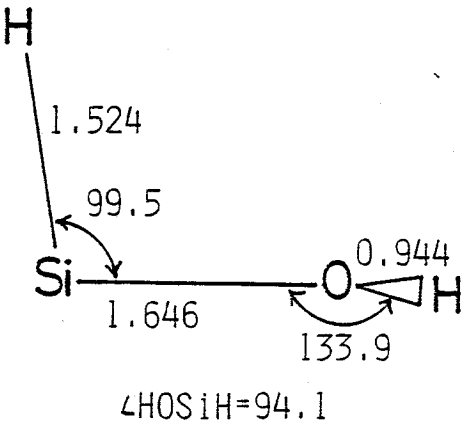

D

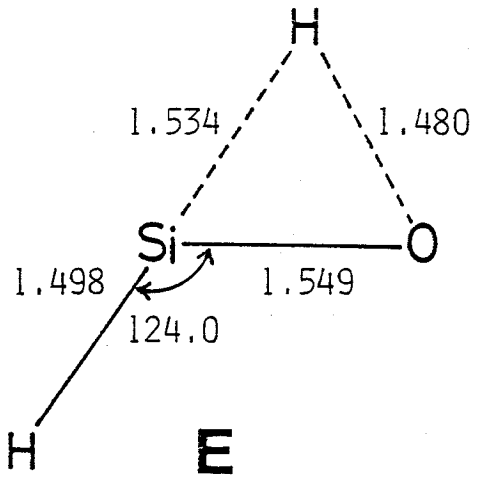

E

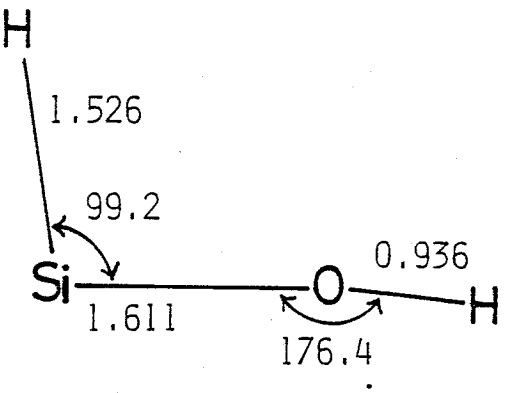

F

Figure 3. Transition structures in angstroms and degrees at the HF/6-31G* level. A, B, C, and D are true transition states. E and F are stationary points with two imaginary vibrational frequencies (see text for detailes).

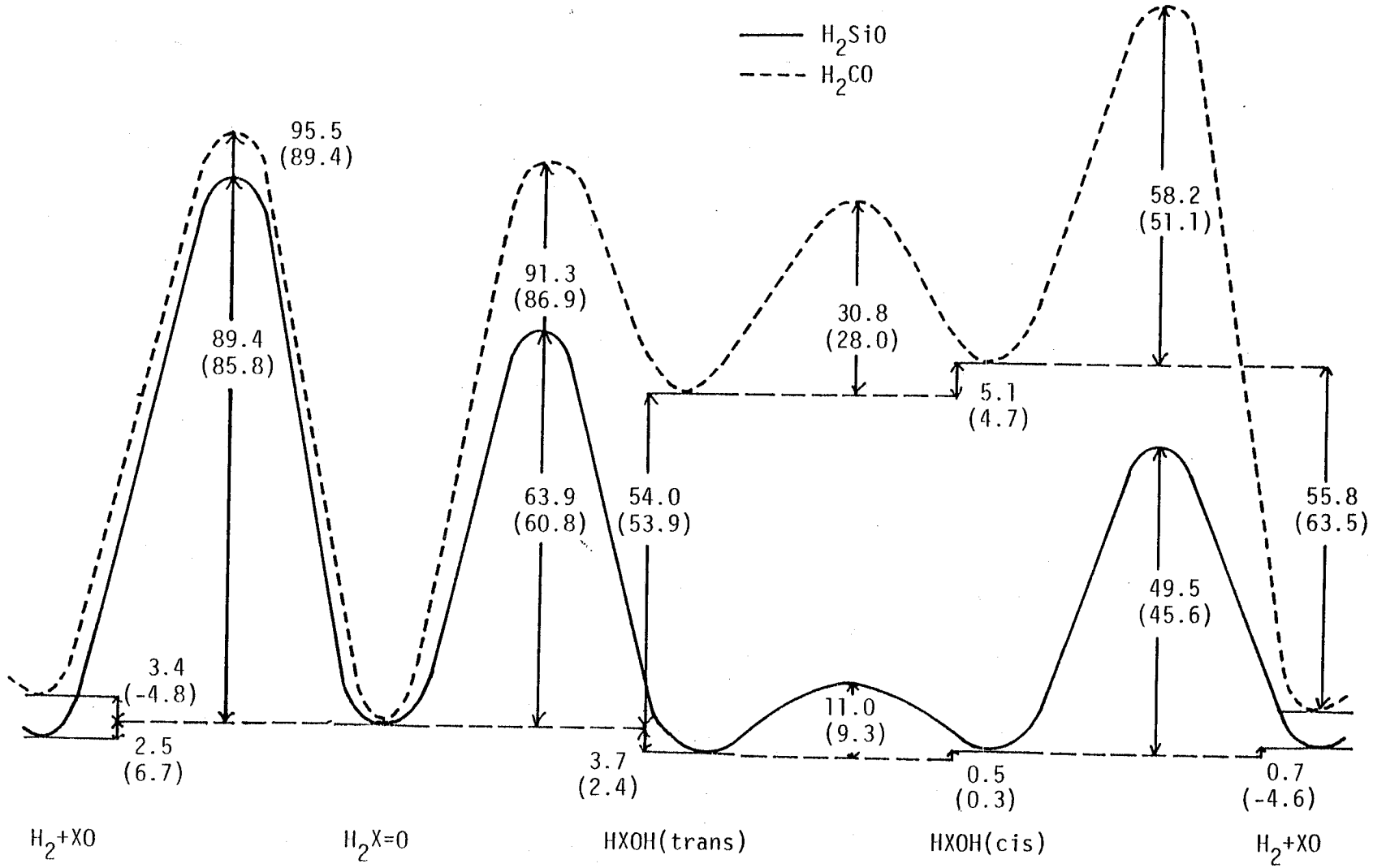

Figure 4. Schematic comparison of energy profiles of H_2SiO(full line) and H_2CO(dotted line). Relative energies in kcal/mol are CI(S+D+QC)/6-31G** values calculated at the HF/6-31G* geometries. The values in parenthesis are corrected for zero-point vibrational energies. The zero-point energies for the H_2CO species are taken from ref.16a.

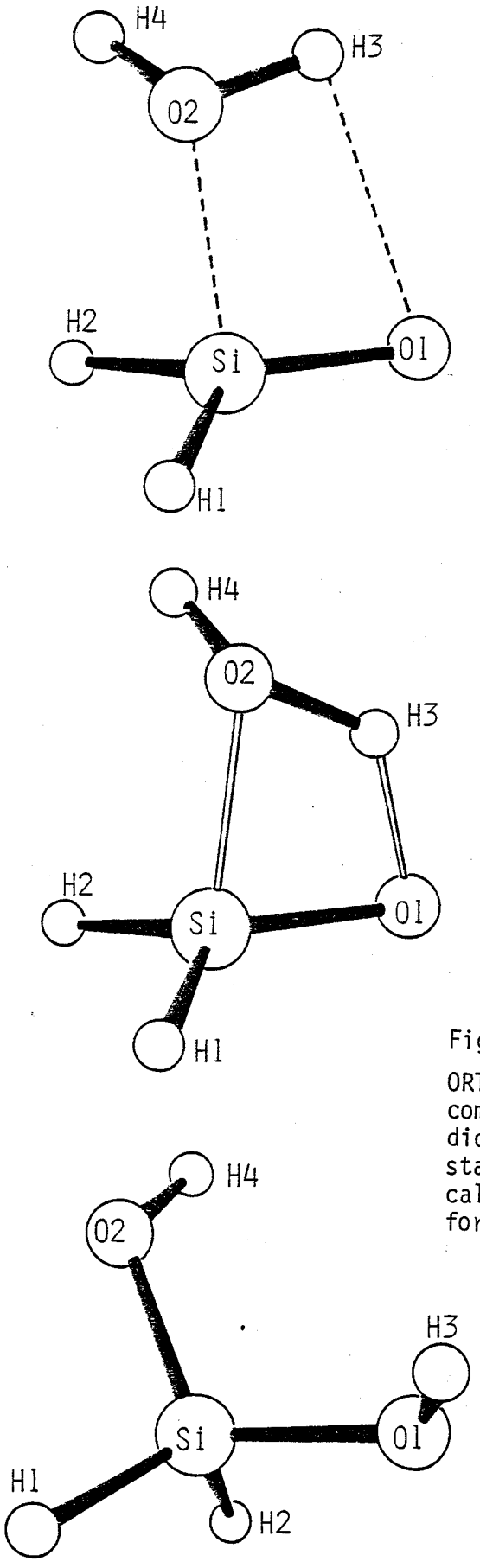

Figure 5.

ORTEP drawings of an intermediate complex(top), the product silanediol(bottom), and the transition state(middle) connecting them, calculated at the HF/6-31G* level for the H_2O + H_2SiO reaction.

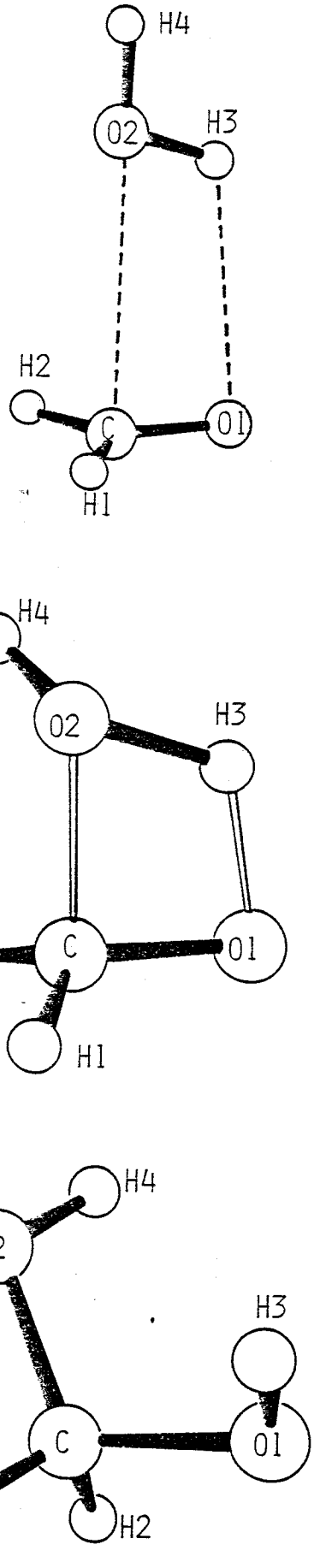

Figure 6.

ORTEP drawings of a intermediate complex(top), the product methanediol(bottom), and the transition state(middle) connecting them, calculated at the HF/6-31G* level for the H_2O + H_2CO reaction.

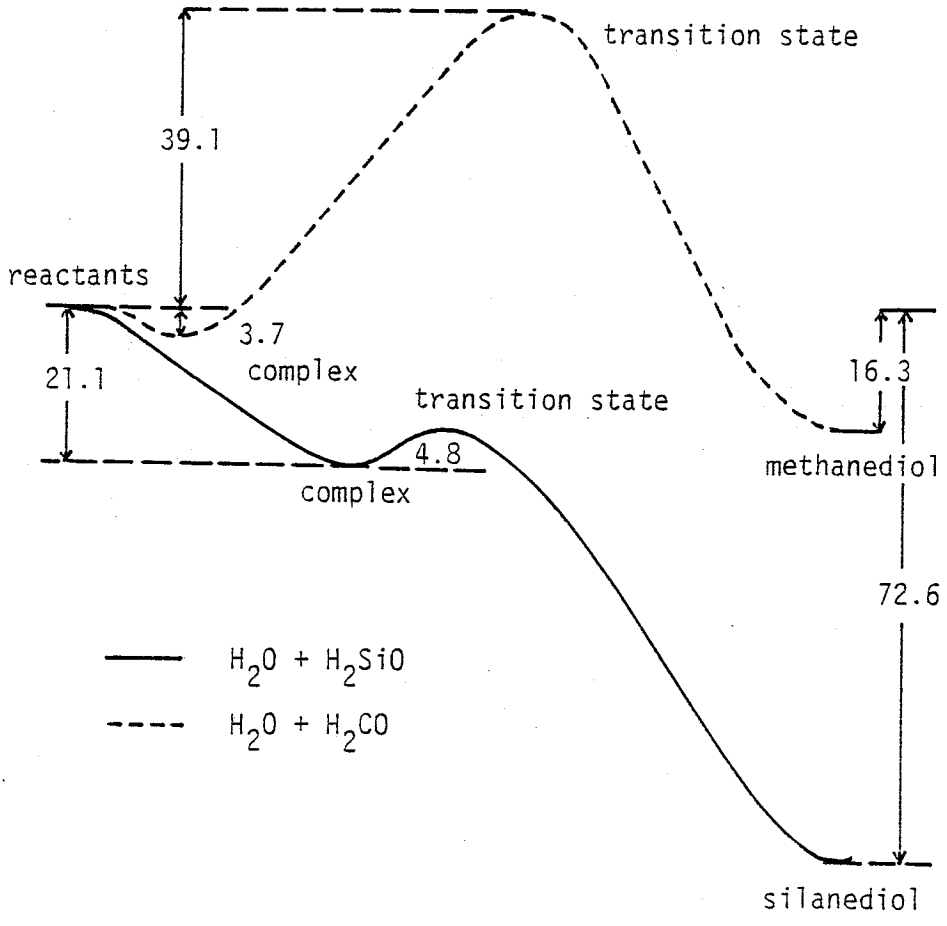

Figure 7. Energy profiles(kcal/mol) at the MP3/6-31G* level at the $H_2O + H_2SiO$(full line) and $H_2O + H_2CO$(dotted line) reactions.

CHAPTER 2

Effects of Fluorine Substitution on the Thermodynamic Stability

In view of intense current interest in a silicon-oxygen double bond, the singlet potential energy surface of H_2SiO has been explored through ab initio calculations, which is found to differ significantly from the H_2CO potential energy surface. Also examined are the effects of fluorine substitution on the relative stabilities of H_2SiO and its isomers.

For many years π-bonded silicon intermediates have attracted a great deal of attention in organosilicon chemistry[1]. Now that compounds containing silicon-carbon[2,3] or silicon-silicon[4,5] double bonds can be synthesized and isolated at room temperature, it is inevitable that considerable attention is directed toward the preparation of silicon-oxygen doubly bonded compounds, silanones. Although schemes for the synthesis of silanones have been devised, up to now only indirect evidence is available which suggests the transient existence[6]. We here report preliminary studies of the singlet potential energy surface of H_2SiO and the effects of fluorine substitution on the silicon-oxygen double bond. The reactions considered are (1a) the hydrogen elimination and (1b) the isomerization to hydroxysilylene.

$$H_2SiO \longrightarrow H_2 + SiO \qquad (1a)$$

$$H_2SiO \longrightarrow H\ddot{S}iOH \qquad (1b)$$

In this work, stationary points on the potential energy surface were located with the 3-21G[7] SCF analytical gradient technique and characterized by calculating routinely their harmonic vibrational frequencies. The harmonic frequencies obtained at this level were used to compute zero-point vibrational energies. Following the full optimizations of stationary point geometries, additional single-point calculations were carried out with electron correlation incorporated through configuration interaction(CI) or third-order Møller-Plesset perturbation(MP3) theory[8], using the larger 6-31G** basis set[9], these being denoted by CI/6-31G**//3-21G or

MP3/6-31G**//3-21G. In the correlation calculations, all single(S) and double(D) substitutions were included, with the restriction that the core-like orbitals (1s,2s and 2p for Si, 1s for O and F in character) were excluded. The final CI energies were obtained by adding the Davidson correction[10] to allow for unlinked cluster quadruple correction(QC).

A schematic energy profile and transition state geometries for the reactions (1a) and (1b) are presented in Figure 1. For comparison the analogous reactions (2a) and (2b) of H_2CO were also calculated at the same level of theory and the results are included in the figure.

$$H_2CO \longrightarrow H_2 + CO \qquad (2a)$$

$$H_2CO \longrightarrow H\ddot{C}OH \qquad (2b)$$

Although our interest is at the characteristic comparison of H_2SiO with H_2CO, the present energy values for H_2CO are very close to those obtained previously with more sophisticated calculations[11-13].

Comparing H_2SiO with H_2CO, the following similarities and differences are worth mentioning. (i) Both hydrogen elimination reactions (1a) and (2a) are slightly exothermic and undergo considerable energy barriers of 84.9 and 88.7 kcal/mol, respectively. The "widths" of the barriers, as characterized by the imaginary (reaction coordinates) vibrational frequencies of 2292i and 2212i cm^{-1}, were comparable to each other. The transition states for these reactions are planar with both hydrogens on the same side of the SiO or CO bond axis. (ii) For the isomerization of the doubly bonded to the divalent species, the reaction (2b) is 54.2 kcal/mol

endothermic while the reaction (1b) is only 2.2 kcal/mol exothermic. This small energy difference between $H_2Si{=}O$ and HSiOH is a distinct feature of silicon compounds. As for the divalent species, both HSiOH and HCOH were calculated to be 0.3 and 4.4 kcal/mol more stable in the trans conformer than in the cis form. The energies required from the trans to the cis were 9.5 and 28.0 kcal/mol for HSiOH and HCOH, respectively. (iii) As shown in Figure 1, the isomerization of H_2SiO to HSiOH(trans) prefers a non-planar transition state with the HOSiH dihedral angle of 116.5°, while the corresponding reaction of H_2CO proceeds via a planar transition state. The imaginary frequencies of 1912i and 2705i cm^{-1} calculated for these transition states indicate that the former reaction gives rise to the larger "width" of the barrier than does the latter. The barrier height for the isomerization $H_2SiO \rightarrow$ HSiOH(trans) is 26.2 kcal/mol smaller than that for $H_2CO \rightarrow$ HCOH(trans), but still as large as 60.3 kcal/mol. These suggest that H_2SiO is sufficiently stable to isomerization.

In Figure 2 are shown the effects of fluorine substitution on the relative stabilities of silanones and hydroxysilylenes. It should be noted that the relative stabilities of the doubly bonded and the divalent species are dramatically reversed when hydrogens were replaced by fluorines. The effect of difluoro substitution is of special interest since it strongly stabilizes silanone relative to hydroxysilylene. In case of monofluoro substitution, HFSiO is more stable than HSiOF, but less stable than FSiOH. These effects of fluorine substitution are explained most probably in terms of the strength of the Si-F bonds. In addition, fluorine substitution causes

the shortening of the silicon-oxygen double bond lengths (Å); 1.559 for H_2SiO, 1.542 for HFSiO and 1.534 for F_2SiO. Thus, it appears that fluorine substitution strengthens the Si=O double bond, as far as bond energy - bond length relationships are valid.

The present work predicts that silanone itself is at the deep bottom of the potential energy surface and can be strongly stabilized in a thermodynamical sense with a proper choice of substituents. According to our preliminary calculations, however, silanone is even more reactive than are silene ($H_2Si=CH_2$) and disilene ($H_2Si=SiH_2$). In view of the interest in isolating a silicon-oxygen double bond, it is important to search for the substituents which reduce the high reactivity. A theoretical study along this line is in progress in our group.

Acknowledgment. All calculations were carried out at the Computer Center of the Institute for Molecular Science, using the center library programs IMSPAK (WF10-9), GAUS80 (WF10-25), and GUGACI (WF10-21).

References

1 L.E. Gusel'nikov and N.S. Nametkin, Chem. Rev., 79 (1979) 529.

2 A.G. Brook, F. Abdesaken, B. Gutekunst, G. Gutekunst and R.K. Kallury, J. Chem. Soc., Chem. Commun., (1981) 191.

3 A.G. Brook, R.K.M.R. Kallury and Y.C. Poon, Organometallics, 1 (1982) 987.

4 R. West, M.J. Fink and J. Michl, Science, 214 (1981) 1343.

5 S. Masamune, Y. Hanzawa, S. Murakami, T. Bally, J.F. Blount, J. Am. Chem. Soc., 104 (1982) 1150.

6 For recent papers, A. Sekiguchi and W. Ando, J. Am. Chem. Soc., 103 (1981) 3579; A.V. Tomadze, N.V. Yablokova, V.A. Yablokov, G.A. Razuvaev, J. Organometal. Chem., 212 (1981) 43; T.J. Barton, S.K. Hoekmann, S.A. Burns, Organometallics, 1 (1982) 721; G. Hussmann, W.D. Wulff, T.J. Barton, J. Am. Chem. Soc., 105 (1983) 1263; I.S. Alnaimi, W.P. Weber, J. Organometal. Chem., 241 (1983) 171.

7 J.S. Binkley, J.A. Pople and W.J. Hehre, J. Am. Chem. Soc., 102 (1980) 939; M.S. Gordon, J.S. Binkley, J.A. Pople, W.J. Pietro and W.J. Hehre, J. Am. Chem. Soc., 104 (1982) 2797.

8 J.A. Pople, J.S. Binkley and R. Seeger, Int. J. Quantum Chem., Quantum Chem. Symp., 10 (1976) 1.

9 R. Ditchfield, W.J. Hehre and J.A. Pople, J. Chem. Phys., 54 (1971) 724; P.C. Hariharan and J.A. Pople, Theor. Chim. Acta, 28 (1973) 213; M.M. Francl, W.J. Pietro, W.J. Hehre, J.S. Binkley, M.S. Gordon, D.J. DeFrees and J.A. Pople, J. Chem. Phys., 77 (1982) 3654.

10 S.R. Langhoff and E.R. Davidson, Int. J. Quantum Chem., 8 (1974) 61; E.R. Davidson and D.W. Silver, Chem. Phys. Lett., 52 (1978) 403.

11 J.D. Goddard and H.F. Schaefer, J. Chem. Phys., 70 (1979) 5117; J.D. Goddard, Y. Yamaguchi and H.F. Schaefer, J. Chem. Phys., 75 (1981) 3459.

12 G.F. Adams, G.D. Bent, R.J. Barlett and G.D. Purvis, J. Chem. Phys., 75 (1981) 834.

13 L.B. Harding, H.B. Schlegel, R. Krishnan and J.A. Pople, J. Phys. Chem., 84 (1980) 3394; M.J. Frisch, R. Krishnan, and J.A. Pople, J. Phys. Chem., 85 (1981) 1467.

Figure 1. Schematic energy profiles and transition state geometries for the hydrogen elimination and isomerization reactions of H_2SiO and H_2CO. Relative energies in kcal/mol are CI(S+D+QC)/6-31G**//3-21G values with zero-point correction. Geometries are in angstroms and degrees. The arrows indicate the displacement vector of reaction coordinates at transition states.

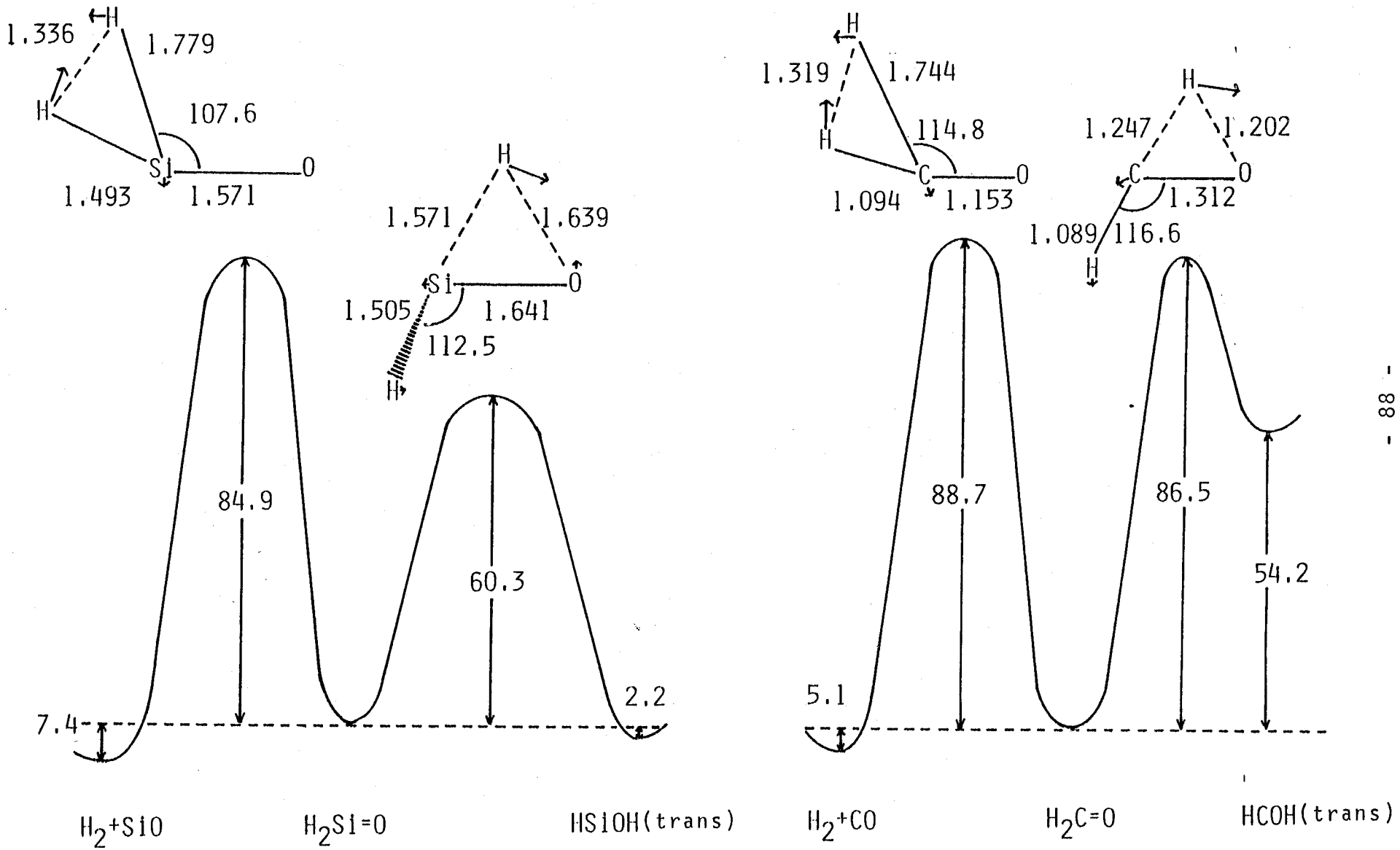

Figure 2. Relative energies of silanones and hydroxysilylenes. Energies in kcal/mol are MP3(S+D)/6-31G**//3-21G values without zero-point correction.

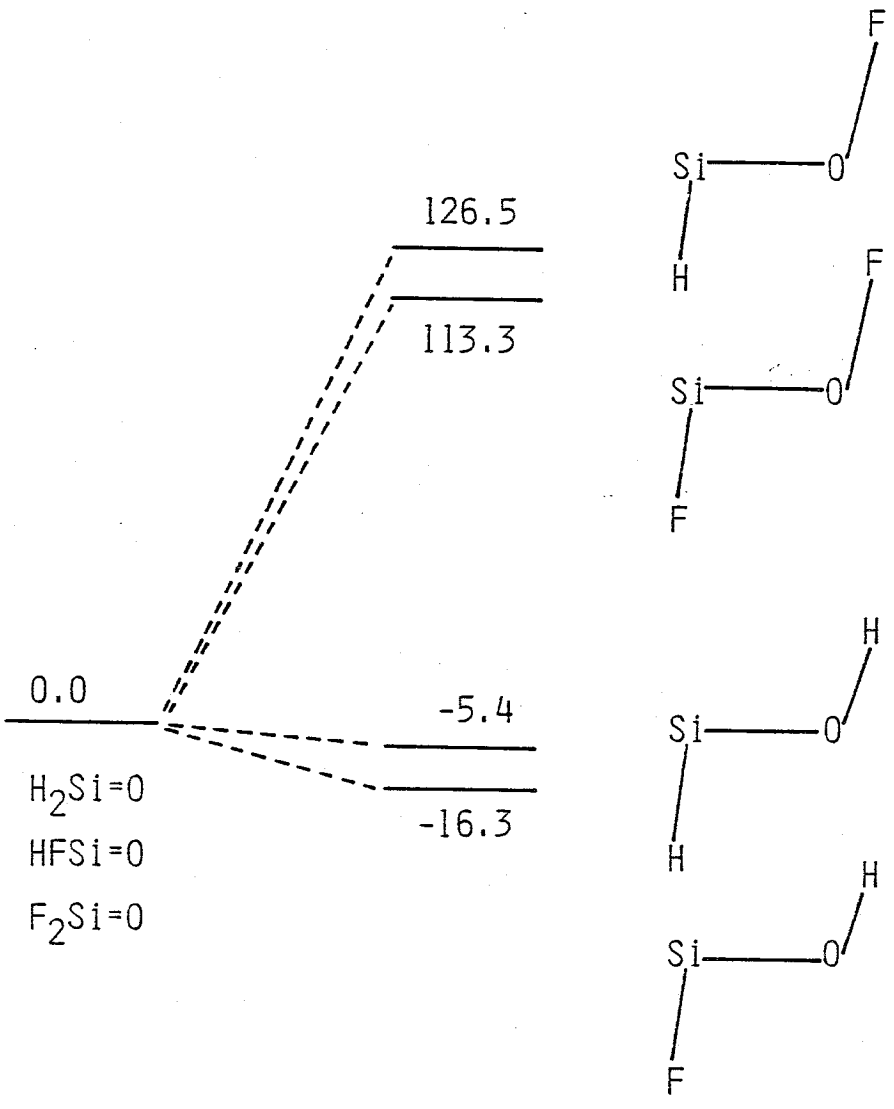

CHAPTER 3

The Dimerization of Silanone and the Properties of the Polymeric Products $(H_2SiO)_n$ (n = 2, 3, and 4)

In an attempt to extend knowledge of the reactivity of silicon-oxygen doubly bonded compounds (silanones), the potential energy surface of the dimerization of $H_2Si{=}O$ was investigated by means of ab initio molecular orbital calculations. The dimerization is found to proceed with no barrier to yield the cyclic product $(H_2SiO)_2$ by forming stepwise two new bonds. The structure, vibrational frequencies, and dimerization energy for the dimeric product $(H_2SiO)_2$ are compared with those for the similar cyclic dimers $(H_2SiS)_2$ and $(H_2CO)_2$ at the same level of theory. All these dimers have a planar four-membered ring with D_{2h} symmetry. The unusually short Si-Si distance in $(H_2SiO)_2$ is explained in terms of the greater affinity of silicon for oxygen. Also discussed are the structures and stability of the cyclic trimer $(H_2SiO)_3$ and tetramer $(H_2SiO)_4$.

There has currently been considerable interest in the possible existence of silicon-oxygen doubly bonded compounds, silanones.[1,2] Experimental evidence for the transient existence has accumulated in the last few years.[3] Since, however, most of the evidence is rather indirect, we have recently undertaken the theoretical studies of the thermodynamic and kinetic stability of the parent compound, $H_2Si{=}O$.[2,4] In an attempt to extend knowledge of the reactivity, we report here the first ab initio calculations of the reaction of two $H_2Si{=}O$ molecules to form the dimeric product cyclodisiloxane $(H_2SiO)_2$.

There has been active work on polymeric cyclosiloxanes $(R_2SiO)_n$, because of the practical importance. However, the lowest member (n=2) of the series is almost unknown and its chemistry is only recently starting to develop.[5] In view of the situation we tried to explore the structure, vibrational frequencies, and dimerization energy for the cyclic dimer $(H_2SiO)_2$ from a theoretical point of view. To characterize the properties of $(H_2SiO)_2$, we compared these results with those calculated for the similar cyclic dimers $(H_2SiS)_2$ and $(H_2CO)_2$ at the same level of theory. Also examined were the properties of the cyclic trimer $(H_2SiO)_3$ and tetramer $(H_2SiO)_4$.

Computational Details

All calculations were carried out for closed-shell singlets. Geometries were fully optimized at the Hartree-Fock (HF) level with

the split-valence 3-21G[6] and polarized 6-31G*[7] basis sets by using the analytical energy gradient technique. The harmonic vibrational frequencies obtained at the HF/3-21G level were used to compute zero-point vibrational energies. The effects of electron correlation were calculated by means of second-order Møller-Plesset perturbation (MP2) theory,[8] with all orbitals included except the corelike orbitals (1s,2s, and 2p for Si and S, and 1s for C and O in character). In this paper, notations like MP2/6-31G*//6-31G* denote a single-point calculation at the MP2/6-31G* level on the HF/6-31G* optimized geometry.

Results and Discussion

The Process of Dimerization Our primary concern is how the dimerization of $H_2Si{=}O$ proceeds and whether there is a significant barrier or not. For these purposes, we chose the parameter R which specifies the distance between the midpoints of two SiO bonds and defined this as the reaction coordinate.

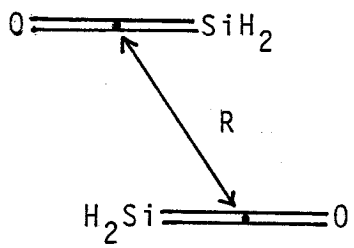

For the selected values of R the energy was minimized with respect to all other geometrical parameters by using the 3-21G analytical energy

gradients at the Hartree-Fock (HF) level.

Figure 1 shows the representative optimized geometries thus obtained along the reaction coordinate. As expected from the strongly polarized Si^{+}-O^{-} bond, at a large R the reaction path involves a "head to tail" coplanar-like approach of two $H_2Si{=}O$ molecules, $O^a{=}Si^aH_2$-------$O^b{=}Si^bH_2$. As the distance R decreases, the first molecule $H_2Si^a{=}O^a$ begins to rotate around the Si^a atom on the Si^b-O^b axis so as to cause a favorable overlap between the π^* orbital of $H_2Si^a{=}O^a$ localized strongly around Si^a and one of the lone pair orbitals of the second $H_2Si^b{=}O^b$ molecule (Figure 1a), resulting in the formation of a new Si^aO^b bond. With the further decrease of R, $H_2Si^a{=}O^a$ next rotates around the atom O^b in the vertical bisector plane of $H_2Si^b{=}O^b$ to develop a new bond between the atoms O^a (carring negative charge) and Si^b (carring positive charge) (Figures 1b and 1c), which leads to the cyclic product (Figure 1d). Thus, the dimerization involves the stepwise formation of two new bonds.

The changes in the potential energy along the reaction path are shown in Figure 2 as a function of R. Upon going from two $H_2Si{=}O$ monomers to the dimeric product, the energy decreases monotonously[9], there being no appreciable barrier to dimerization. To confirm this , we have carried out the larger 6-31G* basis set calculation at the 3-21G optimized geometries. As Figure 2 shows, the improvement of the basis set provides a more smooth energy decreasing, and again indicates that the dimerization proceeds without a barrier.[10] At this point, it is of interest to note that the reaction of two silicon monoxides to form the cyclic dimer $(SiO)_2$ have recently been

calculated to proceed with no barrier.[11] This suggests that the two hydrogen atoms in $H_2Si{=}O$ have no significant effect on the barrier to dimerization.

For comparison with the carbon analogue, we have calculated the reaction of two $H_2C{=}O$ molecules to form the cyclic dimer $(H_2CO)_2$ but found that it involves a high energy barrier due to orbital crossing at R ≒ 2.0 Å. The dimerization is formally a 2s + 2s forbidden reaction in terms of the Woodward-Hoffmann rule,[12] though symmetry-allowed. It is to be noted that the much more polarized frontier orbitals π (strongly localized around O) and π* (strongly localized around Si) of $H_2Si{=}O$ can relieve the symmetry restriction in the "head to tail" dimerization via a non-least-motion path shown in Figure 1.

Although we already found that the dimerization of $H_2Si{=}O$ proceeds with no barrier to yield the D_{2h} cyclic product, other structural alternatives were explored at the HF/3-21G level to answer the following questions : (i) are the SiO distances equal ? (ii) what are the preferred orientations of the SiH_2 groups ? (iii) is a "head to head" interaction between two SiO units possible ? (iv) is there a linear complex ?

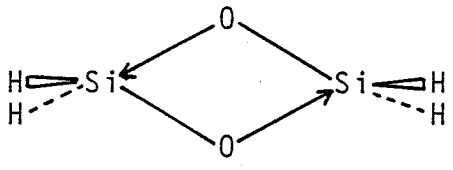

1

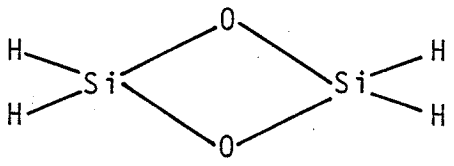

2

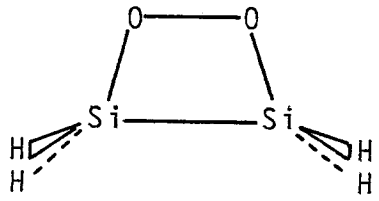

3

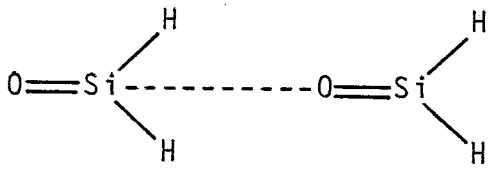

4

To answer (i), a C_{2h} structure 1 was adopted as a starting geometry. However, the geometrical optimization resulted in giving the more symmetrical D_{2h} structure (shown in Figure 1d) with all SiO distances equal. The same was true for the geometrical optimization at the HF/6-31G* level. To answer (ii), we have optimized an all-planar D_{2h} structure 2 and found it to be a stationary point. However, the force constant matrix for the stationary point gave rise to two negative eigenvalues. That is, 2 was a maximum with respect to the conrotatory and disrotatory motions of two SiH_2 groups, leading to the perpendicular arrangement shown in Figure 1d. As expected from the fact that 2 has eight π electrons (antiaromaticity), it was calculated to be 119.0 kcal/mol more unstable than the structure in Figure 1d. As for question (iii), we have undertaken a C_{2v} "head to head" structure 3. As characterized by all positive eigenvalues, the structure was indeed a minimum with the distances of OO=1.489 Å, SiSi=2.351 Å, and SiO=1.752 Å. However, it was found to be 127.2 (141.2 at the HF/6-31G*//3-21G level) kcal/mol more unstable than the structure in Figure 1d. In addition, 3 lies 16.9 kcal/mol above two separated $H_2Si{=}O$ molecules at the HF/6-31G*//3-21G level. This suggests that the "head to head" dimerization must undergo a considerable barrier. Finally, in order to answer (iv) as well as check if there is a true

coplanar approach at the early stage of the "head to tail" dimerization, we have examined a C_{2v} structure 4. By imposing C_{2v} symmetry, we found a stationary point at an intermolecular SiO distance of 3.1 Å, which was 7.1 kcal/mol more stable than two separated $H_2Si{=}O$ molecules. However, the force constant matrix revealed that the stationary point was a maximum which led to a non-coplanar structure shown in Figure 1a. This indicates that the "head to tail" dimerization involves a "coplanar-like" approach at the early stage but never takes a "exact" coplanar conformation.

Structures and Bonding The structure of the dimeric product $(H_2SiO)_2$ optimized at the HF/6-31G* level is shown in Figure 3. For comparison, the HF/6-31G* optimized structures of the cyclic dimers $(H_2SiS)_2$ and $(H_2CO)_2$ are also included in this figure. In the equilibrium structure of the dimer $(H_2SiO)_2$, the Si and O atoms alternate to make a planar four-membered ring with D_{2h} symmetry. It is not surprising that the Si-O bond length of 1.671 Å is comparable to the normal Si-O single bond length of 1.647 Å in silanol. However, the Si-O-Si and O-Si-O bond angles in the dimer are calculated to be highly strained to 91.5 and 88.5°, respectively, compared with the siloxane bond angle of 143 - 149°[13] in $H_3SiOSiH_3$ and the O-Si-O angle of 112.5°[2] in $HOSiH_2OH$. More interesting is the Si-Si distance[14] of 2.394 Å in the cyclic dimer that is only 0.041 Å longer than the Si-Si single bond length of 2.353 Å in disilane. The unusually short Si-Si distance seems to be characteristic of silicon compounds, as is apparent from the fact that the C-C distance in the cyclic dimer $(H_2CO)_2$ is calculated to be 0.414 Å longer at the HF/6-31G* level, as

shown in Fig.3c, than the C-C single bond length in ethane.

Very recently a stable cyclodisiloxane, tetramesitylcyclodisiloxane $(Mes_2SiO)_2$, has been produced from the reaction of tetramesityldisilene with atmospheric oxygen, and its structure has been determined by x-ray diffraction.[5] The four-membered ring in the x-ray crystal structure is not exactly planar but with a small dihedral angle of $\angle$ O-Si-Si-O = 6°. In addition, the SiO distances are not all equal in the crystal structure ; two of them are 1.66 Å (very close to our calculated value of 1.671 Å in $(H_2SiO)_2$) but the remaining two distances slightly lengthen to 1.72 Å most probably due to the bulky substituents. Interestingly, the Si-Si distance of 2.31 Å in $(Mes_2SiO)_2$ is further shorter by 0.084 Å than that in $(H_2SiO)_2$ and it is 0.159 Å shorter than the HF/6-31G* value of 2.469 Å[11] in the cyclic dimer $(SiO)_2$. This may suggest that substituents on silicon atoms are in part responsible for shortening of the Si-Si distance in the cyclic dimer.[15] Accompanied by the shortening of the Si-Si distance, the O-O distance increases ; 2.289 Å for $(SiO)_2$, 2.333 Å for $(H_2SiO)_2$, and 2.47 Å for $(Mes_2SiO)_2$. The increase in the O-O distance may be ascribed to the steric repulsion between the lone-pair orbitals on the oxygen atoms and the substituents on the silicon atoms. As a result, the cyclic dimer $(Mes_2SiO)_2$ becomes a rhombus where the Si-Si distance is rather shorter than the O-O distance, while the dimers $(SiO)_2$ and $(H_2SiO)_2$ have a rhomboid structure which is distorted in the opposite sense.

For the nature of bonding in the cyclic siloxane ring, one may consider two models (A) and (B).[5]

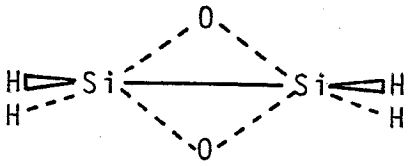

(A)

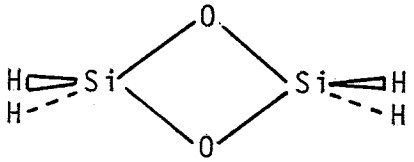

(B)

In model (A) there are a localized two-electron bond between the silicon atoms, leading to the short Si-Si distance, and a delocalized four-center six-electron bond about the periphery of the ring. Probably the most convenient procedure for seeing this possibility is the use of localized molecular orbitals since they provide the conventional picture of chemical bonding. The localized orbitals of $(H_2SiO)_2$ obtained by the Foster-Boys method[16] are shown in Figure 4. There are four equivalent SiH bonds and two equivalent lone pair orbitals on each oxygen. The lone pair orbitals are spatially directed above and below the planar ring, respectively, to make an angle of ca.120° with the ring. Noteworthy is a localized orbital description of bonding in the siloxane ring. Quite unlike model (A), no appreciable localized bond orbital is seen between the silicon atoms[17] and the ring is described as the arrangement of four equivalent localized SiO bonds. The centroids of the charge distributions of the localized SiO bond orbitals are shown in Figure 5. Each position of the centroids is much closer to O than to Si, reflecting the strong ionic character in the SiO bonds, but it is almost on the Si-O axis, indicating that there is no appreciable bent character in the SiO bonds. This finding is interesting since the formation of bent bonds has usually been seen in highly strained compounds.[18]

We now turn to model (B). In this model it is suggested[5] that severe lone pair-lone pair repulsions between the oxygen atoms are responsible for the short Si-Si distance. If this would be true, one should observe an unusual C-C distance even in $(H_2CO)_2$. As already pointed out, this is not the case. Although the importance of O-O repulsion cannot be ruled out, we do suggest[19] that the short Si-Si distance in cyclodisiloxane is the result of very strong attraction between the silicon and oxygen atoms. To demonstrate this, we have calculated the dimeric structure for silanethione $(H_2Si{=}S)$[20] because SiS bonds are less polarized and expected to be weaker than SiO bonds. As seen in Figure 3, the Si-Si distance of 2.858 Å in cyclodisilthiane $(H_2SiS)_2$ is 0.464 Å longer than that in $(H_2SiO)_2$. This results undoubtedly from the fact that sulfur has a much less affinity for silicon than does oxygen.[21]

In 1955 an electron diffraction structure was reported for tetramethylcyclodisilthiane $(Me_2SiS)_2$.[22] By using the assumed geometrical parameters for the methyl group parts, the distance of SiS=2.18 $\pm$ 0.03 Å and bond angles of $\angle$SiSSi=75 and $\angle$SSiS=105° were determined in the electron diffraction study. The determined values for the bond angles differ significantly from our calculated values in $(H_2SiS)_2$. In addition, the Si-Si distance in the electron diffraction structure seems too short compare to our calculated value in $(H_2SiS)_2$. However, one should note that the Si-Si distance of 2.65 Å[23] in $(Me_2SiS)_2$ is 0.34 Å longer than that in $(Mes_2SiO)_2$.

In a very recent report[24] on the x-ray structure it is found that the four-membered ring in $(Me_2SiS)_2$ is planar (D_{2h} symmetry) with the

distance of SiS=2.152 Å and bond angles of ∠SiSSi=82.5 and ∠SSiS=97.5°. These are all very close to our calculated results (SiS=2.150 Å, ∠SiSSi=83.3°, and ∠SSiS=96.7°) for $(H_2SiS)_2$. Furthermore, the Si-Si distance of 2.837 Å in the x-ray structure is in good agreement with our calculated value (2.858 Å) in $(H_2SiS)_2$, and 0.527 Å longer than that in $(Mes_2SiO)_2$.

Vibrational Frequencies Table I summarizes the HF/3-21G harmonic vibrational frequencies and zero-point energies for the cyclic dimers $(H_2SiO)_2$, $(H_2SiS)_2$, and $(H_2CO)_2$. The vibrational modes are schematically shown in Figure 6. To our knowledge no experimental values are available for comparison, but one may refer to two ring deformation frequencies 439-443 (b_{2u}) and 527-536 (b_{3u}) cm^{-1} assigned recently for tetramethylcyclodisilthiane.[25] These assigned values may be compared with our calculated values of 433 (b_{2u}) and 579 (b_{3u}) cm^{-1} for $(H_2SiS)_2$.

In Table I, the following points are noteworthy. First, the vibrational frequencies of the silicon-containing dimers $(H_2SiO)_2$ and $(H_2SiS)_2$ are generally much lower than those of $(H_2CO)_2$. When comparison is made between $(H_2SiO)_2$ and $(H_2SiS)_2$, ring deformation frequencies are higher in the former than in the latter, as is obvious from the comparison of the frequencies ν_5-ν_{11}. This suggests that the Si_2O_2 ring is rigid compared with the Si_2S_2 ring. In contrast, $(H_2SiO)_2$ and $(H_2SiS)_2$ have similar values for the frequencies associate with the SiH_2 part. Second, in all the dimers the lowest frequency corresponds to out-of plane distortion and the values are calculated to be as small as 253 cm^{-1} for $(H_2SiO)_2$, 109 cm^{-1} for

$(H_2SiS)_2$, and 234 cm^{-1} for $(H_2CO)_2$. This reveals that the planarity of the cyclic rings is loose. Third, the Si-Si stretching frequency (ν_2=608 cm^{-1}) of $(H_2SiO)_2$ is higher than that (ν_2=465 cm^{-1}) of $(H_2SiS)_2$, and it is comparable to the Si=Si stretching frequency (621 cm^{-1}) of a planar disilene ($H_2Si=SiH_2$).

Dimerization Energies The total energies of the monomers and dimers were calculated at several levels of theory. These results are given in Table II. The calculated dimerization energies are listed in Table III where entries are ordered according to the increasing quality of computation. The values with zero-point correction (ZPC) are also given in this table. The dimerization energy for $(H_2SiO)_2$ is relatively sensitive to the level of theory employed and it is overestimated by the smaller basis set probably due to the basis set superposition error. However, at all levels of theory there is a remarkable and general trend ; the dimerization energies increase dramatically in the order $(H_2CO)_2 < (H_2SiS)_2 < (H_2SiO)_2$, as expected from electrostatic[26] and frontier orbital[27] interactions.[28]

At the MP2/6-31G*//6-31G* level[29] the dimerization of $H_2Si=O$ is calculated to be 109.4 (104.0 after ZPC) kcal/mol exothermic and that of $H_2Si=S$ is 70.8 (67.7 after ZPC) kcal/mol exothermic. These high exothermicities result from the greater strength of four single bonds than two double bonds, indicating that silicon is reluctant to form double bonding. The much smaller exothermicity in the $H_2Si=S$ dimerization is the result of the cleavage of stronger SiS π bonds (compared with SiO π bonds)[20] as well as the formation of weaker SiS single bonds (compared with SiO single bonds). In contrast,

the dimerization of $H_2C{=}O$ is calculated to be rather endothermic by -0.2 (6.1 after ZPC) kcal/mol, because of the greater advantage in strength of the CO double over single bonds.

The dimerization energies are likely to be observed in the near future. In an attempt to predict theoretically the values, we have evaluated the thermodynamic quantities such as enthalpies (H), entropies (S), and Gibbs free energies (G) by using the HF/6-31G* geometries, MP2/6-31G*//6-31G* relative energies, and HF/3-21G vibrational frequencies. Based on the statistical treatment,[30] the molecular partition functions for translational, rotational, and vibrational motions (assumed to be separated) were calculated within the ideal gas, rigid rotor, and harmonic oscillator approximations. The enthalpy ($\Delta H°$) and entropy ($\Delta S°$) changes thus obtained at a standard state (pressure = 1 atom and temperature = 298 K) are given in Table IV where $\Delta S°$ is decomposed into translational ($\Delta S°_{trans}$), rotational ($\Delta S°_{rot}$), and vibrational ($\Delta S°_{vib}$) entropies.

It is interesting to note that the enthalpic stabilization and destabilization ($\Delta H°$) for dimerization are close to the zero-point corrected potential energy values given in Table III. This means that the effect of excited vibrational states (accounted for in $\Delta H°$) is rather minor, while zero-point correction is significant. Upon incorporation of two separated monomers into the dimer, the entropy ($S°$) decreases due to the loss of the translational ($S°_{trans}$) and rotational ($S°_{rot}$) entropies. However, the degree of the entropy decrease is essentially the same for all dimerizations, because of the structural resemblance. The silicon-containing dimers can compensate

the entropy cost by a large enthalpic stabilization, but $(H_2CO)_2$ cannot repay it because of the enthalpic destabilization. Finally, the Gibbs free energy changes for the dimerizations are calculated to be,

$2\ H_2Si{=}O \rightarrow (H_2SiO)_2 \quad \Delta G° = -92.1$ kcal/mol

$2\ H_2Si{=}S \rightarrow (H_2SiS)_2 \quad \Delta G° = -55.8$ kcal/mol

$2\ H_2C{=}O \rightarrow (H_2CO)_2 \quad \Delta G° = 17.1$ kcal/mol

Polymerization The formation of cyclic polymers is generally typical.[31] We are now in a possition to assess the structures and stability of the trimer $(H_2SiO)_3$ and the tetramer $(H_2SiO)_4$ with respect to those of the dimer $(H_2SiO)_2$. The calculated total energies of the trimer and tetramer are given in Table II. Because of the size of the molecules, our discussion is meant to be qualitative and interpretive rather than quantitative.

Figure 7 shows the HF/3-21G optimized structure of the cyclic trimer $(H_2SiO)_3$. The optimized structure has D_{3h} symmetry with alternate silicon and oxygen atoms arranged in a planar six-membered ring. The planarity of the Si_3O_3 ring has also been observed in the electron diffraction study of hexamethylcyclotrisiloxane $(Me_2SiO)_3$.[32] However, there also is a report[33] which claims that the Si_3O_3 ring deviates from planarity in the x-ray crystal structure. In order to see the degree of planarity of the ring, distortions to "boat" and "chair" forms were examined.

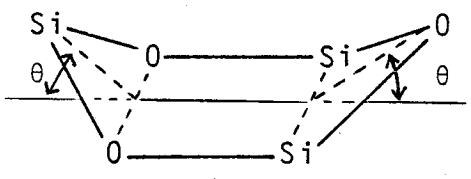

boat

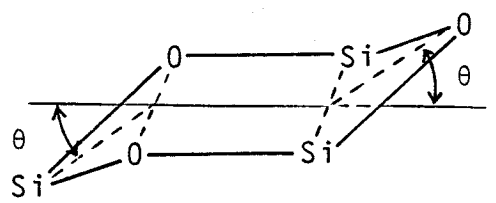

chair

In both distortions, Si and O atoms on the stern and prow were displaced with the angles of θ from the planar base of the remaining heavy atoms in the same direction for the boat and in the opposite direction for the chair. As Figure 8 shows, the "boat" and "chair" distortions undergo increasing destabilization. The increase in destabilization is smaller in the boat form than in the chair form at all the values of θ. This is ascribed to the more favorable electrostatic attraction between the stern and prow in the boat form. Even at the angle of θ=10° the destabilization due to the "boat" distortion is as small as 1.2 kcal/mol. Inclusion of d-type polarization functions on the Si and O atoms (i.e. HF/6-31G*//3-21G calculation) reduces the destabilization to 0.8 kcal/mol. This suggests that the ring is considerably flexible.

The Si-O-Si and O-Si-O angles of 137.7 and 102.3° in the trimer $(H_2SiO)_3$ are much larger (i.e. less constrained), respectively, than those in the dimer $(H_2SiO)_2$. Reflecting this, the disproportion energies for $3(H_2SiO)_2 \rightarrow 2(H_2SiO)_3$ are calculated to be -162.3 kcal/mol at the HF/3-21G level and -110.4 kcal/mol at the HF/6-31G*//3-21G level. These large nagative values clearly favor the trimer over the dimer.[34] Furthermore, the insertion of $H_2Si{=}O$ into the SiO bond of $(H_2SiO)_2$, $(H_2SiO)_2 + H_2Si{=}O \rightarrow (H_2SiO)_3$, is calculated to be 150.1 (HF/3-21G) and 117.3 (HF/6-31G*//3-21G) kcal/mol exothermic. These high exothermicities suggest that the ring expansion proceeds rapidly with no significant barrier.[35]

Figure 9 shows the HF/3-21G optimized structure of the tetramer $(H_2SiO)_4$ obtained by imposing D_{4h} symmetry.[36] The energy released upon

going from $4(H_2SiO)_3$ to $3(H_2SiO)_4$ is calculated to be 74.2 kcal/mol. At the HF/3-21G level this energy is 88.1 kcal/mol smaller than that from $3(H_2SiO)_2$ to $2(H_2SiO)_3$, suggesting that the formation of the tetramer is less favorable than the formation of the trimer. However, the tetramerization is likely to occur readily, as expected from the fact that the reactions $(H_2SiO)_3 + H_2Si{=}O \rightarrow (H_2SiO)_4$ and $(H_2SiO)_2 + (H_2SiO)_2 \rightarrow (H_2SiO)_4$ are calculated to be 120.8 and 132.9 kcal/mol exothermic, respectively, at the HF/3-21G level. To the extent that the difference in the exothermicity is meaningful, the tetramer may be produced more favorably by the reaction of two dimers than by the insertion of $H_2Si{=}O$ into the SiO bond of the trimer.[37]

Finally, it may be interesting to mention the net atomic charges and frontier orbital energies of $H_2Si{=}O$ and $(H_2SiO)_n$ (n=2-4). As Table V shows, with increasing "n" the silicon and oxygen atoms in $(H_2SiO)_n$ carry more positive and negative charges, respectively, than those in $H_2Si{=}O$. Accompanied by the increase in ionic character, the Si-O single bond distances in $(H_2SiO)_n$ decrease in the order 1.717(n=2) >1.667(n=3) >1.646(n=4) Å. This may suggest that the strength of the Si-O single bond increases with the increase in "n", as far as bond energy - bond length relationships are valid. As shown in Table V, the HOMO energy levels of $H_2Si{=}O$ and $(H_2SiO)_n$ are essentially the same. With increasing "n", however, the LUMO levels of $(H_2SiO)_n$ become much higher than that of $H_2Si{=}O$. This indicates that $(H_2SiO)_n$ becomes less reactive toward nucleophiles[38] with the increase in the size of the ring in terms of frontier orbital theory.

Concluding Remarks

The dimerization of $H_2Si{=}O$ proceeds with no barrier along a non-least-motion path to yield the cyclic "head to tail" dimer $(H_2SiO)_2$ by forming stepwise two new bonds. The equilibrium structure of the dimeric product has D_{2h} symmetry with alternate silicon and oxygen atoms in a planar four-membered ring. The unusually short Si-Si distance in the ring is explained in terms of the strength of the SiO bonds and the less severe exchange repulsion between the Si atoms. The dimerization energy for $(H_2SiO)_2$ is calculated to be much larger than those for the similar cyclic dimers $(H_2SiS)_2$ and $(H_2CO)_2$. Finally, it is found that trimerization and tetramerization are both more favorable than dimerization and very likely to proceed with no appreciable barrier.

Acknowledgment

We are grateful to Professor R. West for bringing the unusual structure of cyclodisiloxane to our attention and for making ref.5 available prior to publication. All calculations were carried out at the Computer Center of the Institute for Molecular Science by using the IMSPAK(WF10-9)[39] and GAUSSIAN80(WF10-25)[40] programs in the IMS Computer Center library program package.

References and Notes

(1) For a review, see: Gusel'nikov, L.E.; Nametkin, N.S. Chem. Rev. 1979, 79, 529.

(2) Kudo, T.; Nagase, S. J. Phys. Chem. 1984, 88, 2833.

(3) See a number of references summarized in refs 1 and 2.

(4) Kudo, T.; Nagase, S. J. Organomet. Chem. 1983, 253, C23. See also: Gordon, M.S.; George, C. J. Am. Chem. Soc. 1984, 106, 609.

(5) Fink, M.J.; Haller, K.J.; West, R.; Michl, J. J. Am. Chem. Soc. 1984, 106, 822.

(6) Binkley, J.S.; Pople, J.A.; Hehre, W.J. J. Am. Chem. Soc. 1980, 102, 939. Gordon, M.S.; Binkley, J.S.; Pople, J.A.; Pietro, W.J.; Hehre, W.J. J. Am. Chem. Soc. 1982, 104, 2797.

(7) Hariharan, P.C.; Pople, J.A. Theor. Chim. Acta (Berl.) 1973, 28, 213. Francl, M.M.; Pietro, W.J.; Hehre, W.J.; Binkley, J.S.; Gordon, M.S.; DeFrees, D.J.; Pople, J.A. J. Chem. Phys. 1982, 77, 3654.

(8) Møller, C.; Plesset, M.S. Phys. Rev. 1934, 46, 618. Pople, J.A.; Binkley, J.S.; Seeger, R. Int. J. Quantum Chem., Quantum Chem. Symp. 1976, 10, 1.

(9) One sees that the HF/3-21G energy curve changes somewhat irregularly at the distances of R = 2.8-3.2 Å. In fact, in the region we managed to locate a complex and a transition state whose structure were very similar to each other, at the HF/STO-3G level. The transition state was calculated to be only 0.3 kcal/mol as unstable as the complex. However, the complex and transition state are found to be quite artificial for the use of the minimal basis set and disappear at the HF/3-21G as well as HF/6-31G* level.

(10) The choice of the midpoint-to-midpoint distance (R) as the reaction coordinate clearly establishes the lack of a barrier in the dimerization. Since, however, the choice is somewhat arbitrary, there may be other purely downhill paths and the interpretation of Figure 1 may be one possible picture.

(11) Snyder, L.C.; Raghavachari, K. J. Chem. Phys. 1984, 80, 5076.

(12) Woodward, R.B.; Hoffmann, R. "The Conservation of Orbital Symmetry", Academic Press, New York, N.Y., 1969.

(13) For the experimental values of 144.1 and 149°, see: Almenningen, A.; Bastian, O.; Ewing, V.; Hedberg, K.; Traetteberg, M. Acta Chim. Scand. 1963, 17, 2455. Durig, J.R.; Flanigan, M.J.; Kalasinsky, V.F. J. Chem. Phys. 1977, 66, 2775. For the calculated value of 143.3°, see: Oberhammer, H.; Boggs, J.E. J. Am. Chem. Soc. 1980, 102, 7241.

(14) To see the effect of the d-type polarization functions on the Si-Si distance, the structure of $(H_2SiO)_2$ was also optimized by omitting either d(Si) or d(O) functions. The omissions of d(Si) and d(O) functions lengthened the Si-Si distance to 2.470 and 2.440 Å, respectively. This indicates that d(Si) and d(O) functions are equally important.

(15) For instance, the Si-Si distance in $(F_2SiO)_2$ was calculated to be 0.053 Å shorter than that in $(H_2SiO)_2$, accompanied by the Si-O distance shortening of 0.026 Å. On the other hand, the Si-Si distance in $(Me_2SiO)_2$ was calculated to be very slightly longer than that in $(H_2SiO)_2$. It seems that the stronger is the charge

separation (or ionic character) in the Si^{+}-O^{-} bonds, the shorter is the Si-Si distance. The charge separation strengthens the SiO bond but also may reduce the short-range exchange repulsion between the Si atoms because of the decrease in the electron clouds around the Si atoms.

(16) Foster, J.M.; Boys, S.F. Rev. Mod. Phys. 1960, 32, 300.

(17) The Mulliken overlap populations between the silicon atoms were calculated to be -0.12 (HF/3-21G) and -0.002 (HF/6-31G*), indicating an antibonding interaction. Since it is well-known that the Mulliken population analysis works much better with minimal basis sets, we calculated the overlap population at the HF/STO-3G level, but again obtained the negative value of -0.11.

(18) For instance, see: Newton, M.D. in "Modern Theoretical Chemistry"; Schaefer, H.F. Ed., Plenum, New York, 1977; vol 4, PP.223-268.

(19) If the O-O repulsion would be severe in cyclodisiloxane, one should see a significant increase and decrease in the Si-O-Si angle and Si-O distance, respectively, on going from $(H_2SiO)_2$ to disilene oxide $H_2\overline{SiSiH_2}O$ because of the complete absence of the O-O repulsion. However, the angle (81.2°) and distance (1.687 Å) in the three-membered ring of disilene oxide were calculated to be 10.3° smaller and 0.016 Å longer, respectively, than those in the four-membered ring of $(H_2SiO)_2$ at the HF/6-31G* level.

(20) For a theoretical study on $H_2Si{=}S$ in the ground and excited states, see: Kudo, T.; Nagase, S. (manuscript in preparation).

(21) One may consider that the longer Si-Si distance in $(H_2SiS)_2$ is

due to the smaller S-S repulsion. However, Figure 3 reveals that the Si-S-Si angle of 83.3° in $(H_2SiS)_2$ is significantly smaller than the Si-O-Si angle of 91.5° in $(H_2SiO)_2$. It should be rather emphasized that the exchange repulsion between the less positive Si atoms in $(H_2SiS)_2$ is more severe than that between the much more positive Si atoms in $(H_2SiO)_2$.

(22) Yokoki, M.; Nomura, T.; Yamasaki, K. J. Am. Chem. Soc. 1955, 77, 4484. Yokoki, M. Bull. Chem. Soc. Jpn. 1957, 30, 100.

(23) Note that the authors of ref.5 misevaluated the Si-Si distance to be 2.34 Å when they cited ref.22 and considered that there also was a unusual Si-Si distance in $(Me_2SiS)_2$; this is a misunderstanding.

(24) Schklower, W.E.; Strutschkow, Yu.T.; Gusel'nikow, L.E.; Wolkowa, W.W.; Awakyan, W.G. Z. Anorg. Allg. Chem. 1983, 501, 153.

(25) Gusel'nikov, L.E.; Volkova, V.V.; Avakyan, V.G.; Nametkin, N.S.; Voronkov, M.G.; Kirpichenko, S.V.; Suslova, E.N. J. Organomet. Chem. 1983, 254, 173. See also : Krigsmann, H.; Clauss, H. Z. Anorg. Allg. Chem. 1959, 20, 210.

(26) The HF/6-31G* dipole moments are 2.67 ($H_2C=O$), 3.70 ($H_2Si=S$), and 4.13 ($H_2Si=O$) Debyes.

(27) At the HF/6-31G* level the frontier orbital π levels are -14.7 ($H_2C=O$), -10.3 ($H_2Si=S$), and -12.3 ($H_2Si=O$) eV while the π^* levels are 4.0, 0.5, and 1.5 eV, respectively.

(28) According to the energy component analysis based on the method by Morokuma, K. Acc. Chem. Res. 1977, 10, 294, for instance, in $(H_2SiO)_2$ the attractive term consists of 38% electrostatic, 30%

polarization, and 32% charge transfer interactions at the HF/6-31G* level.

(29) We may need calculations at the more sophisticated levels of theory. However, it is instructive to note that in the dimerization of SiO the exothermicity of 43.3 kcal/mol calculated at the MP2/6-31G*//6-31G* level differs little from that of 43.7 kcal/mol at the MP4/6-31G+2d//6-31G* level.[11]

(30) Herzberg, G. "Molecular Spectra and Molecular Structure. II. Infrared and Raman Spectra of Polyatomic Molecules", Van Nostrand: New York, 1945; PP.501-530.

(31) For instance, see: ref.1 and Barton, T.J. Pure Appl. Chem. 1980, 52, 615.

(32) Aggarwal, E.H.; Bauer, S.H. J. Chem. Phys. 1950, 18, 42. Peyronel, G. Chim. Industr. 1954, 36, 441. See also : Peyronel, G. Atti. Accad. Naz. Lincei. Rend. 1954, 16, 231.

(33) Hernandez, R.P. Acta Crystallogr. Sect.A, 1978, S406.

(34) In contrast, the disproportion energy for $3(H_2SiS)_2 \rightarrow 2(H_2SiS)_3$ is calculated to be much less negative (-30.3 kcal/mol). The details will be discussed elsewhere.

(35) In fact, our preliminary calculations at the HF/STO-2G level show that the ring expansion proceeds with no appreciable barrier via a path similar to that shown in Figure 1.

(36) For a puckered Si_4O_4 ring in cyclotetrasiloxanes, see : Hossain, M.A.; Hursthouse, M.B.; Malik, K.M.A. Acta Cryst. 1979, B35, 522 and references cited therein. Since the Si_4O_4 ring is supposed to be unusually flat, we did not carry out the optimization of the

puckered structure for the present purpose.

(37) For a related experiment, see: Tomadze, A.V.; Yablokova, N.V.; Yablokov, V.A.; Razuvaev, G.A. J. Organomet. Chem. 1981, 212, 43.

(38) For the high reactivity of $H_2Si=O$ toward nucleophiles, see ref.2.

(39) Morokuma, K.; Kato, S.; Kitaura, K.; Ohmine, I.; Sakai, S.; Obara, S. 1980.

(40) An IMS version of the GAUSSIAN80 series of programs by: Binkley, J.S.; Whiteside, R.A.; Krishnan, R.; Seeger, R.; DeFrees, D.J.; Schlegel, H.B.; Topiol, S.; Kahn, L.R.; Pople, J.A. QCPE 1981, 13, 406.

Table I. HF/3-21G Vibrational Frequencies (cm^{-1}) and Zero-Point Energies (kcal/mol) for the Cyclic Dimers.

modes and symmetry[a]	dimers		
	$(H_2SiO)_2$	$(H_2SiS)_2$	$(H_2CO)_2$
ν_1 (b_{3u})	253	109	234
ν_2 (a_g)	608	465	1154
ν_3 (a_u)	635	650	1201
ν_4 (b_{1g})	649	622	1164
ν_5 (b_{2g})	713	566	1182
ν_6 (b_{3g})	730	391	1030
ν_7 (b_{2u})	749	433	935
ν_8 (b_{3u})	820	579	1240
ν_9 (a_g)	925	315	946
ν_{10}(b_{1u})	941	443	1098
ν_{11}(b_{3g})	947	768	1425
ν_{12}(b_{2u})	1052	898	1539
ν_{13}(b_{1u})	1074	996	1711
ν_{14}(a_g)	1118	1018	1752
ν_{15}(b_{2g})	2365	2376	3344
ν_{16}(b_{1u})	2370	2360	3273
ν_{17}(b_{3u})	2370	2377	3353
ν_{18}(a_g)	2383	2364	3287
zero-point[b]	29.6	25.3	42.7

a See Figure 6. b Zero-point energies for the monomers are 12.1 ($H_2Si{=}O$), 11.1 ($H_2Si{=}S$), and 18.2 ($H_2C{=}O$) kcal/mol.

Table II. Total Energies (hartrees) Calculated at Several Level of Theory.

species	HF/3-21G//3-21G	HF/6-31G*//3-21G	HF/6-31G*//6-31G*	MP2/6-31G*//6-31G*
$H_2Si{=}O$	-362.95590	-364.90995	-364.91440	-365.18094
$H_2Si{=}S$	-684.10514	-687.58346	-687.58729	-687.78346
$H_2C{=}O$	-113.22183	-113.86529	-113.86633	-114.16525
$(H_2SiO)_2$	-726.13171	-730.01789	-730.02682	-730.53622
$(H_2SiS)_2$	-1368.30526	-1375.26998	-1375.28879	-1375.67976
$(H_2CO)_2$	-226.45374	-227.72150	-227.73111	-228.33088
$(H_2SiO)_3$	-1089.32687	-1095.11481	____	____
$(H_2SiO)_4$	-1452.47524	____	____	____

Table III. Dimerization Energies (kcal/mol).[a]

level of theory	dimers		
	$(H_2SiO)_2$	$(H_2SiS)_2$	$(H_2CO)_2$
HF/3-21G//3-21G	-138.0	-59.6	-6.3
HF/6-31G*//3-21G	-124.2	-64.7	5.7
HF/6-31G*//6-31G*	-124.3	-71.7	1.0
MP2/6-31G*//6-31G*	-109.4	-70.8	-0.2
+ zero-point correction[b]	-104.0	-67.7	6.1

a Negative (positive) values indicated stabilization (destabilization) relative to two separated monomers. b Zero-point energies in Table I are used for correction.

Table IV. Enthalpy (ΔH) and Entropy (ΔS) Changes for Dimerization.

	dimers		
	$(H_2SiO)_2$	$(H_2SiS)_2$	$(H_2CO)_2$
$\Delta H°_{298}$ (kcal/mol)	-105.7	-68.5	4.2
$\Delta S°_{298}$ (cal/mol.K)[a]	-45.6	-42.7	-43.4
ΔS_{trans}	-35.3	-36.2	-34.1
ΔS_{rot}	-13.6	-14.6	-11.7
ΔS_{vib}	3.3	8.1	2.4

a $\Delta S°_{298} = \Delta S_{trans} + \Delta S_{rot} + \Delta S_{vib}$

Table V. Comparison in the Net Atomic Charges and Frontier Orbital Energies of $H_2Si=O$ and $(H_2SiO)_n$ (n=2-4) at the HF/3-21G Level.

	atomic charge		energy level (eV)	
species	Si	O	HOMO	LUMO
$H_2Si=O$	1.12	-0.70	-11.6	1.5
$(H_2SiO)_2$	1.46	-0.97	-11.9	3.2
$(H_2SiO)_3$	1.61	-1.06	-11.6	4.7
$(H_2SiO)_4$	1.66	-1.10	-11.4	5.0

Figure 1. ORTEP drawings of the dimerization $2H_2Si{=}O \rightarrow (H_2SiO)_2$ in angstroms and degrees, obtained at the HF/3-21G level. (a) R=4.0 Å, (b) R=2.8 Å, (c) R=2.4 Å, and (d) R=1.717 Å (product).

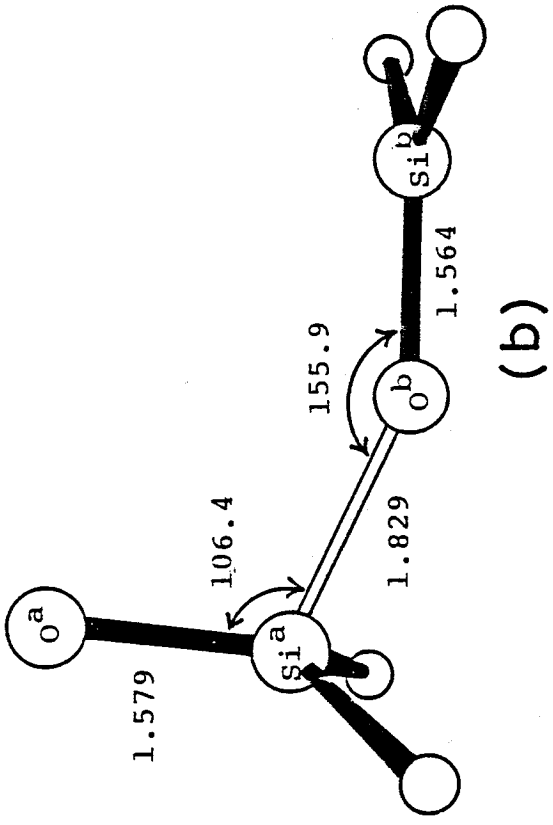

(b)

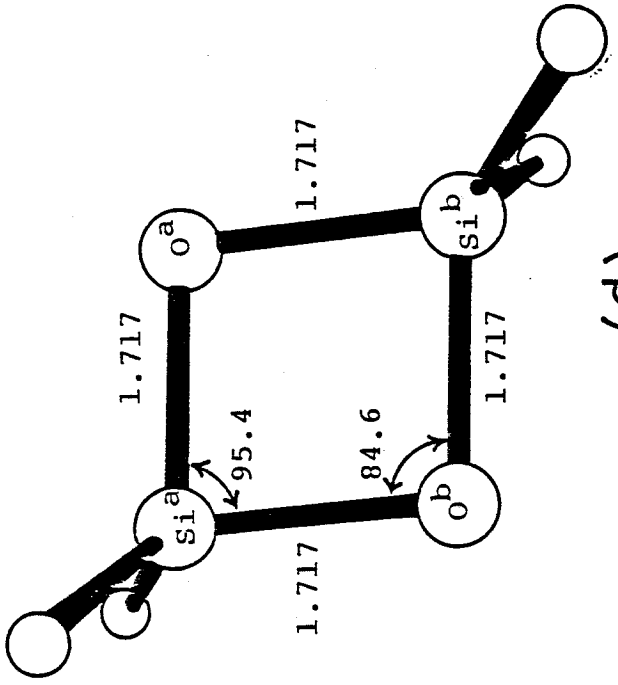

(d)

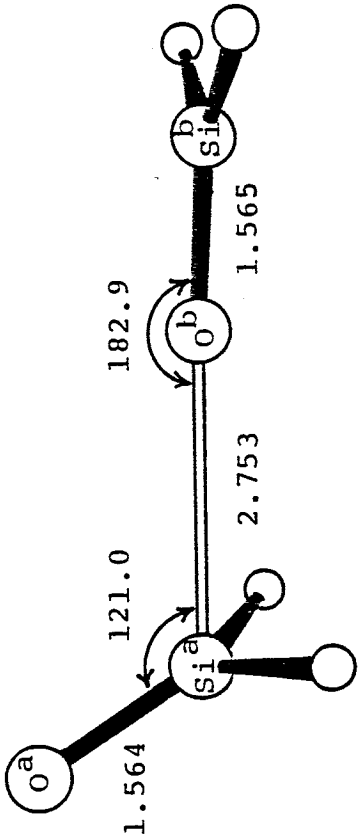

(a)

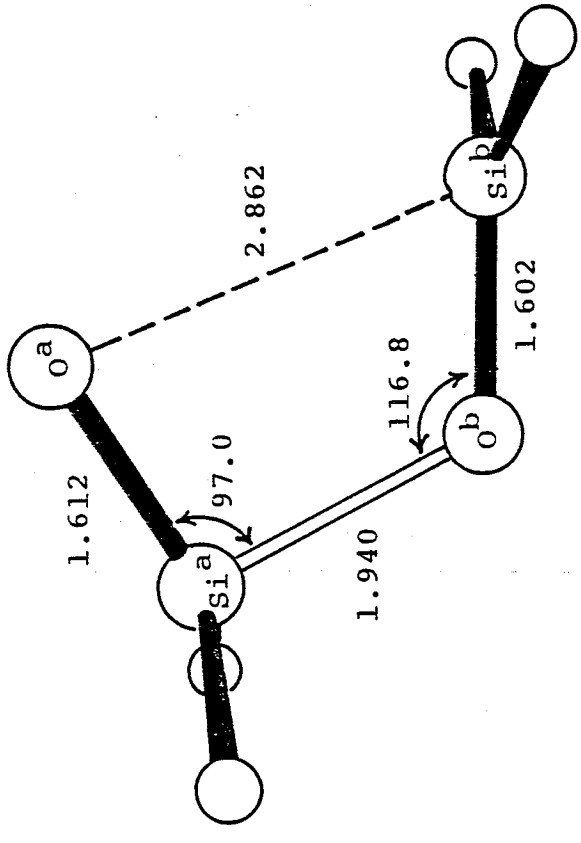

(c)

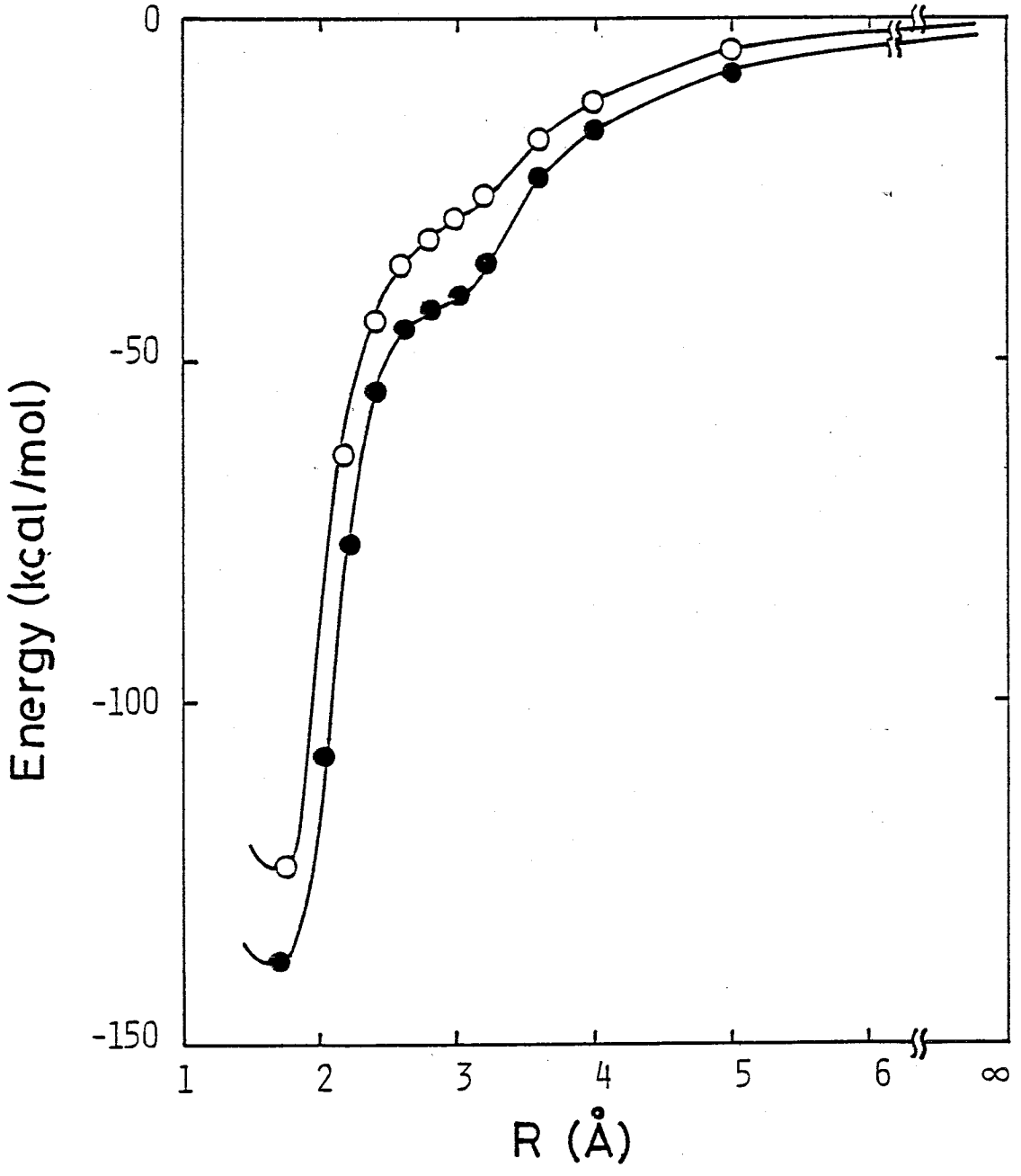

Figure 2. Potential energy curves for the dimerization of $H_2Si=O$ along the reaction path as a function of R, obtained at the HF/3-21G (●) and HF/6-31G*//3-21G (○) levels.

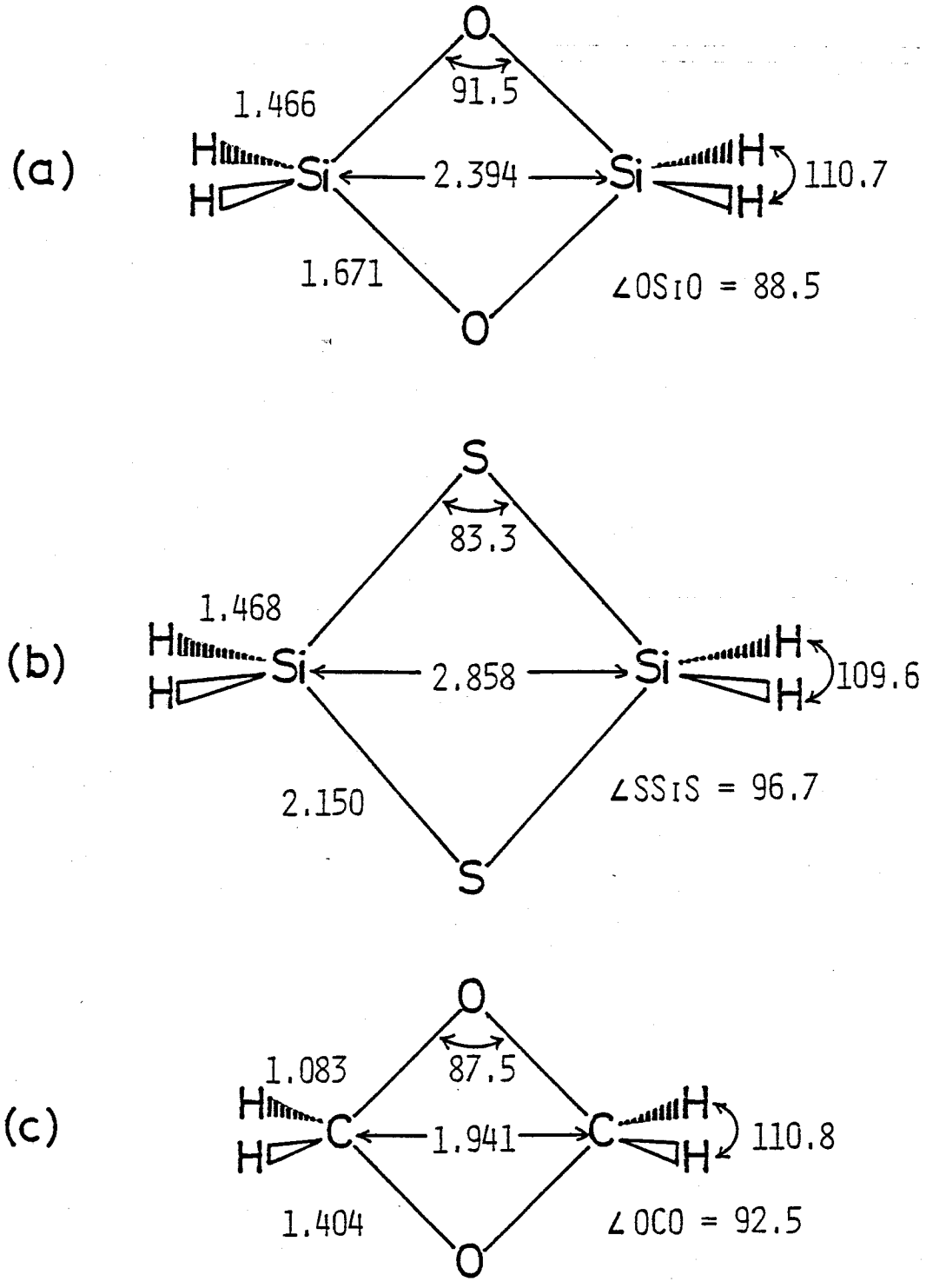

Figure 3. HF/6-31G* optimized structures of the cyclic dimers $(H_2SiO)_2$, $(H_2SiS)_2$, and $(H_2CO)_2$ in angstroms and degrees.

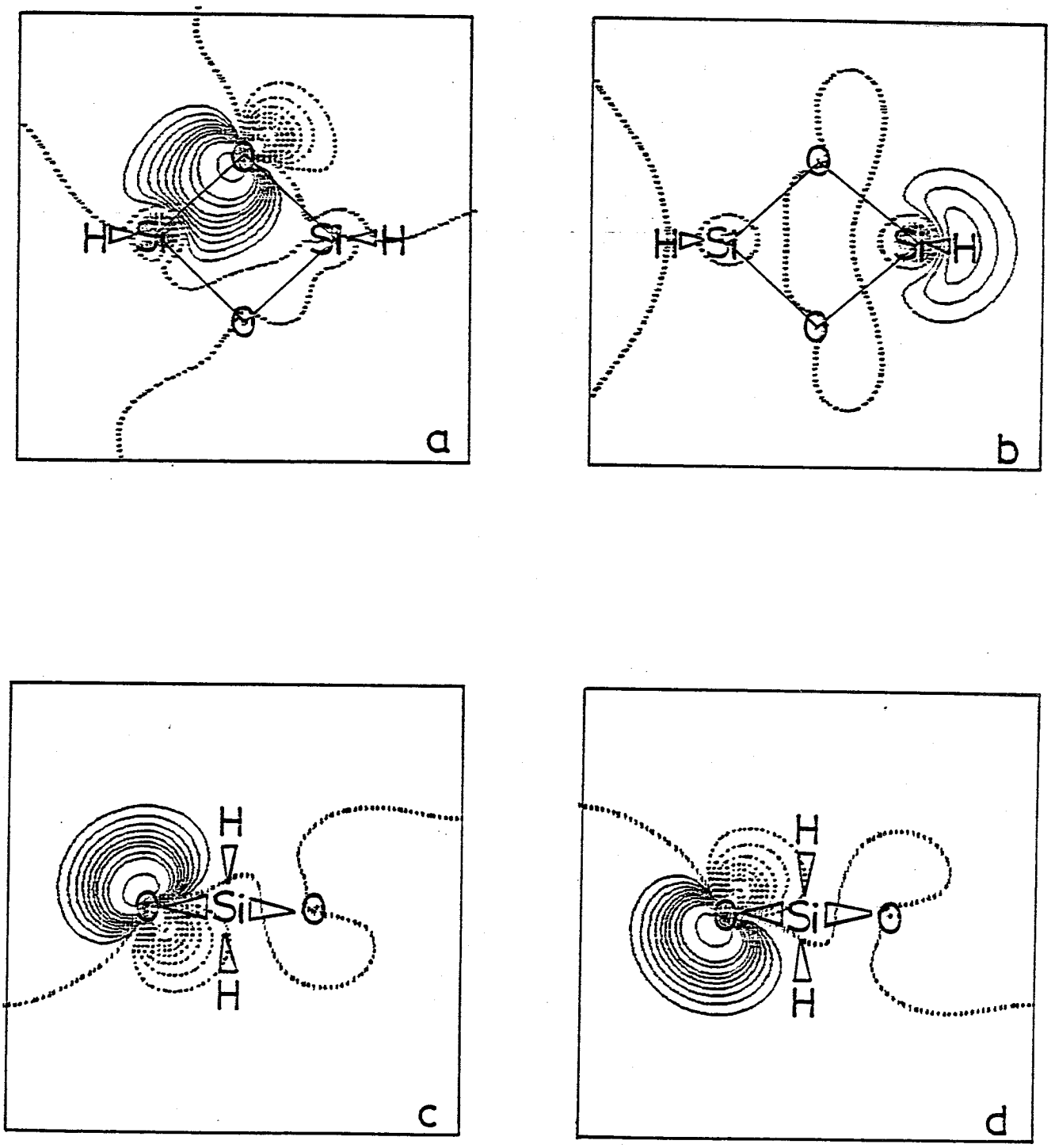

Figure 4. Contour plots of the localized molecular orbitals for the SiO bond (a), SiH bond (b), and lone-pair orbitals (c and d) in $(H_2SiO)_2$ obtained by the HF/3-21G Foster-Boys method.

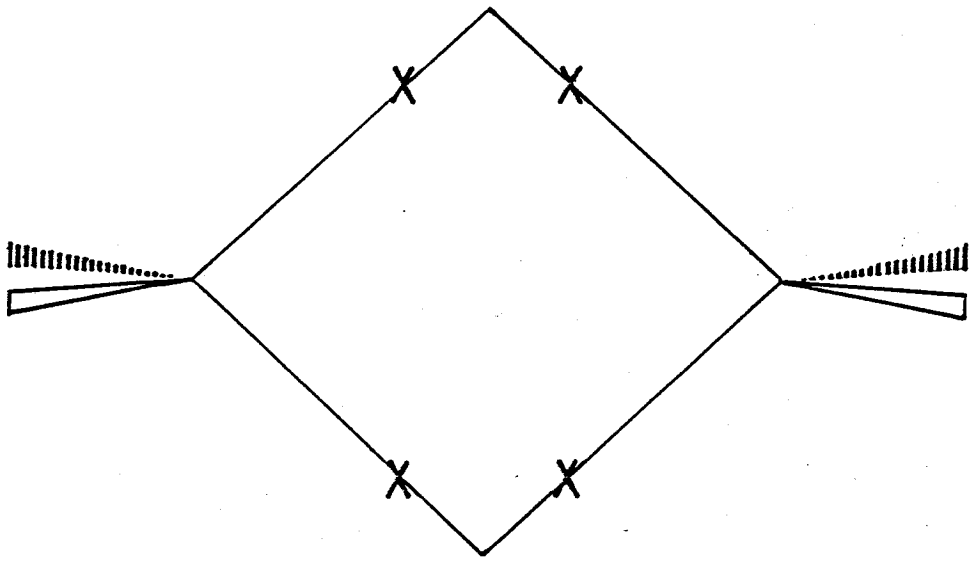

Figure 5. Centroids of the charge distributions of four SiO bond orbitals in $(H_2SiO)_2$.

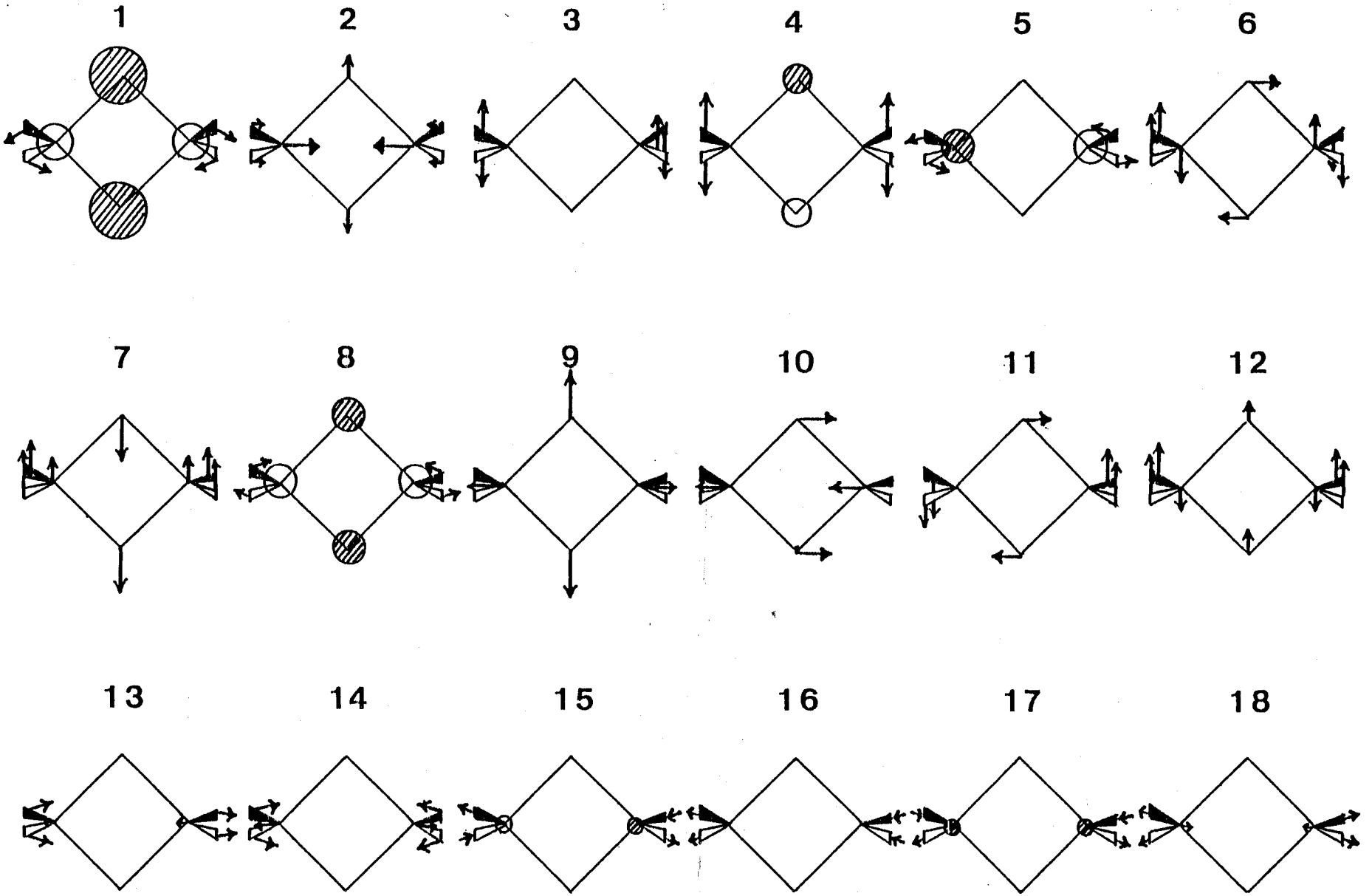

Figure 6. Schematic description of the vibrational modes for cyclic dimers.

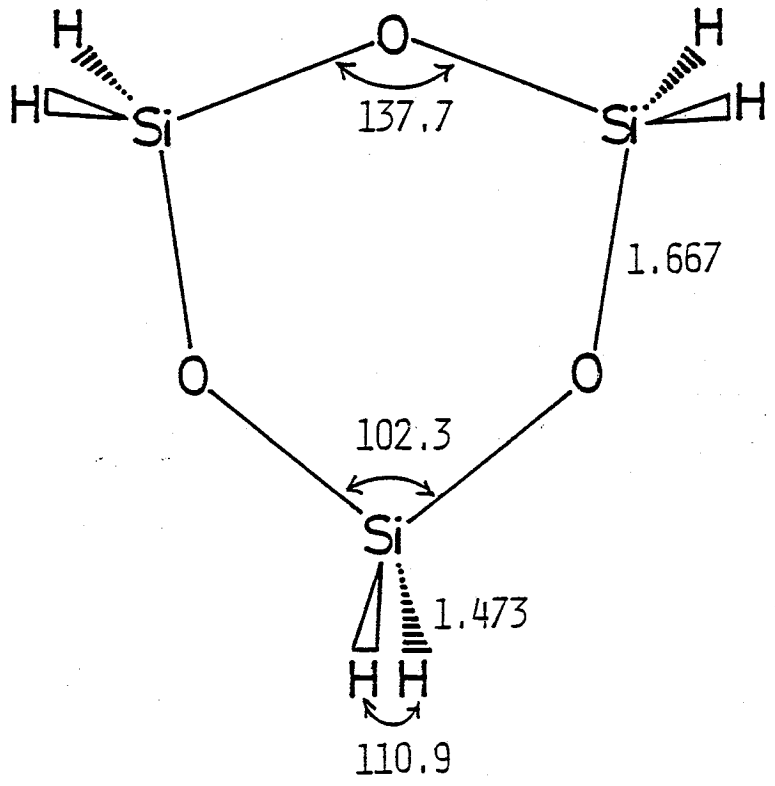

Figure 7. HF/3-21G optimized structure of the $(H_2SiO)_3$ trimer in angstroms and degrees.

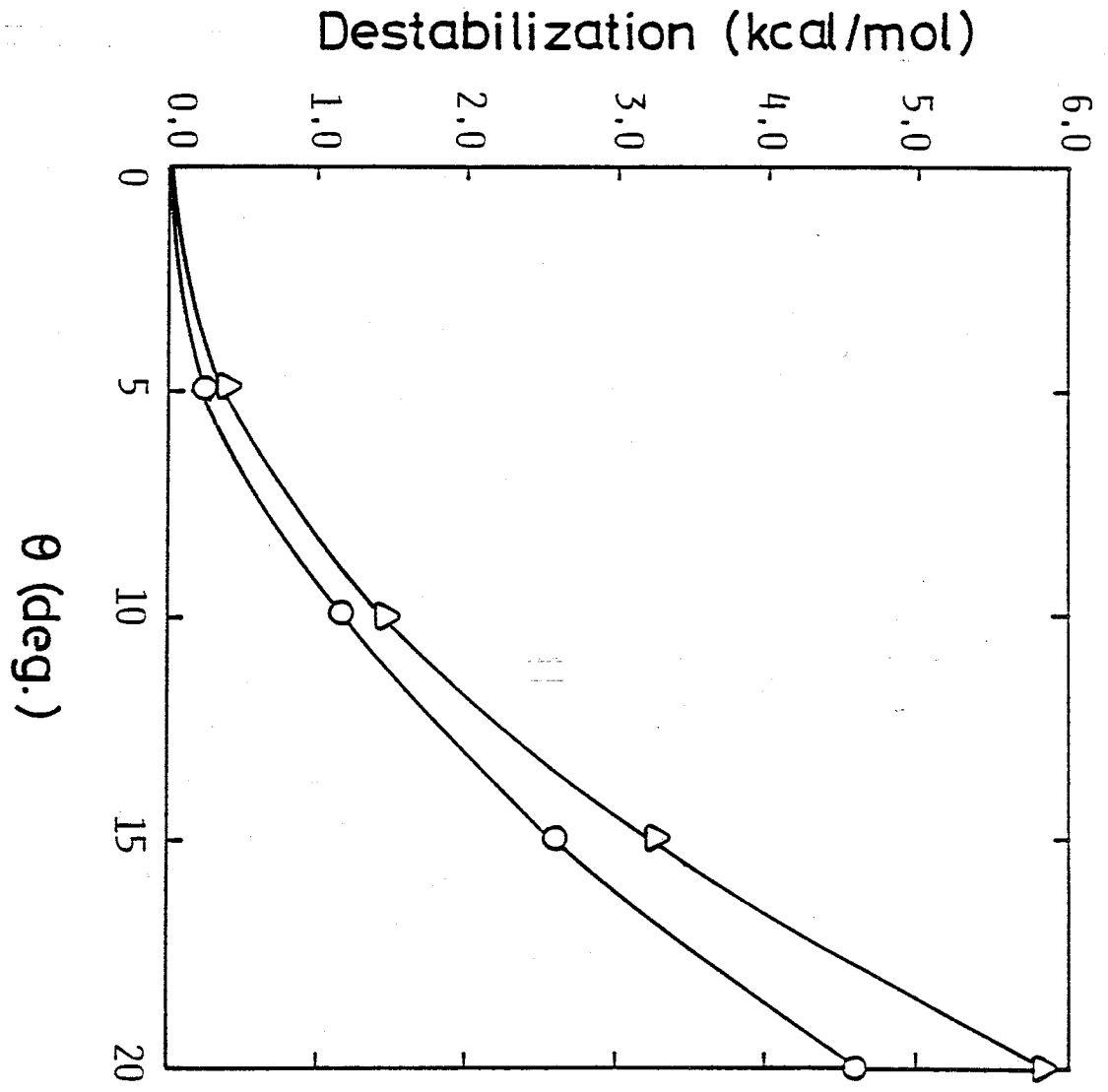

Figure 8. Destabilization energies due to the boat (○) and chair (△) distortions as a function of θ.

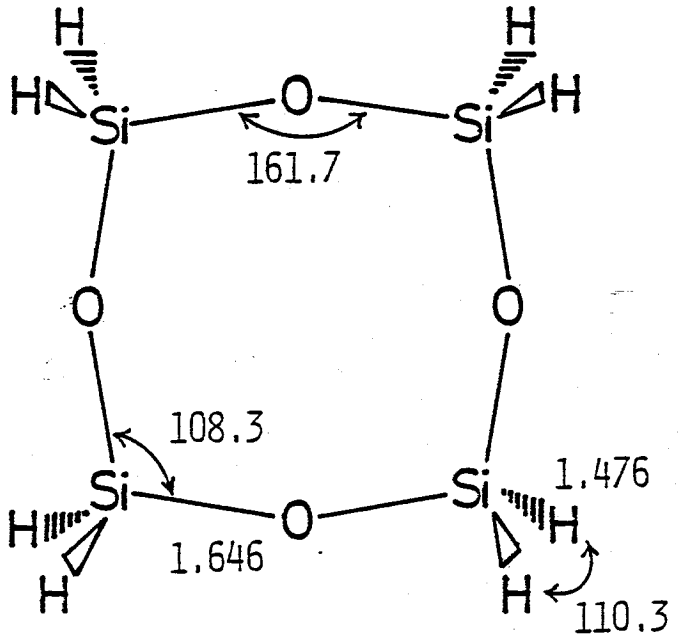

Figure 9. HF/3-21G optimized structure of the $(H_2SiO)_4$ tetramer in angstroms and degrees, obtained by imposing D_{4h} symmetry.

CHAPTER 4

The Thermodynamic and Kinetic Stability of Silanethione.

The Ground, Excited, and Protonated States

To extend knowledge of silicon-sulfur double bonds, several properties of silanethione were investigated and compared with those of silanone and formaldehyde, by means of ab initio calculations including polarization functions and electron correlation. $H_2Si{=}S$ is found to be kinetically stable enough to its unimolecular destructions such as $H_2Si{=}S \rightarrow H_2{+}SiS$, $H_2Si{=}S \rightarrow H{+}HSiS$, and $H_2Si{=}S \rightarrow \ddot{H}SiSH$, which is certainly the existing species. Furthermore, $H_2Si{=}S$ is found to be thermodynamically more stable than $H_2Si{=}O$ and rather resemble $H_2C{=}O$ in stability. Through these comparisons, it is emphasized that silicon is less reluctant to form doubly bonding with sulfur than with oxygen. The singlet-triplet energy differences in $H_2Si{=}S$ and $H_2Si{=}O$ are calculated to be considerably smaller than that in $H_2C{=}O$. In the protonated states, the S-protonated singlet species, H_2SiSH^+, is the most stable and separated by sizable barriers from the isomers such as H_3SiS^+ and $\ddot{H}SiSH_2^+$, as are H_2SiOH^+ and H_2COH^+. Finally, the potential energy surface for the reaction of $H_2Si{=}S$ with water is investigated to characterize the reactivity toward polar reagents.

Introduction

Compounds which feature doubly bonding to silicon are of current interest.[1] As the silicon analogues of ethenes, silicon-carbon (silenes)[2] and silicon-silicon (disilenes)[3] doubly bonded compounds have been characterized and isolated in the last few years. In contrast, the study of the formaldehyde analogues seems to be still in the early stages.[1] Recently we have studied the thermodynamic and kinetic stability of silicon-oxygen doubly bonded compounds (silanones).[4-6] Silanones are found to be less stable and more reactive than formaldehydes. This may arrise from the following ; unfavorable overlapping between $p_{\pi}(Si)$ and $p_{\pi}(O)$ orbitals owing to a size difference gives a weaker π-bonding, while a large electronegativity difference between Si and O atoms causes strongly polarized Si^{+}-O^{-} bonding which results in the higher reactivity. To the extent that the view is valid, silicon-sulfur doubly bonded compounds (silanethiones) are expected to be more stable and less reactive. However, the number of the experimental studies of silanethiones are fairly limited to date ; only indirect evidence is at present available which suggests the transient existence of the important species.[7]

In view of the situation theoretical information is helpful for further advance in silanethione chemistry. Thus, we have undertaken the ab initio calculations of the properties of the ground and excited states of the parent compound, $H_2Si{=}S$, to extend knowledge of silicon-sulfur double bonds. To characterize

the stability and reactivity, comparisons with $H_2Si{=}O$ and $H_2C{=}O$ are made with use of results obtained at the same level of theory. Also investigated is the protonation of $H_2Si{=}S$ and $H_2Si{=}O$, because of the long-standing interest in the protonation of the carbon analogues $H_2C{=}S$[8] and $H_2C{=}O$.[8,9]

To this end, silicon-sulfur double bonds are found to be thermodynamically and kinetically more stable than silicon-oxygen double bonds. Successful schemes for the synthesis and isolation of silanethiones are expected to be soon devised.

Computational Details

Stationary points (equilibrium and transition structures) on potential energy surfaces were all located at the Hartree-Fock (HF) level with the split-valence 6-31G* d-polarized basis set[10] by using analytical gradient procedures. In these calculations, open-shell systems were treated with the spin-unrestricted HF formalism.

Subsequent to the full optimization of the stationary point structures, single-point calculations were carried out to obtain more reliable energies ; with the larger 6-31G** basis set[10], electron correlation was incorpolated via configuration interaction (CI) or second- and third-order Møller-Plesset perturbation (MP2 and MP3)[11] theories. In the CI and MP calculations, all single (S) and double (D) excitations from the respective HF reference configurations were included, with the

constraint that core-like orbitals (1s,2s, and 2p for Si and S and 1s for C and O) were "frozen" (i.e., doubly occupied). The energies by the CI method were further improved with the Davidson formula[12] to allow for unlinked cluster quadruple correction (QC), these being denoted by CI(S+D+QC). Zero-point correction (ZPC) was made with harmonic vibrational frequencies calculated at the HF/3-21G level.[13]

For $H_2Si{=}S$ only, the harmonic vibrational frequenceis were calculated at the HF/6-31G* level. The zero-point energy of 11.6 kcal/mol at the HF/6-31G* level was found to differ little from that of 11.1 kcal/mol at the HF/3-21G level.

Results and Discussion

A. Closed-Shell Singlet States

The species and unimolecular reactions pertinent to the stability of $H_2Si{=}S$ are shown in Scheme I.

Scheme I

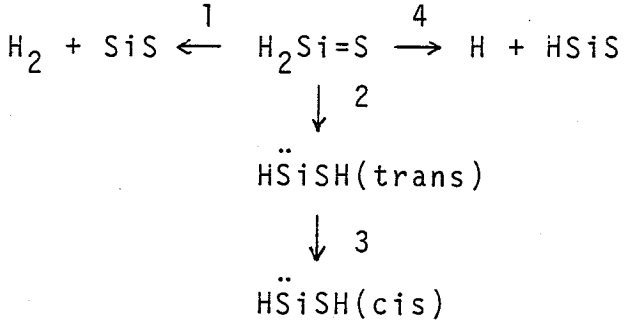

Structures. Figure 1 summarizes the HF/6-31G* equilibrium structures on the ground singlet potential energy surface of the H_2SiS species. At present no experimental data are available for comparison. It may be fruitful to make comparison with the calculated values for the H_2CO[14] and H_2SiO[5] species at the same level of theory.

The equilibrium structure of $H_2Si{=}S$ is calculated to be planar with C_{2v} symmetry, as in the cases of $H_2C{=}O$ and $H_2Si{=}O$. The double bond length (1.936 Å) in $H_2Si{=}S$ is 0.752 Å and 0.438 Å longer, respectively, than those in $H_2C{=}O$ and $H_2Si{=}O$. However, the Si-S double bond length is 0.216 Å shorter than the Si-S single bond length (2.152 Å) in H_3SiSH. The shortening of 0.216 Å is comparable to that of 0.215 Å from H_3COH (1.399 Å) to $H_2C{=}O$ (1.184 Å), and it is significantly greater than that of 0.149 Å from H_3SiOH (1.647 Å) to $H_2Si{=}O$ (1.498 Å). These suggest not only that there is a certain strength of π bonding between the Si and S atoms, but also that the p_π-p_π overlapping is more favorable in $H_2Si{=}S$ than in $H_2Si{=}O$.

The elimination of a hydrogen atom from $H_2Si{=}S$ gives the HSiS radical. For this silicon radical, two distinct equilibrium structures with the same $^2A'$ symmetry were located on the potential energy surface, whose electronic configurations are described, respectively, as

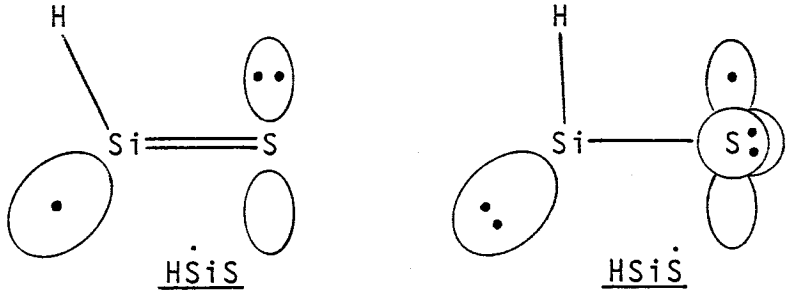

HSiS and HSiS differ greatly in their Si-S bond lengths and HSiS bond angles. The Si-S bond length (1.941 Å) in HSiS is only 0.005 Å longer than the double bond in $H_2Si{=}S$, while the Si-S length (2.070 Å) in

HSiṠ is rather close to the Si-S single bond in H_3Si-SH. In addition, the HSiS bond angle (123.0°) in HṠiS is 27.2° larger than that (95.8°) in HSiṠ. As for the relative stability, HṠiS was calculated to be 6.2 kcal/mol more stable at the MP3/6-31G**//6-31G* level than HSiṠ. Thus, only HṠiS will be considered in this paper. For the HSiO radical, two minima were also found which correspond to HṠiO (SiO=1.501 Å and ∠ HSiO=122.8°) and HSiȮ (SiO=1.626 Å and ∠HSiO=94.1°). At the MP3/6-31G**//6-31G* level, the energy difference (12.3 kcal/mol) favoring HṠiO over HSiȮ is twice larger than that favoring HṠiS over HSiṠ. For the carbon radical HCO, however, only one minimum corresponding to HĊO (CO=1.159 Å and ∠HCO=126.3°) was located on the potential energy surface.

The further hydrogen eliminations from HṠiS, HṠiO, and HĊO shorten the Si-S, Si-O, and C-O bond lengths, respectively, by 0.024, 0.014, and 0.045 Å. Consequently, the double bond lengths in Si=S, Si=O, and C=O are 0.019, 0.011, and 0.070 Å shorter, respectively, than those in H_2Si=S, H_2Si=O, and H_2C=O.

The divalent HS̈iSH species, the 1,2-H shifted isomers of H_2Si=S, have a planar structure in trans and cis forms. The Si-S length as well as the HSiS and HSSi angles is significantly larger in the cis form than in the trans form ; These trends are also seen in HC̈OH and HS̈iOH,[5] and well explained in terms of steric repulsion between the hydrogens.

Figure 2 shows the transition structures for reactions 1-3 in Scheme I. A and B are the transition structures for the 1,2-hydrogen shift in H_2Si=S to HS̈iSH (reaction 2) and trans to cis isomerization of HS̈iSH (reaction 3). Both are calculated to be nonplanar. C is the transition structure for molecular

dissociation of $H_2Si{=}S$ leading to H_2 + SiS (reaction 1), which is planar. The overall features of these transition structures are very similar to those calculated previously for H_2CO and H_2SiO reactions, except that the 1,2-hydrogen shift in $H_2C{=}O$ to $H\ddot{C}OH$ proceeds via a planar transition state.[14]

Nevertheless, it may be interesting to refer to the geometrical changes in the trans to cis isomerization of the divalent species. As Figure 2 shows, the isomerization proceeds via rotation (not via inversion). During the isomerization, no appreciable change occurs in the Si-O bond length of $H\ddot{S}iOH$ while the Si-S and C-O lengths of $H\ddot{S}iSH$ and $H\ddot{C}OH$ increase by ca. 0.08 and 0.04 Å, respectively, at the transition states in which the dihedral angles are ∠HSiSH = 90.6° and ∠HCOH = 90.1°. As suggested by Goddard and Schaefer,[15] the increasings may be related to the presence of some double bond character in the SiS and CO bonds (not in the SiO bond). At this point, it is interesting to note that the Si-S and C-O lengths of $H\ddot{S}iSH$ and $H\ddot{C}OH$ are 0.019 and 0.099 Å shorter, respectively, than those of H_3SiSH and H_3COH, while the Si-O length of $H\ddot{S}iOH$ is rather 0.004 Å longer than that of H_3SiOH.

Vibrational Frequenceis. Table I compares the harmonic vibrational frequencies of $H_2Si{=}S$ and $H_2Si{=}O$ at the HF/6-31G* level. It is now well-known that HF/6-31G* frequencies are calculated to be too high by an average of 12.6 % compared with experimental (anharmonic) frequencies but the errors are

relatively constant.[16] In view of the fact, the scaled-down frequencies ($\nu_{calcd}/1.126$) are also presented in Table I. It is to be noted that the scaled value (1203 cm^{-1}) for the Si=O stretching frequency of $H_2Si{=}O$ is comparable to the experimental value (1204 cm^{-1}) assigned recently for dimethylsilanone.[17]

No experimental data on silanethiones are available for comparison. As Table I suggests, the Si=S stretching mode should be actually observed near 682 cm^{-1}. Contrary to the expectation just based on the π-bond strength, the Si=S stretching frequency is predicted to be ca. 520 cm^{-1} lower than the corresponding Si=O frequency. This is because the much stronger SiO σ bonding (compared with the SiS σ bonding) overwhelms the weaker SiO π bonding (compared with the SiS π bonding),[18] resulting in the greater ($\sigma+\pi$) strength of the Si=O bond than the Si=S bond.[19]

Energies. The total and relative energies of the H_2SiS species at several levels of theory are given in Tables II and III, respectively. The relative energies at the CI(S+D+QC)/6-31G**//6-31G* level are schematically summarized in Figure 3, together with the zero-point correction (ZPC) values. Since comparison of the H_2CO and H_2SiO species has already been made in our recent paper[5], we here concentrate mainly on the similarities and differences between the H_2SiO and H_2SiS species. For this purpose, the energy profile of the H_2SiO species calculated previously[5] at the same level of theory is included in

Figure 3.

As seen in Figure 3, $H_2Si{=}O$ is 3.7 (2.4 after ZPC) kcal/mol less stable than $\ddot{H}SiOH$, reflecting a preference for divalent silicon (At this point, note that $H_2C{=}O$ is 54.0 (53.9 after ZPC) kcal/mol more stable than $H\ddot{C}OH$)[5]. However, $H_2Si{=}S$ is now calculated to be 9.3 (8.9 after ZPC) kcal/mol more stable than $H\ddot{S}iSH$, the relative stability of doubly bonded and divalent species being significantly reversed. This suggests that silicon is less reluctant to form doubly bonding with sulfur than with oxygen.

The thermodynamic stability of silicon-sulfur double bonds can be characterized by comparing the energies released upon the addition of H_2 to $H_2Si{=}S$, $H_2Si{=}O$, and $H_2C{=}O$. At the MP3/6-31G**//6-31G* level the hydrogenation energy of $H_2Si{=}S$ was calculated to be 31.4 kcal/mol. At the same level of theory, this value is 20.2 kcal/mol smaller than the value (51.6 kcal/mol) of $H_2Si{=}O$ and rather comparable to the value (29.6 kcal/mol) of $H_2C{=}O$. These indicate that silicon-sulfur double bonds are much more stable in a thermodynamic sense than silicon-oxygen double bonds.

We turn to the kinetic stability of silicon-sulfur double bonds. As Figure 3 shows, the barrier for the 1,2-H shift in $H_2Si{=}S$ to $H\ddot{S}iSH$ is as sizable as 57.5 (54.8 after ZPC) kcal/mol. The same is true for the molecular and radical dissociations of $H_2Si{=}S$ which lead to H_2 + SiS and H + HSiS, respectively ; the energies required for the former reaction is

79.2 (75.7 after ZPC) kcal/mol, while the latter reaction was calculated to be 82.8 kcal/mol endothermic at the MP3/6-31G**//6-31G* level. These do suggest that $H_2Si{=}S$ itself is kinetically stable enough and is certainly the existing species. The barriers for the unimolecular destructions of $H_2Si{=}S$ are calculated to be somewhat small compared with those of $H_2Si{=}O$. This reflects that the SiH bonds in $H_2Si{=}S$ are weaker than those in $H_2Si{=}O$. In fact, the energy (97.6 kcal/mol) required for the radical dissociation of $H_2Si{=}O$ was 8.6 kcal/mol larger than that of $H_2Si{=}S$ at the MP3/6-31G**//6-31G* level.

The 1,2-H shifted isomers, $\ddot{H}SiSH$ and $\ddot{H}SiOH$, can exist in trans and cis forms, the trans being slightly more stable than the cis, as shown in Figure 3. The barrier for the trans-to-cis isomerization via rotation of $\ddot{H}SiSH$ is 19.3 (18.0 after ZPC) kcal/mol while that of $\ddot{H}SiOH$ is 11.0 (9.3 after ZPC) kcal/mol. The former value is about twice larger than the latter value. This is explained in terms of the double bond character in the Si-S bond of $\ddot{H}SiSH$, as already pointed out.

B. Open-Shell Triplet States

Structures. In Table IV are summarized the structural parameters optimized at the HF/6-31G* level for the n-π^* and π-π^* triplet states of H_2SiS and H_2SiO. With C_{2v} symmetry constraint we initially optimized the structures of these triplet states. In all the cases, however, the resultant optimized structures were found to be the

transition states for molecular deformation from the planar C_{2v} to pyramidalized C_s forms, as in the case of H_2CO.

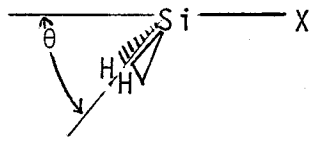

X=S or O

In the $^3A''(n-\pi^*)$ states the out-of-plane angles θ (defined as the angles between the HSiH plane and SiX axis) increase to 57.3° for H_2SiS and 59.8° for H_2SiO ; at the MP3/6-31G**//6-31G* level the pyramidalized forms of H_2SiS and H_2SiO were calculated to be 12.6 (11.8 after ZPC) and 17.5 (16.7 after ZPC) kcal/mol more stable, respectively, than the planar forms. In the $^3A'(\pi-\pi^*)$ states, the out-of-plane angles θ are smaller but still as large as 52.9° (H_2SiS) and 54.5° (H_2SiO).

The difference in the angles θ between the $^3A''(n-\pi^*)$ and $^3A'(\pi-\pi^*)$ states is due to the fact that the π orbitals are delocalized over the two heavy atoms while the n orbitals are strongly localized on the non-silicon atoms. In other words, a larger amount of electron transfer to silicon can take place in the $^3A''(n-\pi^*)$ states than in the $^3A'(\pi-\pi^*)$ states, as is obvious from the net atomic charge densities and dipole moments in Table V, thereby inducing sp_3 hybridization on silicon to a greater extent in the $^3A''(n-\pi^*)$ states. When comparison is made between H_2SiS and H_2SiO, H_2SiO is more pyramidalized in the $^3A''(n-\pi^*)$ and $^3A'(\pi-\pi^*)$ states than is H_2SiS. This is also explained in terms of the amount of electron transfer to silicon (see Table V), as is apparent from the fact that the strongly

polarized π and π^* orbitals of H_2SiO have much smaller and larger electron densities around the Si atom, respectively, than those of H_2SiS.

Upon being excited to the triplet states, the Si-S bond length in H_2SiS increases by 0.211 ($^3A''$) and 0.246 ($^3A'$) Å while the Si-O bond length in H_2SiO increases by 0.188 ($^3A''$) and 0.216 ($^3A'$) Å ; in both the cases the increasings are larger in the $^3A'$ states than in the $^3A''$ states. All these increasings are not surprising since the triplet states result from the excitation from the bonding π or nonbonding n to antibonding π^* orbitals.

Adiabatic Energy Separations. Table VI summarizes the energies of the open-shell triplet states of H_2SiS and H_2SiO, relative to the respective closed-shell singlet states. To refer to the reliability of the calculated values, we also calculated the $^3A''$ and $^3A'$ states of H_2CO because experimental data are available for the $^3A''$ state. The $^1A_1$-$^3A''$ adiabatic energy separation of 3.06 (2.97 after ZPC) eV in H_2CO calculated at the MP3/6-31G**//6-31G* level is in good agreement with the corresponding experimental value of 3.12 eV.[20] Furthermore, it is instructive to note that our MP3/6-31G**//6-31G* values for H_2SiO agree very well (to within 0.02 eV) with the values of 2.24 ($^1A_1$-$^3A''$) and 2.59 ($^1A_1$-$^3A'$) eV calculated recently at similar levels of theory by Dixon et al..[21]

As Table VI shows, $H_2Si{=}S$ and $H_2Si{=}O$ have the ground singlet $^1A_1$ states, respectively, as does $H_2C{=}O$. The $^3A''(n\text{-}\pi^*)$ states of $H_2Si{=}S$ and $H_2Si{=}O$, which are the lowest excited states,[22] lie 1.75

(1.72 after ZPC) and 2.31 (2.27 after ZPC) eV, respectively, above the ground singlet $^1A_1$ states. The $^1A_1$-$^3A''$ energy separations in $H_2Si=S$ and $H_2Si=O$ are considerably smaller than that in $H_2C=O$. The same is also true for the $^1A_1$-$^3A'$ energy separations. These smaller energy separations are characteristic of silicon-containing compounds and easily understandable from the frontier orbital energy levels shown in Figure 4. Furthermore, it is interesting to note that the energy gaps between the $^3A''(n-\pi^*)$ and $^3A'(\pi-\pi^*)$ states in $H_2Si=S$ and $H_2Si=O$ are very small (ca.0.3 eV) compared with that in $H_2C=O$, because the n and π energy levels almost degenerate in the silicon-containing compounds.

C. Protonated States

The species and reactions considered for the protonation of $H_2Si=X$ (X=S or O) are shown in Scheme II.

Scheme II

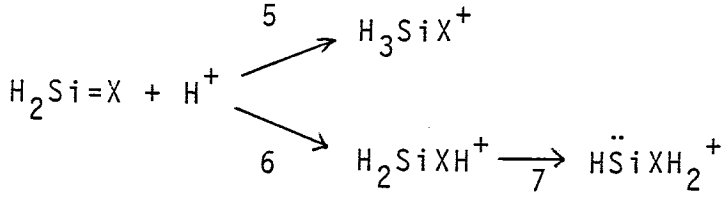

The Sites of Protonation. There are two possible sites available for the protonation of $H_2Si=X$ (X=S or O). Protonation on the X site (reacion 6) leads to the cation, H_2SiXH^+, while protonation on the Si site (reaction 5) results in producing the

cation, H_3SiX^+. The HF/6-31G* optimized structures of these cations are shown in Figure 5.

The X-protonated structure H_2SiXH^+ is found to be planar with C_s symmetry. The Si-X bond length in H_2SiXH^+ is only 0.096 (X=S) and 0.063 (X=O) Å longer than that in $H_2Si{=}X$. This is not surprising since the cation results from the proton-attack on the lone-pair orbitals of $H_2Si{=}X$. Interesting is the SiXH angle which may measure the direction of the lone pair orbitals (or the direction of protonation); the SiSH angle (97.7°) in H_2SiSH^+ is 34.7° smaller than the SiOH angle (132.4°) in H_2SiOH^+.

Protonation on the Si site proceeds by attacking the π orbital of $H_2Si{=}X$. The Si-protonated cation H_3SiX^+ with three equivalent hydrogen atoms has degenerate HOMO levels. According to Hund's rule the most stable should be a triplet of C_{3v} symmetry. However, Jahn-Teller distortion in a singlet state can remove the degeneracy by lowering the symmetry to C_s. For this reason, both singlet and triplet states were examined for the cation H_3SiX^+. As Figure 5 shows, the triplet cation, although optimized without symmetry constraint, is found to prefer a C_{3v} structure, in agreement with Hund's rule. As for two Jahn-Teller-distorted structures for the singlet cation, only one of them was located at the HF/6-31G* level,[23] respectively, for X=S and X=O, which is just shown in Figure 5.

The total and relative energies of the cations H_2SiXH^+ ($^1A'$) and H_3SiX^+ ($^1A'$ and $^3A_1$) are given in Tables VII and VIII, respectively. In both X=S and X=O, the X-protonated cation is

calculated to be much more stable at any levels of theory than the Si-protonated cation.

At the MP3/6-31G**//6-31G* level H_2SiSH^+ ($^1A'$) is 84.0 (83.4 after ZPC) kcal/mol more stable than H_3SiS^+ ($^1A'$) and it is 41.7 (41.2 after ZPC) kcal/mol more stable than H_3SiS^+ ($^3A_1$). We managed to locate a transition state connecting H_2SiSH^+ ($^1A'$) and H_3SiS^+ ($^1A'$) at the HF/6-31G level, but found that the transition state lies in energy rather below H_3SiS^+ ($^1A'$) at the higher calculational levels. This suggests that H_3SiS^+ ($^1A'$) collapses with no barrier to H_2SiSH^+ ($^1A'$) and that the H_3SiS^+ species is likely to exist only in a triplet state. In the protonation of $H_2Si{=}O$, H_3SiO^+ ($^1A'$) and H_3SiO^+ ($^3A_1$) are 172.5 (168.7 after ZPC) and 111.3 (108.4 after ZPC) kcal/mol more unstable at the MP3/6-31G**//6-31G* level, respectively, than H_2SiOH^+ ($^1A'$). In addition, H_3SiO^+ ($^1A'$) is found to be a transition structure for scrambling of the hydrogen atoms.

The sites for the protonation of the carbon analogues $H_2C{=}X$ (X=O or S) have been extensively discussed many times over the past years.[8,9] It is now established through the long-standing controversy that H_2CXH^+ is more stable than H_3CX^+. Here, it is interesting to note that the energy difference favoring H_2SiXH^+ over H_3SiX^+ is calculated to be much larger than that favoring H_2CXH^+ over H_3CX^+.

H_2SiSH^+ vs. H_2SiOH^+. We already found that the most stable conformation of H_2SiXH^+ (X=S or O) is the fully planar structure

with C_s symmetry (Figure 5). As other conformational alternatives, a nonplanar structure a and a linear Si-X-H arrangement b were explored.

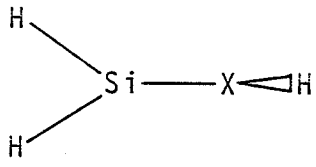

nonplanar (C_s)

a

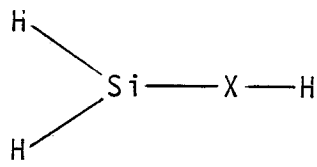

linear (C_{2v})

b

In case of X=S, both a and b are found to be the stationary points on the potential energy surface. However, the force constant matrix analyses reveal that a has one negative eigenvalue while b has two negative eigenvalues. In other words, b is the maximum with respect to both molecular deformation to a and linear inversion at the X center, b being 45.7 kcal/mol less stable at the MP3/6-31G**//6-31G* level than the planar C_s structure in Figure 5. On the other hand, a is the transition structure[24] for the rotation around the Si-X bond ; the rotational barrier is calculated to be 17.5 (16.6 after ZPC) kcal/mol at the MP3/6-31G**//6-31G* level. This considerable barrier suggests a certain degree of π bonding between the Si and S atoms in H_2SiSH^+, allowing us to describe the cation as $H_2Si{=}SH^+$.

In case of X=O, b is found to be the transition structure[25] for inversion at the X center and calculated to lie only 3.4 (3.1 after ZPC) kcal/mol, at the MP3/6-31G**/6-31G* level, above the

planar C_s structure in Figure 5. On the other hand, a is found to be no longer stationary (and collapses to b). Therefore, a rigid rotor model was employed to evaluate approximately the rotational barrier of H_2SiOH^+. The barrier was calculated to be small (6.1 kcal/mol) even for a rigid rotation. These suggest that H_2SiOH^+ is conformationally very flexible compared with H_2SiSH^+.

1,2-H Shifts in H_2SiSH^+ and H_2SiOH^+. Since there is a tendency for silicon to be divalent, the 1,2-H shifts (reaction 7 in Scheme II) were examined to see the stability of the H_2SiSH^+ and H_2SiOH^+ cations.

As Figure 6 shows, the structure of the 1,2-H shifted divalent isomer is significantly pyramidalized for $H\ddot{S}iSH_2^+$ but planar with C_s symmetry for $H\ddot{S}iOH_2^+$.[26] In a way to reach these divalent isomers via a least-motion path, the 1,2-H shift in H_2SiSH^+ prefers a nonplanar transition state (D) while that in H_2SiOH^+ proceeds via a planar transition state (E). As shown in Table VIII, the respective barriers for the 1,2-H shift are 65.0 (61.7 after ZPC) and 76.3 (73.9 after ZPC) kcal/mol at the MP3/6-31G**//6-31G* level. This indicates that both H_2SiSH^+ and H_2SiOH^+ are kinetically stable to the 1,2-H shifts. In addition, H_2SiSH^+ and H_2SiOH^+ are calculated to be 22.5 (21.5 after ZPC) and 15.4 (17.7 after ZPC) kcal/mol more stable, respectively, than the 1,2-H shifted isomers. Apparently, silicon has a much smaller tendency for divalency in cationic species than in neutral species.

Proton Affinities. Table IX compares the calculated proton affinities of $H_2Si=S$, $H_2Si=O$, and $H_2C=O$ at several levels of theory. The zero-point corrected MP3/6-31G**//6-31G* value of 174.7 kcal/mol for $H_2C=O$ agrees well with the experimental value of 177.2 kcal/mol.[27]

The proton affinities increase in the order $H_2C=O$ (174.7 kcal/mol)< $H_2Si=S$ (190.5 kcal/mol)< $H_2Si=O$ (208.3 kcal/mol). This is explained in terms of the predominance of the electrostatic over frontier orbital interactions, because the charge separations in the double bonds increase in the order $H_2C^{\underline{+0.2}}O^{-0.4}$< $H_2Si^{\underline{+0.7}}S^{-0.4}$< $H_2Si^{\underline{+1.0}}O^{-0.7}$ (Table V) while the frontier n orbital levels rise in the order $H_2C=O$ (-11.8 eV) $\leq$ $H_2Si=O$ (-11.9 eV) < $H_2Si=S$ (-9.8 eV) (Figure 4).

D. Reactivity toward Polar Reagents

In an attempt to characterize the reactivity of silanethione toward polar reagents, we have calculated the potential energy surface for the reaction of $H_2Si=S$ with water as a typical example.

As Figure 7 shows, the reaction of $H_2Si=S$ with water initiates the formation of a two-center-like complex with maximum interaction between the oxygen and silicon atoms. The intermediate complex is transformed via a four-center-like transition state to the product $HOSiH_2SH$. The HF/6-31G* structural parameters of the complex, transition state, and product are given in Table X. It is

to be noted that the overall feature of the structural changes in the $H_2Si{=}S + H_2O$ reaction is essentially the same as that calculated previously[5] in the $H_2Si{=}O + H_2O$ reaction, except that the former reaction involves a somewhat "later" transition state than does the latter reaction.

Figure 8 compares the energy profiles for these reactions at the MP3/6-31G*//6-31G* level. It is to be noted that the energy profile for the $H_2Si{=}S + H_2O$ reaction differs considerably from that for the $H_2Si{=}O + H_2O$ reacion. The $H_2Si{=}S + H_2O$ reaction involving a "later" transition state is 23 kcal/mol less exothermic than the $H_2Si{=}O + H_2O$ reaction. Silanethione complexes with water with a stabilization energy of 17.2 kcal/mol more weakly than does silanone with a stabilization of 21.1 kcal/mol. The $H_2Si{=}S + H_2O$ complex must surmount a considerable barrier of 11.5 kcal/mol to accomplish the reaction while the $H_2Si{=}O + H_2O$ complex proceeds just across a small barrier of 4.8 kcal/mol to the silanediol product.

What factors are responsible for the difference in the reactions between silanethione and silanone? As Figure 4 shows, the frontier orbital π (-10.3 eV) and π^* (0.5 eV) energy levels of silanethione are 2.0 eV higher and 1.0 eV lower, respectively, than the π (-12.3 eV) and π^* (1.5 eV) levels of silanone. If the reactions would be "frontier-controlled", one should see a more facile attack of water on silanethione than on silanone. As seen in Figure 8, this is not the case. Apparently, the difference in the reactivity of silanethione and silanone is due to the fact

that the silicon-sulfur double bond is less strongly polarized than the silicon-oxygen double bond.

Despite the difference, silanethione is still too reactive to be isolated under normal conditions. In the interest in preparing an isolable silanethione, one should note that the transition state for the $H_2Si{=}S + H_2O$ reaction lies only 5.7 kcal/mol below the reactants, in marked contrast with the energy difference of 16.3 kcal/mol between the reactants and transition state in the $H_2Si{=}O + H_2O$ reaction. This means that the reactivity of silicon-sulfur double bonds can be more easily controlled not only by the steric effect of very bulky substituents but also by the electronic effect of relatively small substituents.[28] In order that silanethiones become as popular as formaldehydes, it is desirable that protecting substituents are as small as possible. Obviously, the electronic effect of small substituents should reduce further the dipolar character in the silicon-sulfur double bond of $H_2Si{=}S$ (and increase the HOMO-LUMO energy gap).

Concluding Remarks

Comparisons with silanone as well as formaldehyde reveal several intriguing aspects of the structural and energetic properties of silanethione in the ground, excited, and protonated states. An important finding is that silicon is much less reluctant to form doubly bonding with sulfur than with oxygen. Thus, silanethione is more stable and less reactive than silanone. The major obstacle to

the successful isolation of silanethione is the relatively high reactivity. In the interest in designing an isolable silanethione, the hydrogen atoms in $H_2Si=S$ should be replaced by substituents that deduce the polarity of the silicon-sulfur double bond. A theoretical study along this line is in progress.

Acknowledgement. All calculations were carried out at the Computer Center of the Institute for Molecular Science and at the Computer Center of Tokyo University with the IMSPAK (WF10-8) and GAUSSIAN 80 (WF10-24) programs in IMS Computer Center library program package. We are grateful to Dr. D. A. Dixon for sending a preprint of ref 21 prior to publication.

References and Notes

(1) For recent comprehensive reviews, see: (a) Gusel'nikov, L. E.; Nametkin, N. S. Chem. Rev. 1979, 79, 529. (b) Coleman, B.; Jones, M. Rev. Chem. Intermed. 1981, 4, 297. (c) Bertrand, G.; Trinquier, G.; Mazerolles, P. J. Organomet. Chem. Library 1981, 12, 1. (d) Schaefer, H. F. Acc. Chem. Res. 1982, 15, 283. (e) Wiberg, N. J. Organomet. Chem. 1984, 273, 141. (f) West, R. Science (Washington, D.C.) 1984, 225, 1109.

(2) Brook, A. G.; Abdesaken, F.; Gutekunst, B.; Gutekunst, G.; Kallury, R. K. J. Chem. Soc., Chem. Commun. 1981, 191. Brook, A. G.; Nyburg, S. C.; Abdesaken, F.; Gutekunst, B.; Gutekunst, G.; Kallury, P. K. M. R.; Poon, Y. C.; Chang, Y. -N. ; Wong-Ng, W. J. Am. Chem. Soc. 1982, 104, 5667.

(3) West, R.; Fink, M. J.; Michl, J. Science (Washington, D.C.) 1981, 214, 1343. For a current review, see ref 1(f).

(4) Kudo, T.; Nagase, S. J. Organomet. Chem. 1983, 253, C23.

(5) Kudo, T.; Nagase, S. J. Phys. Chem. 1984, 88, 2833.

(6) Kudo, T.; Nagase, S. J. Am. Chem. Soc. 1985, 89, 0000.

(7) Gusel'nikov, L. E.; Sokolova, V. M.; Volnina, E. A.; Zaikin, V. G.; Nametkin, N. S.; Voronkov, M. G.; Kirpichenko, S. V.; Keiko, V. V. J. Organomet. Chem. 1981, 214, 145. Gusel'nikov, L. E.; Volkova, V. V.; Zaikin, V. G.; Tarasenko, N. A.; Tishenkov, A. A.; Nametkin, N. S.; Voronkov, M. G.; Kirpichenko, S. V. J. Organomet. Chem. 1981, 215, 9. Carlson, C. W.; West, R. Organometallics 1983, 2, 1798. Guimon, C.;

Pfister-Guillouzo, G.; Lavayssiere, H.; Dousse, G.; Barrau, J.; Satge, J. J. Organomet. Chem. 1983, 249, C17. Gusel'nikov, L. E.; Volkova, V. V.; Avakyan, V. G.; Nametkin, N. S.; Voronkov, M. G.; Kirpichenko, S. V.; Suslova, E. N. J. Organomet. Chem. 1983, 254, 173. Gusel'nikov, L. E.; Volkova, V. V.; Avakyan, V. G.; Volnina, E. A.; Zaikin, V. G.; Nametkin, N. S.; Polyakova, A. A.; Tokarev, M. I. J. Organomet. Chem. 1984, 271, 191.

(8) Bernardi, F.; Csizmadia, I. G.; Schlegel. H. B.; Wolfe, S. Can. J. Chem. 1975, 53, 1144. Bernardi, F.; Csizmadia, I. G.; Mangini, A.; Schlegel, H. B.; Whangbo, M. -H.; Wolfe, S. J. Am. Chem. Soc. 1975, 97, 2209. Pau, J. K.; Ruggera, M. B.; Kim, J. K.; Caserio, M. C. J. Am. Chem. Soc. 1978, 100, 4242. Dill, J. D.; Mclafferty, F. W. J. Am. Chem. Soc. 1979, 101, 6526. Yamabe, T.; Yamashita, K.; Fukui, K.; Morokuma, K. Chem. Phys. Lett. 1979, 63, 433. Grein, F. Can. J. Chem. 1984, 62, 253. Nobes, R. H.; Bouma, W. J.; Radom, L. J. Am. Chem. Soc. 1984, 106, 2774.

(9) Schleyer, P. v. R.; Jemmis, E. D. J. Chem. Soc., Chem. Commun. 1978, 190. Dill, J. D.; Fischer, C. L.; Mclafferty, F. W. J. Am. Chem. Soc. 1979, 101, 6531. Nobes, R. H.; Radom, L.; Rodwell, W. R. Chem. Phys. Lett. 1980, 74, 269.

(10) Francl, M. M.; Pietro, W. J.; Hehre, W. J.; Binkley, J. S.; Gordon, M. S.; DeFrees, D. J.; Pople, J. A. J. Chem. Phys. 1982, 77, 3654.

(11) Pople, J. A.; Binkley, J. S.; Seeger, R. Int. J. Quantum

Chem., Quantum Chem. Symp. 1976, 10, 1.

(12) Langhoff, S. R.; Davidson, E. R. Int. J. Quantum Chem. 1974, 8, 61. Davidson, E. R.; Silver, D. W. Chem. Phys. Lett. 1978, 52, 403.

(13) Gordon, M. S.; Binkley, J. S.; Pople, J. A.; Pietro, W. J.; Hehre, W. J. J. Am. Chem. Soc. 1982, 104, 2797. For comparable accuracy of HF/3-21G and HF/6-31G* vibrational frequencies, see: Pople, J. A.; Schlegel, H. B.; Krishnan, R. ; DeFrees, D. J.; Binkley, J. S.; Frisch, M. J.; Whiteside, R. A.; Hout, R. F.; Hehre, W. J. Int. J. Quantum Chem., Quantum Chem. Symp. 1981, 15, 269.

(14) Harding, L. B.; Schlegel, H. B.; Krishnan, R.; Pople, J. A. J. Phys. Chem. 1980, 84, 3394.

(15) Goddard, J. D.; Schaefer, H. F. J. Can. Phys. 1979, 70, 5117.

(16) Hout, R. F.; Levi, B. A.; Hehre, W. J. J. Comput. Chem. 1982, 3, 234.

(17) Arrington, C. A.; West, R.; Michl, J. J. Am. Chem. Soc. 1983, 105, 6176.

(18) In our recent study[6], the formation of the cyclic dimer $(H_2SiO)_2$ from $H_2Si{=}O$ is calculated to be 109.4 kcal/mol exothermic at the MP2/6-31G*//6-31G* level, while the corresponding reaction $2H_2Si{=}S \rightarrow (H_2SiS)_2$ is 70.8 kcal/mol exothermic. The much larger exothermicity in the $H_2Si{=}O$ dimerization results undoubtedly from the cleavage of the weaker SiO π bonds (compared with the SiS π bonds) and the formation of the stronger SiO single bonds (compared with the SiS single bonds).

(19) In fact, the dissociation energy (128 kcal/mol) for $H_2Si{=}O \rightarrow H_2Si(^1A_1) + O(^3P)$ is calculated to be 32 kcal/mol larger at the MP3/6-31G**//6-31G* level than that (96 kcal/mol) for $H_2Si{=}S \rightarrow H_2Si(^1A_1) + S(^3P)$.

(20) Herzberg, G. "Electronic Spectra of Polyatomic Molecules", Van Nostrand: New York, 1966.

(21) Glinski, R. J.; Gole, J. L.; Dixon, D. A. J. Am. Chem. Soc., submitted for publication (private communication from Dr. Dixon).

(22) For the calculations of the higher singlet, triplet, and Rydberg excited states at the MRD-CI level, see: Kudo, T.; Nagase, S. (manuscript in preparation).

(23) At the lower levels of theory, however, two Jahn-Teller-distorted structures were located.

(24) The HF/6-31G* structure has SiS = 2.081 Å, SiH = 1.456 Å, SH = 1.336 Å, ∠HSSi = 95.0°, ∠HSiS = 121.2°, and ∠HSiSH = 91.5°.

(25) The HF/6-31G* structure has SiO = 1.530 Å, SiH = 1.450 Å, OH = 0.946 Å, ∠HSiO = 118.6°.

(26) The Walsh rule suggests a pyramidalized C_{3v} structure for the parent cations ; the structure of SH_3^+ is twice more pyramidalized than that of OH_3^+, as characterized by the respective out-of-plane angles θ (θ=0 for a planar structure) of 79.5 and 44.7° at the HF/6-31G* level. Introduction of an electron-donating SiH group relaxes the degree of pyramidalization by producing a more positive charge on the central atom.

(27) Aue, D. H.; Bowers, M. T. In "Gas Phase Ion Chemistry"; Bowers, M. T., Ed.; Academic Press: New York, 1979; Vol. 2, pp 1-51.

(28) For a theoretical attempt to reduce the reactivity of slicon-carbon double bonds by the electronic effect, see: Nagase, S.; Kudo, T.; Itoh, K. In "The Proceedings of the Applied Quantum Chemistry Symposium"; Smith, V. H. et al. Eds.; D. Reidel Publishing: Dordrecht, Netherland, 1985; pp 000-000.

Table I. HF/6-31G* vibrational Frequencies (cm^{-1}) of $H_2Si{=}X$ (X= S and O)[a]

symmetry and mode	$H_2Si{=}S$	$H_2Si{=}O$[b]
a_1 SiH_2 s-stretch	2424 (2153)	2433 (2160)
a_1 SiX stretch	768 (682)	1356 (1203)
a_1 SiH_2 scis.	1110 (986)	1125 (1000)
b_1 SiH_2 a-stretch	2427 (2155)	2432 (2159)
b_1 SiH_2 rock	686 (609)	787 (699)
b_2 SiH_2 wag	724 (643)	812 (721)

a Values in parentheses are scaled-down frequencies (see text). b Taken from ref 5.

Table II. Total Energeis (hartrees) of the H_2SiS Species Based on HF/6-31G* Structures

	6-31G*	6-31G**		
species	HF	HF	CI(S+D)	CI(S+D+QC)
$H_2Si{=}S$	-687.58729	-687.59037	-687.80797	-687.82984
$H_2{+}SiS$	-687.56830	-687.57285	-687.79847	-687.82376
HSiSH(cis)	-687.56604	-687.57140	-687.78834	-687.81075
HSiSH(trans)	-687.56978	-687.57515	-687.79252	-687.81499
A[a]	-687.46967	-687.47502	-687.70913	-687.73819
B[a]	-687.54202	-687.54775	-687.76216	-687.78418
C[a]	-687.43427	-687.44254	-687.67558	-687.70365

a Transition structures in Figure 2.

Table III. Relative Energies (kcal/mol) of the H_2SiS Species Based on HF/6-31G* Structures

	6-31G*	6-31G**		
species	HF	HF	CI(S+D)	CI(S+D+QC)
$H_2Si{=}S$	0.0	0.0	0.0	0.0
H_2+SiS	11.9	11.0	6.0	3.8
HSiSH(cis)	13.3	11.9	12.3	12.0
HSiSH(trans)	11.0	9.6	9.7	9.3
A[a]	73.8	72.4	62.0	57.5
B[a]	28.4	26.7	28.7	28.7
C[a]	96.0	92.8	83.1	79.2

a Transition structures in Figure 2.

Table IV. HF/6-31G* Optimized Structures for the $^3A''(n-\pi^*)$ and $^3A'(\pi-\pi^*)$ States of H_2SiX (X=S or O)

structural parameters[a]	$^3A''(n-\pi^*)$		$^3A'(\pi-\pi^*)$	
	H_2SiS	H_2SiO	H_2SiS	H_2SiO
Si-X	2.147	1.686	2.182	1.714
Si-H	1.477	1.478	1.475	1.476
∠HSiH	110.7	111.4	109.2	109.4
θ[b]	57.3	59.8	52.9	54.5

a Lengths in angstroms and angles in degrees. b Out-of-plane angles (see text).

Table V. Net Atomic Charge Densities and Dipole Moments (D) for the Ground ($^1A_1$) and Excited ($^3A''$ and $^3A'$) States of H_2SiX (X= S or O) at the HF/6-31G**//6-31G* Level

states	atomic charge densities			dipole moments
	Si	X	H	
		H_2SiS		
$^1A_1$(ground)	0.673	-0.416	-0.129	3.72
$^3A''(n-\pi^*)$	0.496	-0.234	-0.131	1.53
$^3A'(\pi-\pi^*)$	0.527	-0.255	-0.136	1.67
		H_2SiO		
$^1A_1$(ground)	0.998	-0.680	-0.159	4.14
$^3A''(n-\pi^*)$	0.726	-0.426	-0.150	1.77
$^3A'(\pi-\pi^*)$	0.769	-0.443	-0.163	1.76

Table VI. Singlet-Triplet Adiabatic Separation Energeis(eV) in H_2SiS, H_2SiO, and H_2CO Based on HF/6-31G* Structures

level of theory	H_2SiS		H_2SiO		H_2CO	
	$^3A''$	$^3A'$	$^3A''$	$^3A'$	$^3A''$	$^3A'$
HF/6-31G*	0.94	1.16	1.05	1.32	1.95	2.89
HF/6-31G**	0.94	1.16	1.06	1.32	1.94	2.88
MP2/6-31G**	1.89	2.20	2.85	3.19	3.43	4.66
MP3/6-31G**	1.75	2.05	2.31	2.65	3.06	4.22

Table VII. Total Energeis (hartrees) of the Protonated States of $H_2Si{=}S$ and $H_2Si{=}O$ Based on HF/6-31G* Structures

species		6-31G*	6-31G**		
		HF	HF	MP2	MP3
H_2SiSH^+	($^1A'$)	-687.89420	-687.90165	-688.10715	-688.13442
H_3SiS^+	($^1A'$)	-687.77651	-687.78124	-687.96604	-688.00051
H_3SiS^+	($^3A_1$)	-687.86160	-687.86632	-688.03619	-688.06801
$HSiSH_2^+$		-687.85603	-687.86500	-688.06618	-688.09852
D[a]		-687.76133	-687.77223	-688.00221	-688.03090
H_2SiOH^+	($^1A'$)	-365.25793	-365.26907	-365.53073	-365.54241
H_3SiO^+	($^1A'$)	-365.01832	-365.02327	-365.23588	-365.26752
H_3SiO^+	($^3A_1$)	-365.14560	-365.15053	-365.33528	-365.36507
$HSiOH_2^+$	($^1A'$)	-365.22414	-365.23891	-365.49962	-365.51786
E[a]		-365.11292	-365.12773	-365.41123	-365.42082

a Transition structures in Figure 6.

Table VIII. Relative Energies (kcal/mol) of Protonated States of $H_2Si{=}S$ and $H_2Si{=}O$ Based on HF/6-31G* Structures

	6-31G*	6-31G**		
species	HF	HF	MP2	MP3
H_2SiSH^+ ($^1A'$)	0.0	0.0	0.0	0.0
H_3SiS^+ ($^1A'$)	73.9	75.6	88.5	84.0
H_3SiS^+ ($^3A_1$)	20.5	22.2	44.5	41.7
$HSiSH_2^+$	24.0	23.0	25.7	22.5
D[a]	83.4	81.2	65.9	65.0
H_2SiOH^+ ($^1A'$)	0.0	0.0	0.0	0.0
H_3SiO^+ ($^1A'$)	150.4	154.2	185.0	172.5
H_3SiO^+ ($^3A_1$)	70.5	74.4	122.6	111.3
$HSiOH_2^+$ ($^1A'$)	21.2	18.9	19.5	15.4
E[a]	91.0	88.7	75.0	76.3

a Transition structures in Figure 6.

Table IX. Proton Affinities (kcal/mol) Calculated on HF/6-31G* Structures

level of theory	$H_2Si=S$	$H_2Si=O$	$H_2C=O$
HF/6-31G*	192.6	215.6	182.0
HF/6-31G**	195.4	220.6	186.6
MP2/6-31G**	193.1	209.4	180.3
MP3/6-31G**	196.1	215.7	183.2
+ ZPC	190.5	208.3	174.7

Table X. Structures and Total Energies Calculated for the Reaction of $H_2Si{=}S$ with H_2O

	complex	transition state	product
Bond Distances, Bond Angles, and Dihedral Angles[a]			
SiS	1.975	2.055	2.146
SiO	2.007	1.795	1.640
SiH1	1.469	1.465	1.464
SiH2	1.475	1.471	1.470
SH3	2.938	1.726	1.329
OH3	0.958	1.215	—
OH4	0.954	0.954	0.947
SSiO	103.7	87.6	112.9
SSiH1	123.6	121.5	111.1
SSiH2	123.5	120.9	103.0
SiSH3	56.1	62.7	98.2
SiOH3	106.9	80.0	—
SiOH4	115.9	120.2	119.2
H1SiSO	-105.7	-108.2	-118.3
H2SiSO	102.1	106.1	121.7
H3SSiO	3.4	-1.4	63.2
H4OSiS	111.7	116.3	54.9
Total Energies in hartrees[b]			
HF/6-31G*	-763.62617	-763.59800	-763.68239
MP2/6-31G*[c]	-764.00931	-763.99422	-764.05910
MP3/6-31G*[c]	-764.03407	-764.01574	-764.08537

a HF/6-31G* structures in angstroms and degrees. For the numberings of atoms, see Figure 7. b Total energies of reactants are -763.59804 (HF/6-31G*), -763.97942 (MP2/6-31G*), and -764.00672 (MP3/6-31G*). c Calculated at the HF/6-31G* structures.

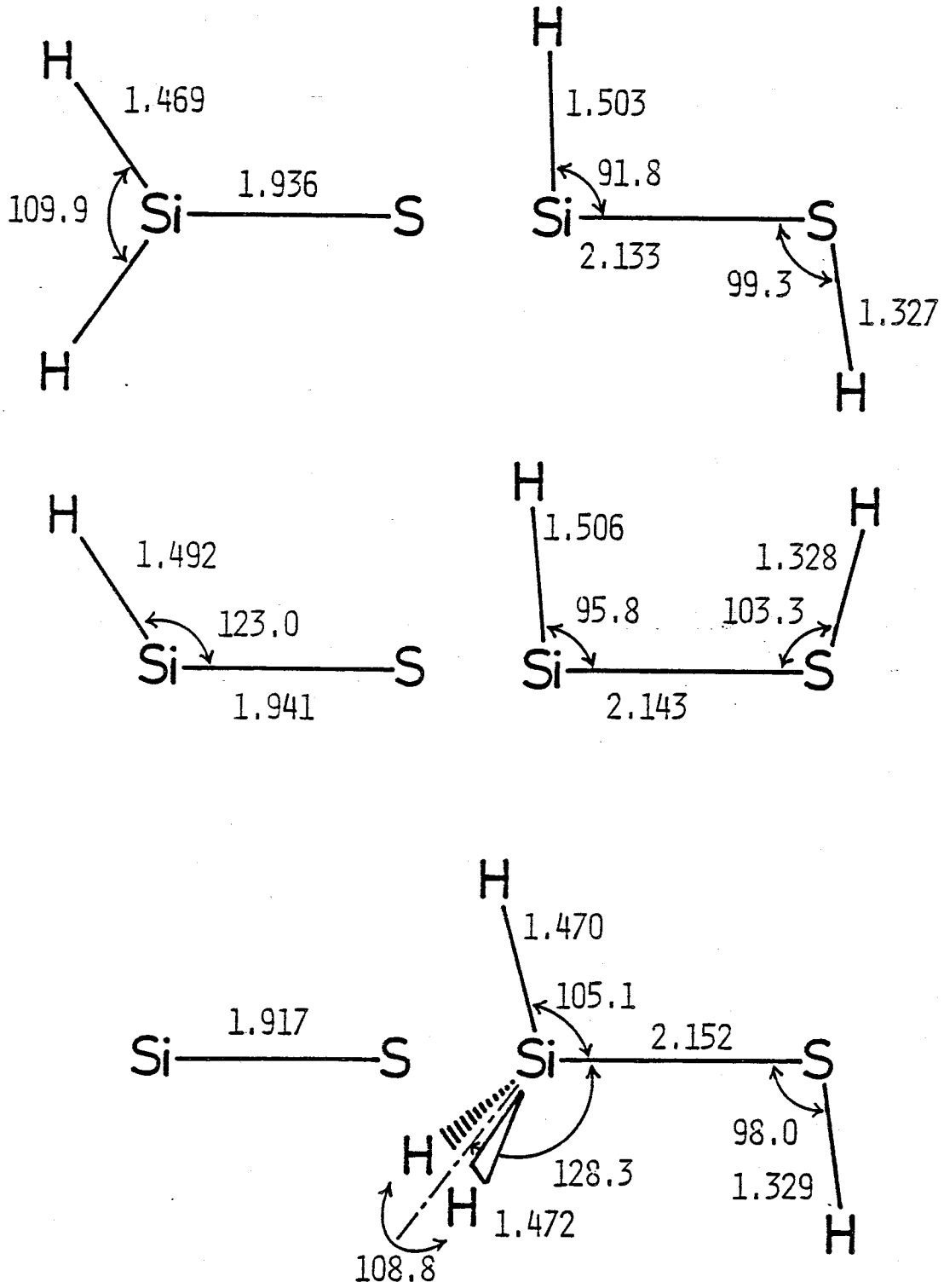

Figure 1. Equilibrium structures in angstroms and degrees calculated at the HF/6-31G* level.

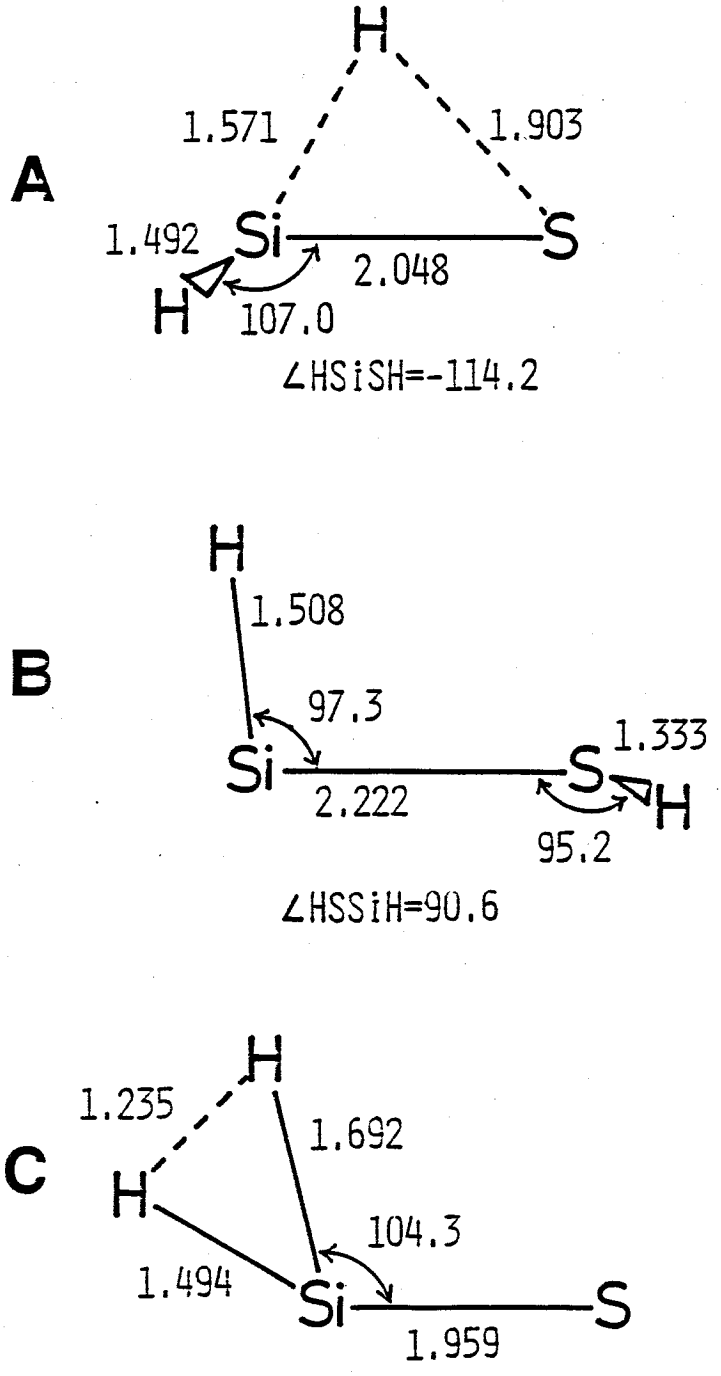

Figure 2. Transition structures in angstroms and degrees calculated at the HF/6-31G* level.

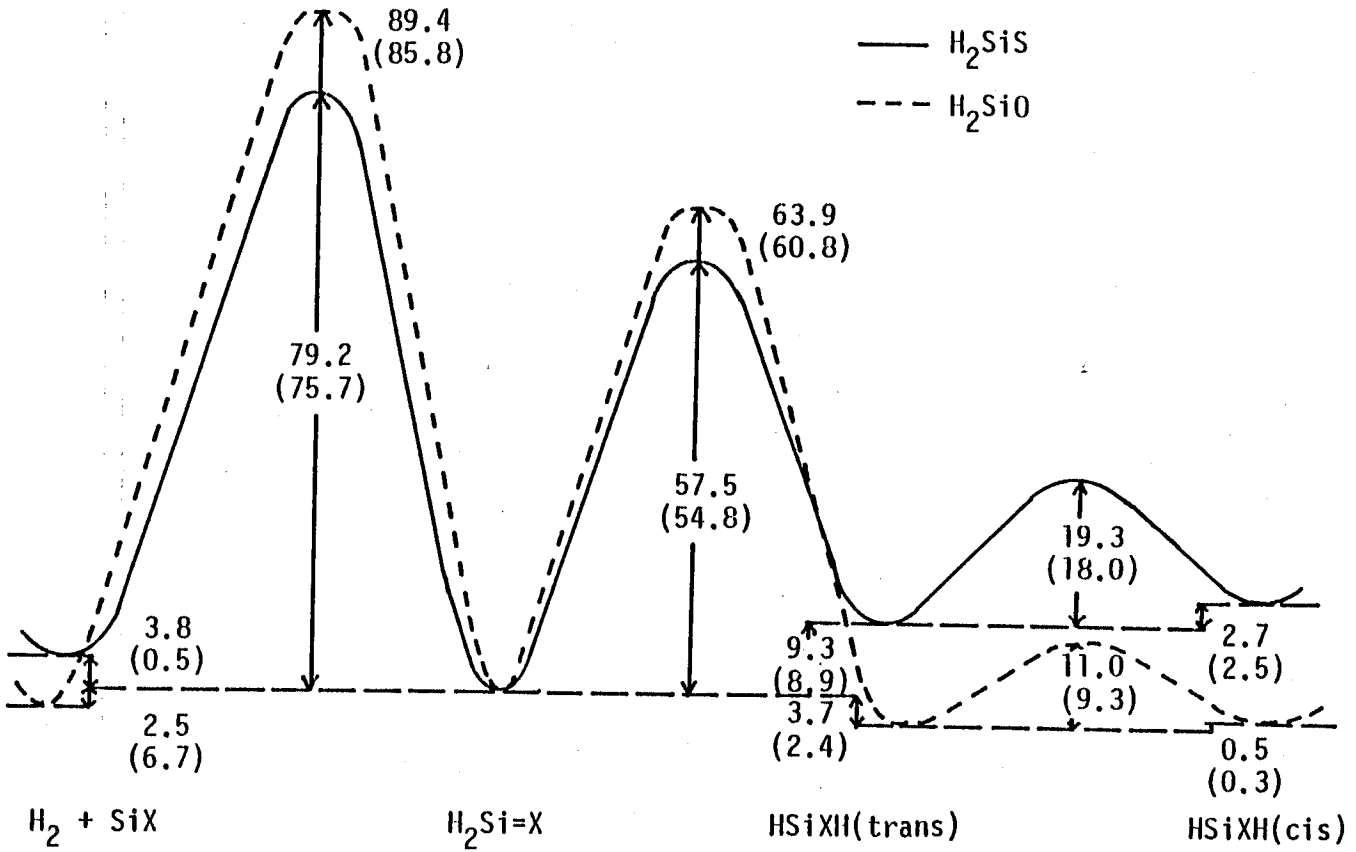

Figure 3. Schematic comparison of the energy profiles (kcal/mol) of H_2SiS (full line) and H_2SiO (dotted line) at the CI(S+D+QC)/6-31G**//6-31G* level. The zero-point corrected values are in parentheses.

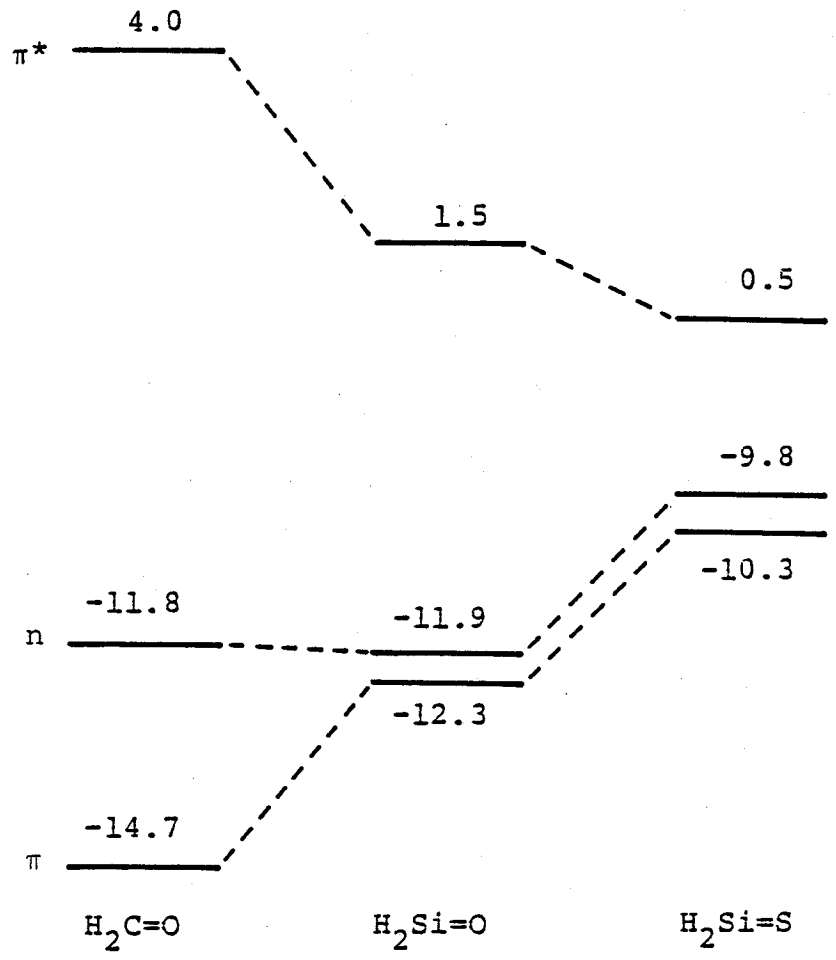

Figure 4. Frontier orbital energy levels (eV) of $H_2C{=}O$, $H_2Si{=}O$, and $H_2Si{=}S$ at the HF/6-31G**//6-31G* level.

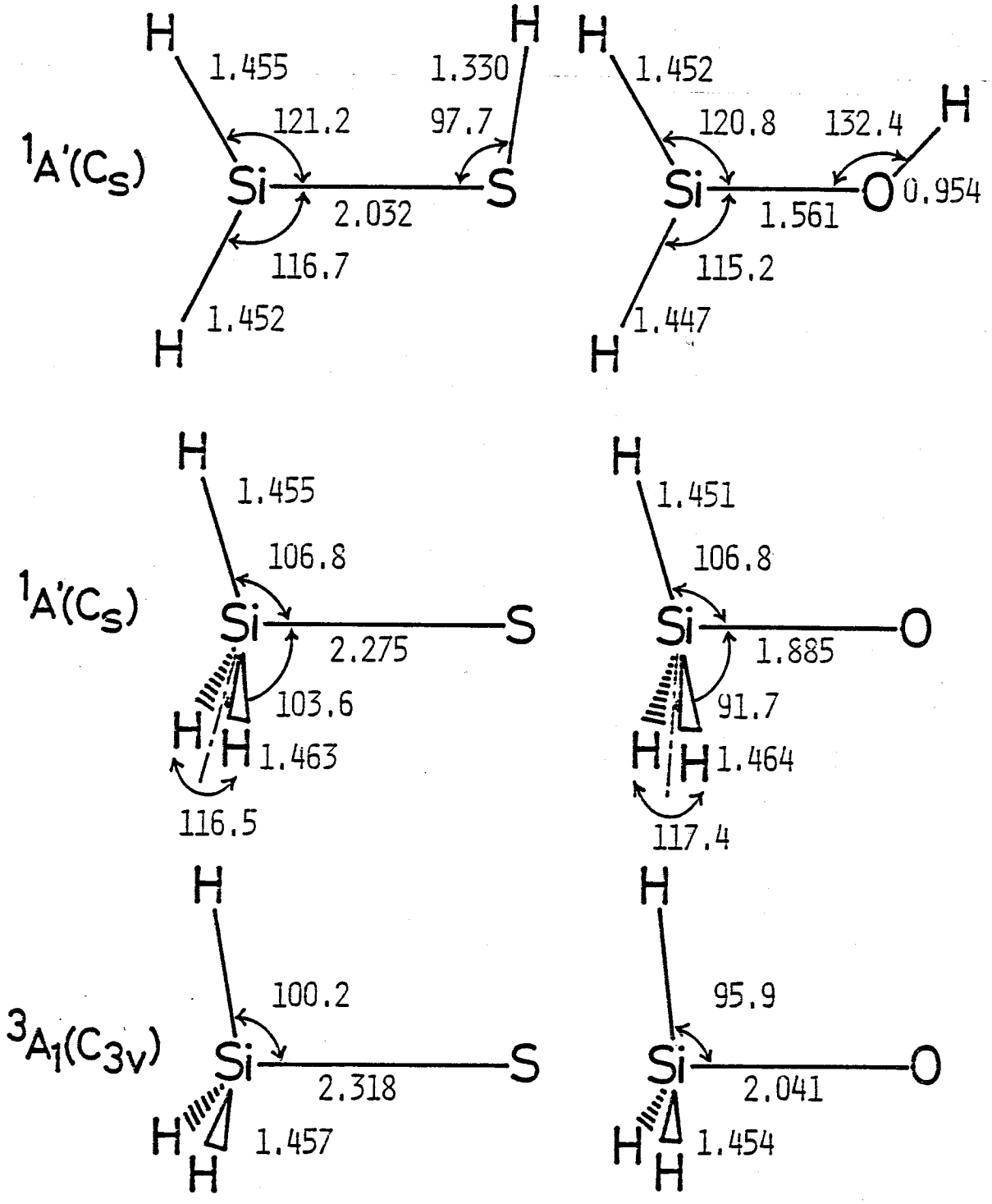

Figure 5. HF/6-31G* structures of the SiH_3S^+ and SiH_3O^+ species in angstroms and degrees.

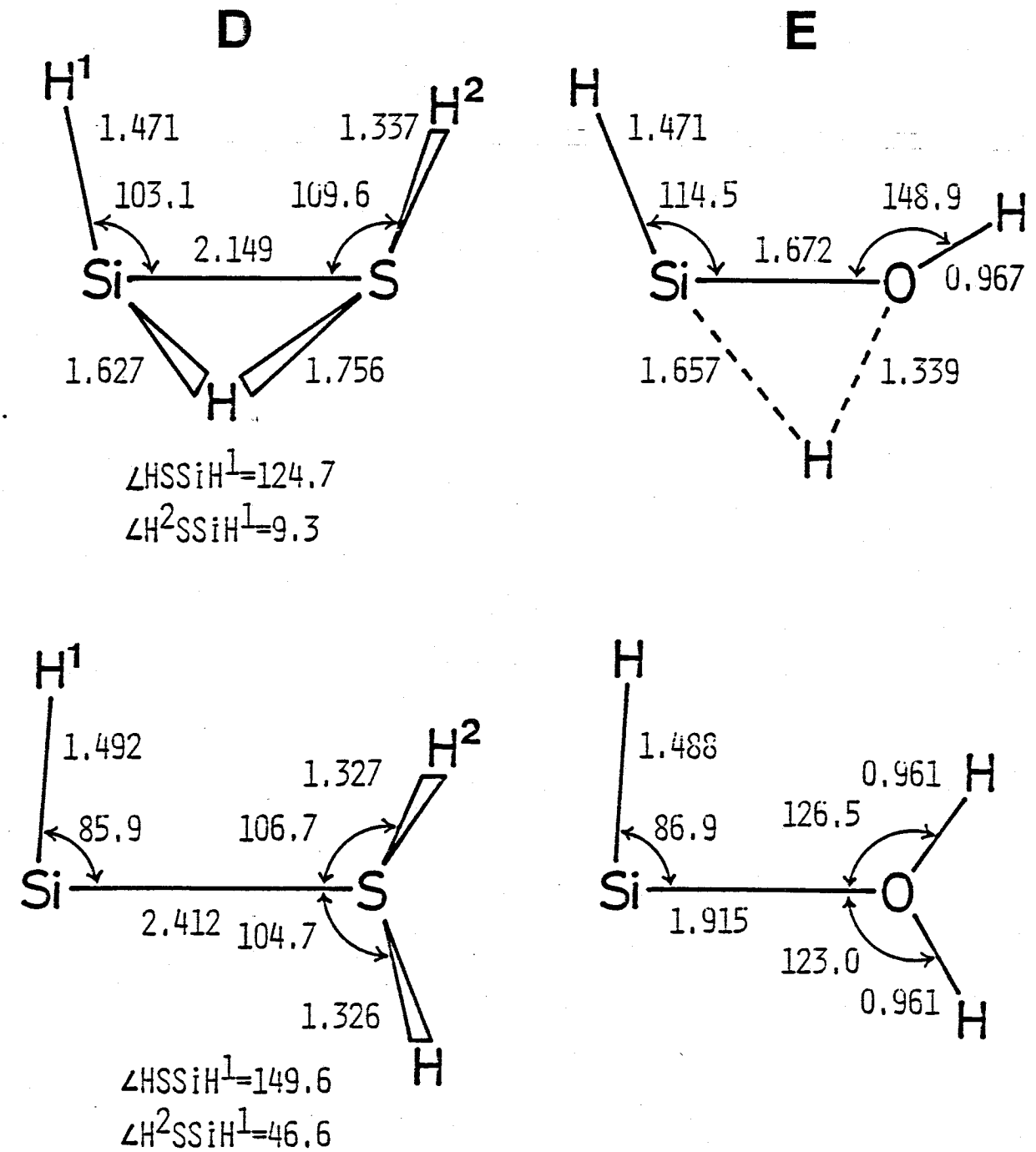

Figure 6. HF/6-31G* optimized structures of the transition states (D and E) and the products for the 1,2-H shifts in H_2SiSH^+ and H_2SiOH^+.

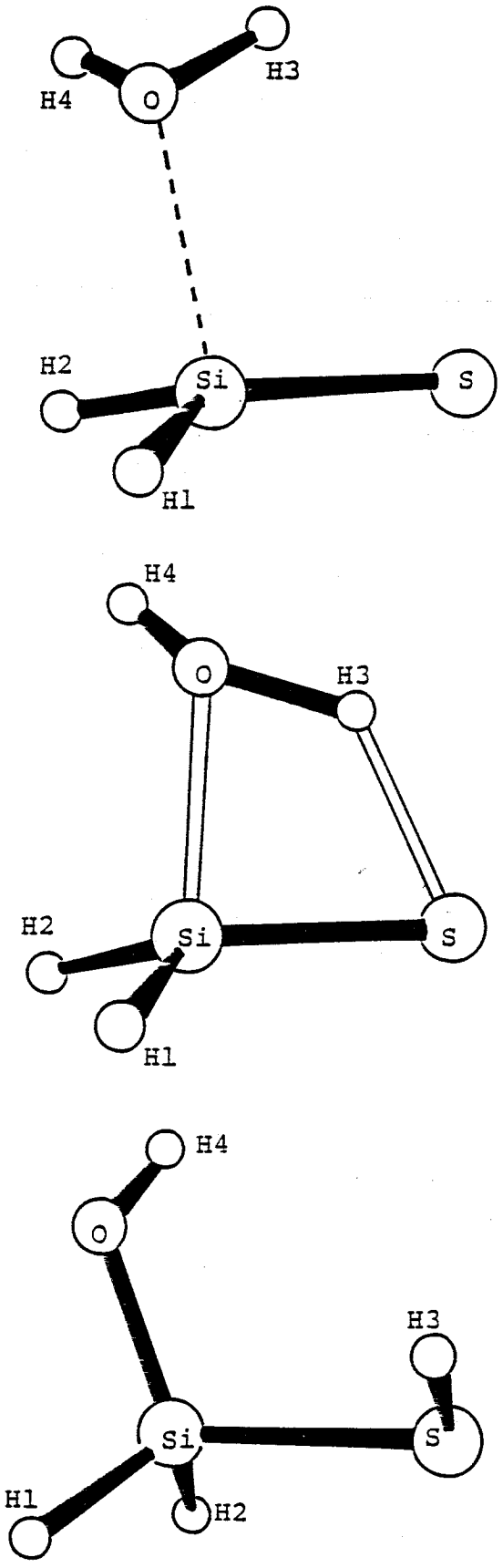

Figure 7. ORTEP drawings of an intermediate complex (top), the product (bottom), and the transition state (middle) connecting them, calculated at the HF/6-31G* level for the H_2O + H_2SiS reaction.

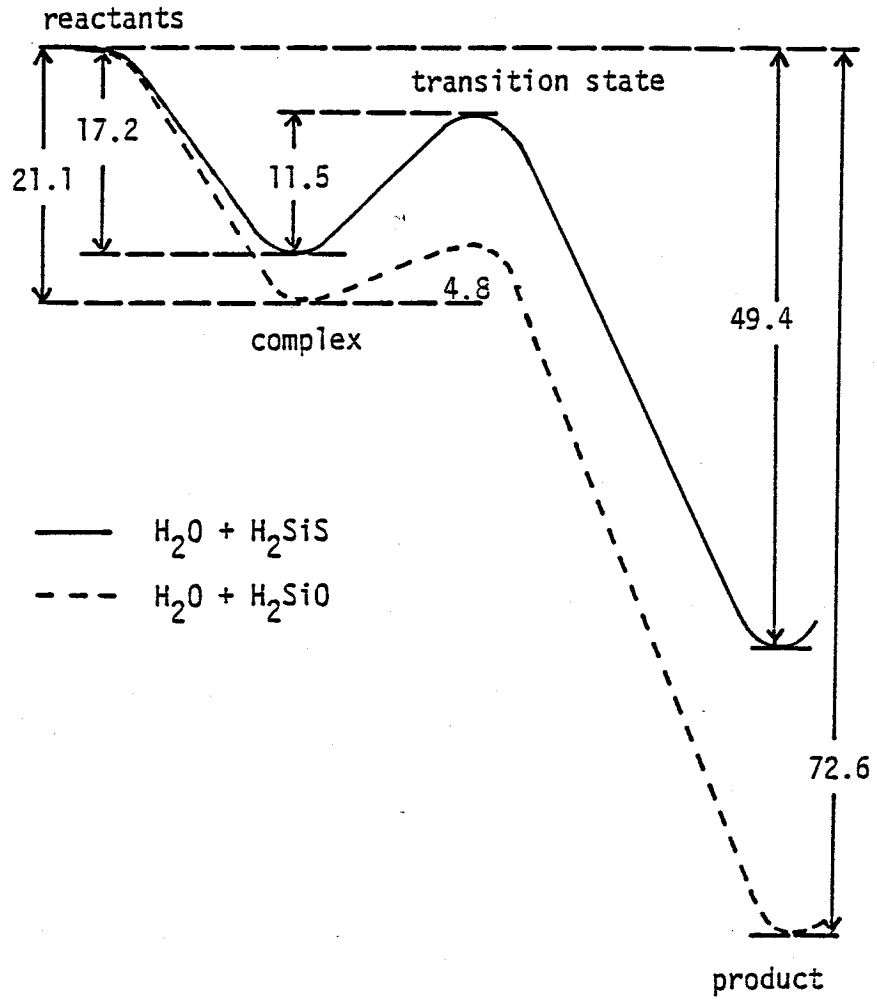

Figure 8. Energy profiles (kcal/mol) at the MP3/6-31G* level for the $H_2O + H_2SiS$ (full line) and $H_2O + H_2SiO$ (dotted line) reactions.

Part III

Germanium - Carbon and Germanium - Germanium Double Bonds

CHAPTER 1

The Relative Stability of Germaethene and Its Isomers

In an attempt to examine the properties of a germanium-carbon double bond, title species were calculated with the ab initio SCF method. The geometry, proton affinity, and thermodynamic stability of $H_2Ge{=}CH_2$ were discussed in comparison with the previous data on $H_2C{=}CH_2$ and $H_2Si{=}CH_2$.

1. Introduction

For many years multiple bonds of group 4B elements have been receiving great interest in organometallic chemistry, as has recently been reviewed[1]. Now that the existence of silicon-carbon double-bonded intermediates has become established, attention should naturally been directed towards the search for the corresponding germanium analogues. At present a few experimental reports[2-5] are available which give evidence consistent with the transient existence of compounds containing a (p,p) π germanium-carbon double bond. Despite an upsurge of interest, up to now a germanium double bond has not been subjected to theoretical investigations except for only one semiempirical CNDO/2 study by Gowenlock and Hunter[6].

We here report the first ab initio SCF MO study of the parent compound $H_2Ge{=}CH_2$ in the anticipation that such theoretical information would be useful for further experimental considerations. The calculations were carried out to determine the geometry of germaethylene and to provide information concerning its proton affinity and its thermodynamic stability to isomerization in comparison with the previous data on ethene and silaethene at the comparable levels of calculations.

2. Computational Details

All calculations with at least a double zeta (DZ) basis set are for closed-shell singlets and within the framework of the restricted Hartree-Fock SCF approximation. The basis set for Ge

was obtained from the Dunning's (13s9p5d) primitive set[7]. The contraction schemes used were as follows. In Basis A (DZ), a contracted [6s4p1d] set[8,9] for Ge and the 4-31G set[10] for C and H were used. Except the seventh primitive s function is uncontracted[8], the [6s4p1d] set is in the spirit of the 4-31G basis set[8]. In Basis B (DZ + POL), a less contracted [7s5p3d] set[8] for Ge and the 6-31G** set[11,12] for C and H which included polarization (POL) functions were used. For POL functions for Ge, a set of d functions (exponent 0.25) was added, where overall s-type functions constructed from $d_{xx}+ d_{yy}+ d_{zz}$ were retained.

All geometries were fully optimized with Basis A. Incidentally, Basis A gave the bond distance of 1.524 Å to GeH_4 as compared to the experimental value of 1.527 Å[13]. Single point calculations were then carried out with Basis B at the geometries determined by Basis A.

3. Results and Discussion

3.1. Thermodynamic stabilities of $CGeH_4$ isomers

We first examined the thermodynamic stabilities for isomerization of $H_2Ge=CH_2$ to methylgermylene and germylmethylene.

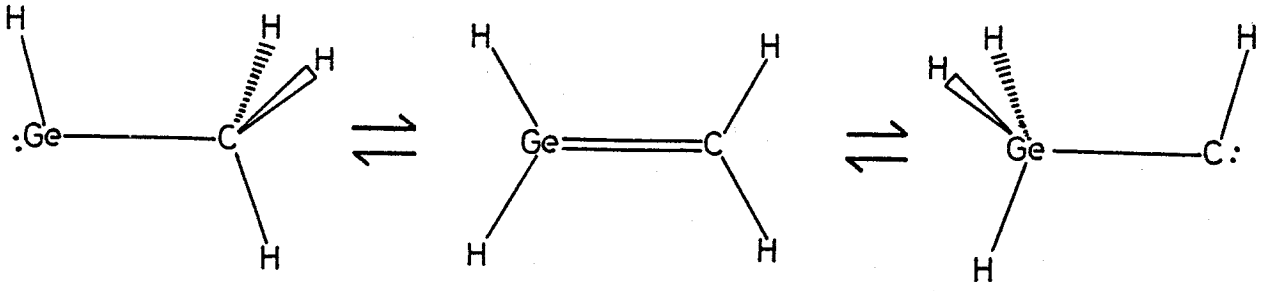

Chart 1

The optimized geometries of these isomers are shown in Figs.1 and 2. The calculated energies relative to $H_2Ge{=}CH_2$ are collected in Table 1 together with the values[14] of the corresponding silicon analogues. As in the silicon analogues, $H_3Ge\ddot{C}H$ is most unstable and lies 65.8 (Basis A) and 56.8 (Basis B) Kcal/mol higher in energy than $H_2Ge{=}CH_2$. $H\ddot{G}eCH_3$ is calculated to be more stable than $H_2Ge{=}CH_2$ and to lie 27.4 (Basis A) and 22.7 (Basis B) Kcal/mol lower in energy. When the energy differences of $H_2Ge{=}CH_2$ and $H\ddot{G}eCH_3$ are compared with those of $H_2Si{=}CH_2$ and $H\ddot{S}iCH_3$ at the similar levels of calculations in Table 1, a noticeable point is that the former differences are much larger than the latter. This suggests that the Ge atom is more reluctant to form a double-bonded compound than is the Si atom.

As was noted in the silicon analogues[14,15], effects of electron correlation (not considered in the present work) will favor to place $H_2Ge{=}CH_2$ closer in energy to $H\ddot{G}eCH_3$. In addition, with a proper choice of substituents such as F and CH_3, a doubly bonded isomer will happen to become thermodynamically most stable, as recently demonstrated for substituted silaethenes[16]. Even if germaethene remains less stable in a thermodynamic sense, however, the existence of a germanium double bond would be likely in the absence of reactive trapping reagents since a significant barrier is expected in going from $H_2Ge{=}CH_2$ to $H\ddot{G}eCH_3$. In fact, a barrier for the 1,2-hydrogen shift reaction of $H_2Si{=}CH_2 \rightarrow H\ddot{S}iCH_3$ is predicted to be as large as $\sim$40 Kcal/mol[14], though the reaction

is approximately thermoneutral.

Divalent germanium species, which are formal analogues to carbenes, are receiving a recent theoretical interest[8,17]. Before we discuss the characteristics of the Ge=C double bond, let us compare briefly the present data on $H\ddot{G}eCH_3$ with the previous ones[17] on $H\ddot{G}eH$ and $CH_3\ddot{G}eCH_3$ obtained with a pseudopotential method at the DZ + POL level. As Table 2 shows, the regular trends are seen for the substitution of hydrogen atoms by methyl groups. The methyl group increases the 'germylenic' angle, as expected from the steric effect, while it decreases the ionization potential. A net charge on Ge is increased to some extent upon substitution, and the methyl group seems to work as an electron acceptor in divalent germanium species.

3.2. Properties of germaethene

For comparison purpose, the silaethene geometries calculated by Hood and Schaefer[18] and Ahlrichs and Heinzmann[19] are also given in Fig.1. The computed Ge=C double bond length of 1.756 Å is longer than 1.715[18] and 1.69 Å[19] for the Si=C bond, while other geometrical parameters for both molecules are of very similar values except for the Ge-H and Si-H single bonds. The HCH angle obtained by Ahlrichs and Heinzmann[19] is smaller by 3°.

The Si=C bond has been found to possess considerable dipolar character $H_2\overset{\delta+}{S}i{=}\overset{\delta-}{C}H_2$ rather than a diradical[20], as supported by theoretical calculations[19]. In contrast, Gowenlock and Hunter

[6] claimed based on their CNDO/2 calculations that the electron density was higher at the Ge atom in $H_2Ge=CH_2$ and that the polarity of the Ge=C bond was opposite to that found for the Si=C one. As Table 3 shows, however, in our calculations the Ge atom always bears a net positive charge and the C atom a net negative charge, this being described as $H_2\overset{\delta+}{G}e\!-\!\overset{\delta-}{C}H_2$. The Ge=C bond seems somewhat more strongly polar as compared with the Si=C one[19]. It is to be noted that the introduction of POL functions decreases the extent of charge separations. The total POL d orbital atomic populations were 0.272 for Ge and 0.033 for C, and significant use of the germanium vacant d orbitals was observed. Gowenlock and Hunter[6] also concluded from their bond-order analysis that $H_2Ge=CH_2$ had a relatively week σ bond and much stronger π bond. As far as one sees the atomic overlap population between Ge and C in Table 3, that π strength is smaller than the σ one and any unusual characteristics are not seen even in the Ge=C bond as compared with the Si=C bond.

The first ionization potentials ($-\varepsilon_{HOMO}$) obtained with Koopmans theorem were 8.4 (Basis A) and 8.3 eV (Basis B). These values are comparable with 8.6[19] and 8.4 eV (6-31G**) for $H_2Si=CH_2$ and significantly smaller than 10.3[19] and 10.2 eV (6-31G**) for $H_2C=CH_2$, where a 6-31G** basis set for the Si atom was taken from the Gordon's paper[21]. It is of interest to note that very recent experimental values are 10.5[22] for ethene and 8.3 eV[23] for 1,1-dimethylsilaethene. The similar trends were also seen for the LUMO energies (ε_{LUMO}); 2.4 eV (Basis A) and 2.5 eV (Basis B) for

$H_2Ge{=}CH_2$, 2.4 eV (6-31G**) for $H_2Si{=}CH_2$, and 5.0 eV (6-31G**) for $H_2C{=}CH_2$. These results imply that the Ge=C as well as the Si=C bond is open to both electrophilic and nucleophilic attacks. The high reactivity due to the larger ε_{HOMO} and the smaller ε_{LUMO} is one of reasons why it is not easy to detect the double-bonded intermediates including the heaviers group 4B elements.

3.3. Protonated germaethene

We finally calculated the $CGeH_5^+$ ion in an attempt to examine the proton affinity of Ge=C bond. To our knowledge, $CGeH_5^+$ has not been observed yet, though $CSiH_5^+$ is a well characterized ion in the gas phase[24,25]. Three geometrical structures were considered for $CGeH_5^+$; two classical forms I (methylgermyl cation) and II (germylmethyl cation), and a non-classical bridged form III.

Chart 2

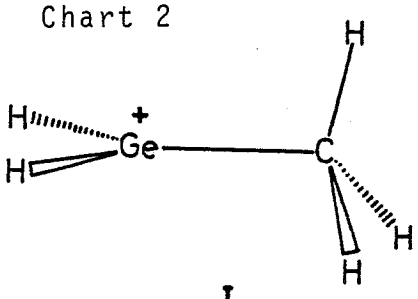

I

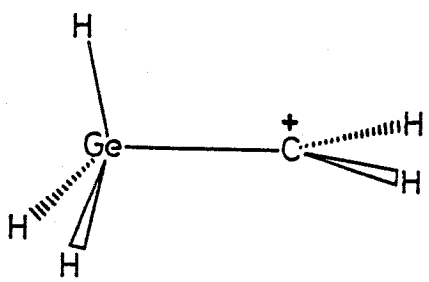

II

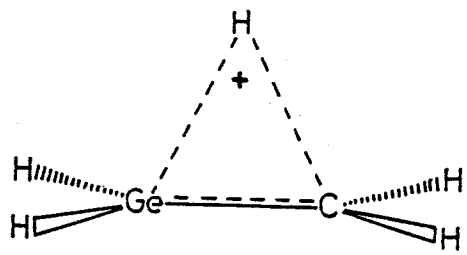

III

III was less stable at the present levels of SCF calculations than I and II. In Fig.3 are shown the optimized geometries of I and II. A large difference in geometry between I and II is that the opening up of the GeH_3 group in II is much larger than that of the CH_3 group in I. I is calculated to be more stable than II by 51.3 (Basis A) and 48.0 Kcal/mol (Basis B), the Ge atom preferring

to accomodate a positive charge. In Table 4 are summarized the calculated proton affinities together with the available values [26] of $H_2C=CH_2$ and $H_2Si=CH_2$. As may be expected from the above-mentioned ionization potentials, the proton affinities increase in the order of $H_2C=CH_2 < H_2Si=CH_2 \leq H_2Ge=CH_2$.

Acknowledgement

All calculations were carried out at the Computer Center of the Institute for Molecular Science, using the IMSPAC and IMSPAK programs[27].

References

[1] L.E. Gusel'nikov and N.S. Nametkin, Chem. Rev. 79 (1979) 529.

[2] N.S. Nametkin, L.E. Gusel'nikov, R.L. Ushakova, V.Yu. Orlov, O.V. Kuz'min, and V.M. Vdovin, Dokl. Akad. Nauk SSSR. 194 (1970) 1096.

[3] T.J. Barton, E.A. Kline, and P.M. Garvey, J. Am. Chem. Soc. 95 (1973) 3078.

[4] T.J. Barton and S.K. Hoekman, J. Am. Chem. Soc. 102 (1980) 1584.

[5] P. Riviere, A. Castel, and J. Satge, J. Am. Chem. Soc. 102 (1980) 5413.

[6] B.G. Gowenlock and J.A. Hunter, J. Organomet. Chem. 111 (1976) 171;
ibid. 140 (1977) 265.

[7] T.H. Dunning, J. Chem. Phys. 66 (1977) 1382.

[8] G. Olbrich, Chem. Phys. Lett. 73 (1980) 110.

[9] R.A. Eades and D.A. Dixon, J. Chem. Phys. 72 (1980) 3309.

[10] R. Ditchfield, W.J. Hehre, and J.A. Pople, J. Chem. Phys. 54 (1971) 724.

[11] W.J. Hehre, R. Ditchfield, and J.A. Pople, J. Chem. Phys. 56 (1972) 2257.

[12] P.C. Hariharan and J.A. Pople, Theor. Chim. Acta. 28 (1973) 213.

[13] L.E. Sutton, editor, Chem. Soc. Spec. Pub. 11 (1958).

[14] J.D. Goddard, Y. Yoshioka, and H.F. Schaefer, J. Am. Chem. Soc. 102 (1980) 7644.

[15] M.S. Gordon, Chem. Phys. Lett. 54 (1978) 9.

[16] M. Hanamura, S. Nagase, and K. Morokuma, Tetrahedron Lett. (1981) 1813 and unpublished results.

[17] J.-C. Barthelat, B.S. Roch, G. Trinquier, and J. Satgé, J. Am. Chem. Soc. 102 (1980) 4080.

[18] D.M. Hood and H.F. Schaefer, J. Chem. Phys. 68 (1978) 2985.

[19] R. Ahlrichs and R. Heinzmann, J. Am. Chem. Soc. 99 (1977) 7452.

[20] R.D. Bush, C.M. Golino, and L.H. Sommer, J. Am. Chem. Soc, 96 (1974) 7105.

[21] M.S. Gordon, Chem. Phys. Lett. 76 (1980) 163.

[22] P. Mosclet, D. Grosjeam, G. Mouvier, and J. Dubois, J. Electron Spectrosc. Related. Phenom. 2 (1973) 225.

[23] T. Koenig and W. Mckenna, J. Am. Chem. Soc. 103 (1981) 1212.

[24] T.H. Mayer and F.W. Lample, J. Phys. Chem. 78 (1974) 2422; ibid. 78 (1974) 2645.

[25] G.W. Stewart, J.M.S. Henis, and P.P. Gaspar, J. Chem. Phys. 57 (1972) 1990.

[26] A.C. Hopkinson and M.H. Lien, J. Org. Chem. 46 (1981) 998.

[27] K. Morokuma, S. Kato, K. Kitaura, I. Ohmine, S. Sakai and S. Obara, IMS Computer Center Library Program (1980).

Table 1 Relative energies (Kcal/mol) of $CGeH_4$ and $CSiH_4$ isomers

Molecule	X = Ge		X = Si[a)]	
	Basis A	Basis B	DZ	DZ+POL
$H_2X{=}CH_2$	0.0	0.0	0.0	0.0
$H_3X\ddot{C}H$	65.8	56.8	63.3	54.7
$H\ddot{X}CH_3$	-27.4	-22.7	-11.6	-4.9

a) Values are taken from ref.[14].

Table 2 The trends in the germylenic angle (degree), net charge on Ge, and Koopmans' ionization potential (eV) for the lowest singlet states of substituted germylenes

	$H\ddot{G}eH$ [a]	$H\ddot{G}eCH_3$ [b]	$CH_3\ddot{G}eCH_3$ [a]
germylenic angle	92.9	94.9	97.8
ionization potential	9.05	8.60	8.12
net charge on Ge	+0.31	+0.39	+0.41

a) Ref.[17].

b) Values by Basis B are given except for the angle by Basis A.

Table 3 Mulliken population analysis for $H_2Ge{=}CH_2$

	Basis A	Basis B
Atomic charge		
Ge	0.694	0.472
C	-0.811	-0.647
H(Ge)	-0.137	-0.065
H(C)	0.195	0.153
Overlap population between Ge and C		
Total[a)]	0.546	0.608
σ component	0.316	0.356
π component	0.230	0.252[b)]

a) Total = σ component + π component.

b) σ component of 7.342×10^{-4} is included.

Table 4 Proton affinities (Kcal/mol)

Molecule			Basis set
$H_2C=CH_2$	172.8		DZ[d]
$H_2Si=CH_2$	223.0[a]	176.6[b]	DZ[d]
$H_2Ge=CH_2$	229.7[a]	178.4[c]	Basis A
	233.2[a]	185.1[c]	Basis B

a) C protonation. b) Si protonation. c) Ge protonation.

d) Ref.[26].

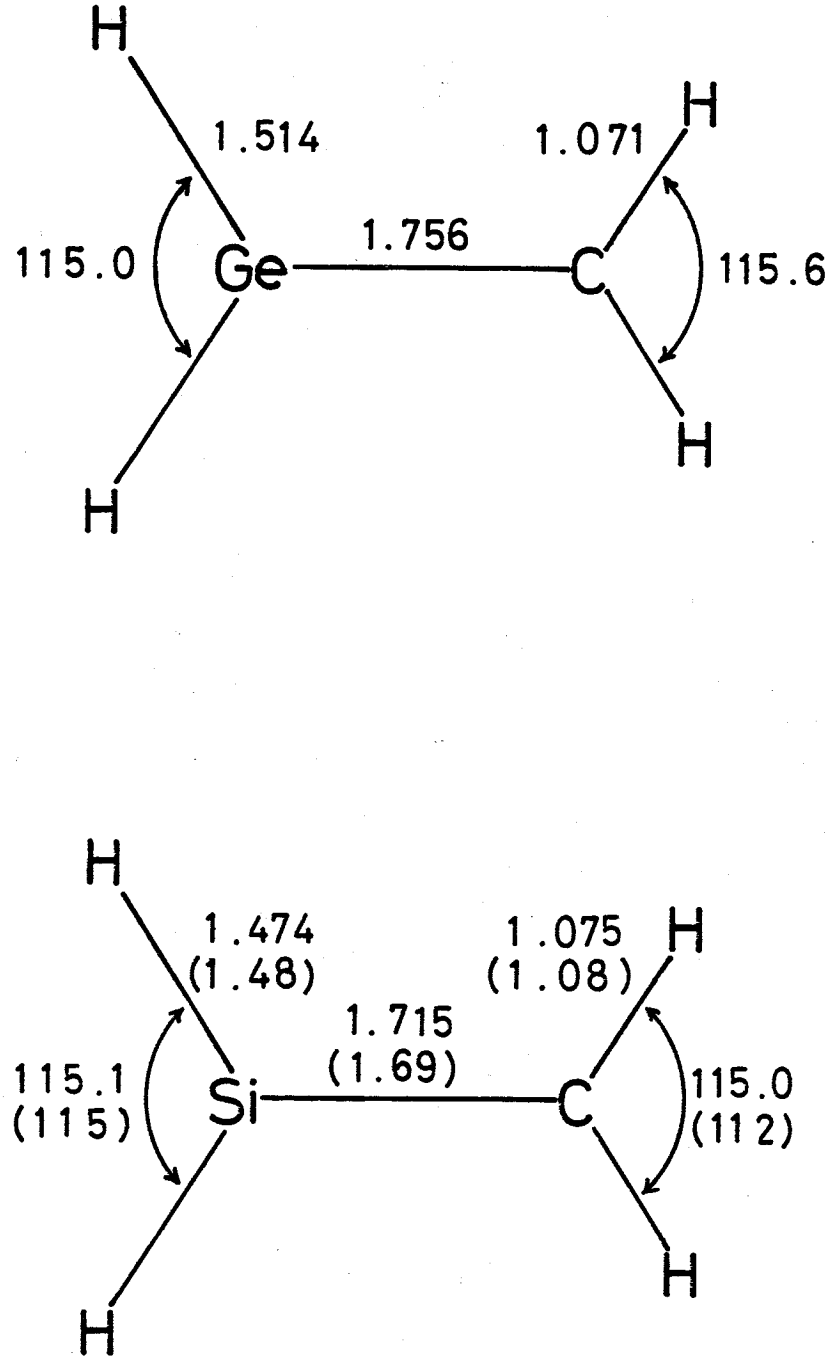

Figure 1. Comparison of calculated equilibrium geometries of $H_2Ge{=}CH_2$ and $H_2Si{=}CH_2$. The geometrical parameters for $H_2Si{=}CH_2$ are taken from refs.[14] and [15] in parentheses.

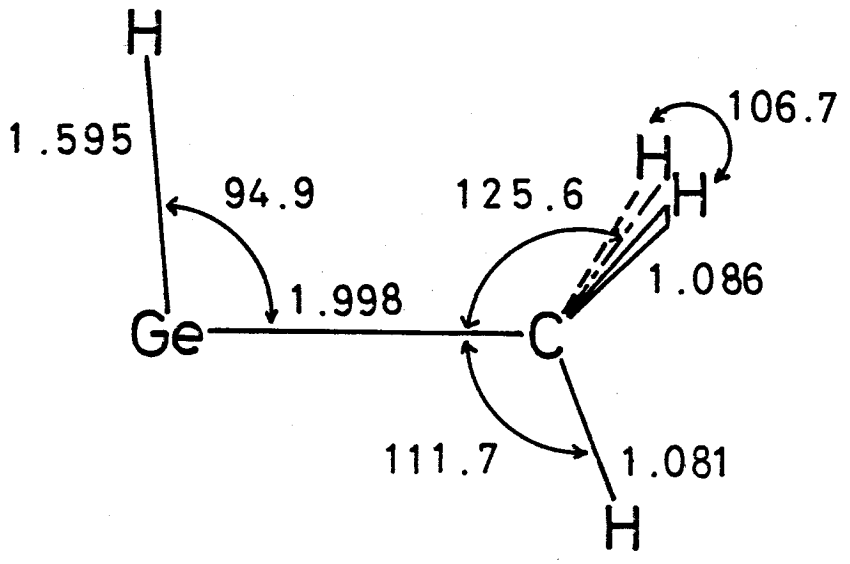

I

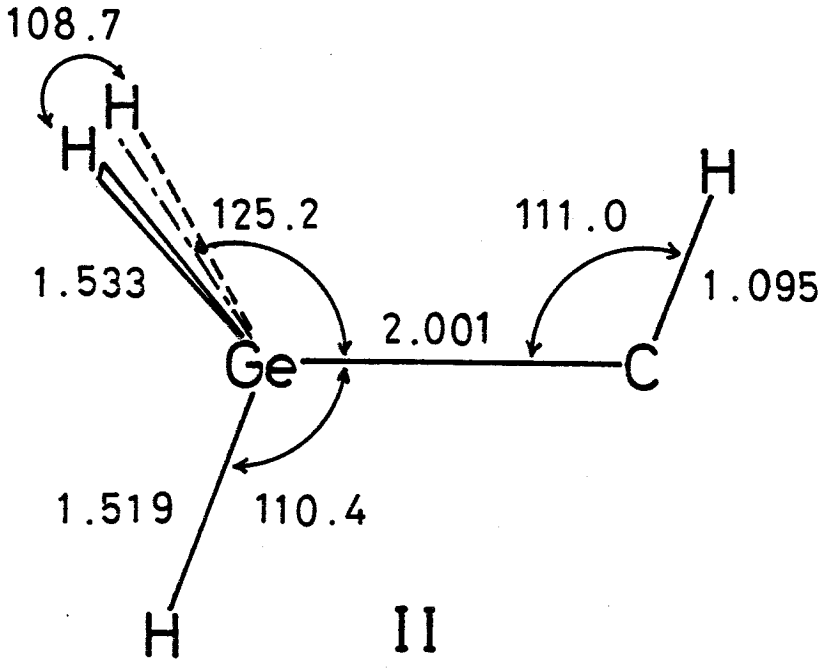

II

Figure 2. Optimized geometries of methylgermylene (I) and germylmethylene (II).

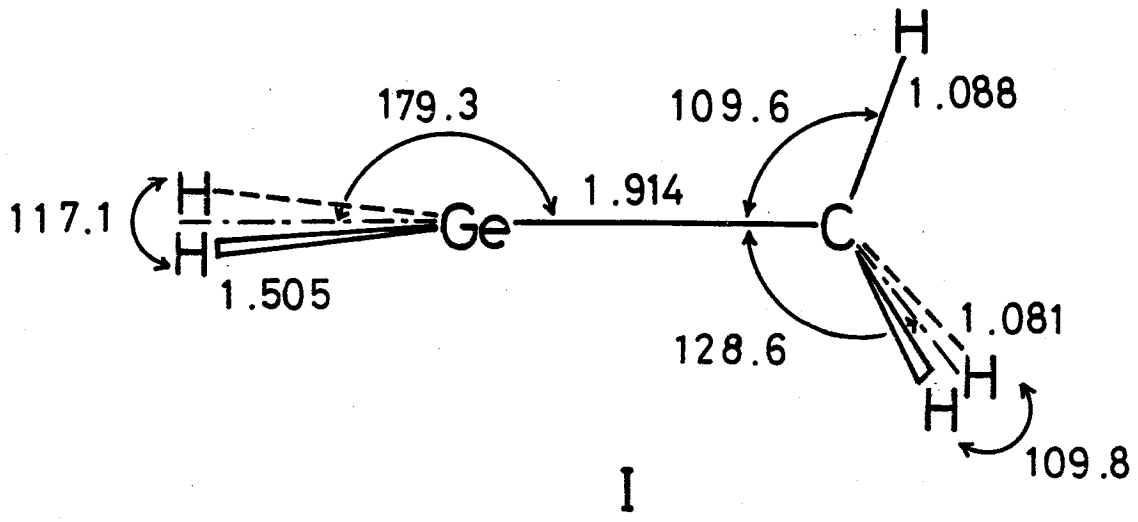

I

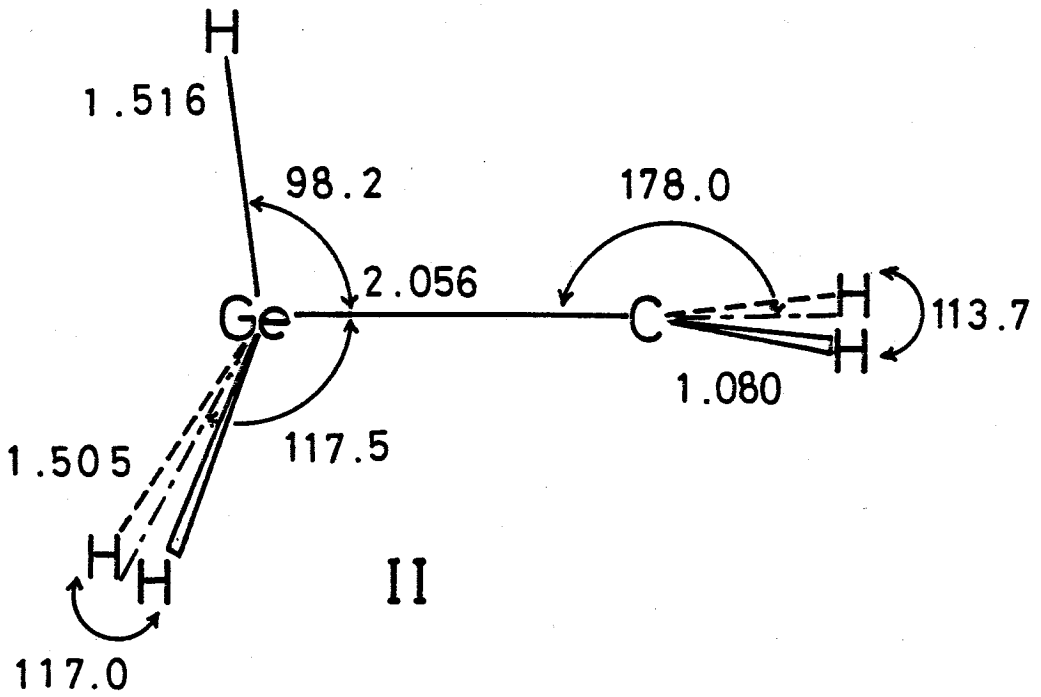

II

Figure 3. Optimized geometries of methylgermyl (I) and germylmethyl (II) cations.

CHAPTER 2

Barrier Heights for the Germaethene to Germylene Isomerization and for the Reaction with Water

To extend knowledge of the germanium-carbon double bond, the title reactions of singlet germaethene were investigated with ab initio calculations. It is found that germaethene resembles silaethene closely in stability and reactivity, though germanium is more reluctant to form doubly bonded compounds than silicon.

In view of recent dramatic developments in silaethene chemistry[1], analogous extensive studies of germanium-carbon doubly bonded compounds, germaethenes, should soon be forthcoming and open up new areas. Evidence consistent with the transient existence has accumulated in the last few years[2]. However, most of the experimental evidence is only indirect. In addition, very little is known about the mechanistic aspects of reaction of the important intermediates.

Theory should provide helpful information in this regard, and two reports of calculations on germaethene and its 1,2-hydrogen shifted isomers have already appeared[3,4]. Although much more stable than germylmethylene[3], germaethene was predicted to be 24[3]- 15[4] kcal/mol less stable in a thermodynamic sense than methylgermylene. However, none of the reports dealt with the nature of the transition state or the energy barrier separating the doubly bonded from the more stable divalent species, still less with the reactivity toward trapping reagents. In an attempt to characterize the stability and reactivity of germaethene, we here report ab initio calculations of the 1,2-hydrogen shift as well as the reaction with water, and compare these with data on silaethene at comparable levels of theory.

All calculations for closed-shell singlets were carried out with the double-zeta(DZ) and DZ+d basis sets[5]. Geometries were fully optimized at the Hartree-Fock(HF) level with the analytical gradient technique, using the DZ basis. Electron correlation was

incorporated at the DZ optimized geometries through third order Møller-Plesset perturbation(MP3) theory[6].

The 1,2-Hydrogen Shift. The optimized geometries of germaethene, methylgermylene, and the transition state connecting them are shown in Figure 1[7]. Germaethene is again calculated to be considerably less stable than methylgermylene by 24.8(HF/DZ), 24.2(HF/DZ+d), and 17.6(MP3/DZ+d) kcal/mol. This is in contrast with the relative stability of silaethene and its isomer methylsilylene, since these silicon isomers are calculated to be nearly degenerate in energy[8]. The large energy difference favoring $\ddot{H}Ge\text{-}CH_3$ over $H_2Ge{=}CH_2$ indicates that germanium is more reluctant to form doubly bonded compounds than silicon.

The transition state in Fig.1 is "early" only in a sense that the shifting hydrogen is still bound to Ge with a small increase in bond length (0.124 Å). In several of the remaining geometrical parameters, however, the transition state resembles methylgermylene and is "late". Reflecting the "late" transition state, the energy barrier for the isomerization of germaethene to methylgermylene is calculated to be 38.1(HF/DZ) and 36.2(HF/DZ+d) kcal/mol. Even at the MP3/DZ+d level, the barrier is as large as 37.5 kcal/mol, suggesting that germaethene itself is kinetically, sufficiently stable to isomerization. It is of interest to note that the calculated barriers are only a few kcal/mol smaller than that of ca.41 kcal/mol calculated for the isomerization of silaethene[8b].

The Reaction with Water. In Fig.2 are shown the optimized geometries of an intermediate complex, the product, and the transition state connecting them. The reaction with water initiates with the formation of a weak complex (1.5 kcal/mol at the HF/DZ+d level and 2.6 kcal/mol at the MP3/DZ level) in a fairly early stage, in which one of the lone pairs of water is oriented for maximum interaction with the π^* orbital of germaethene localized strongly around Ge. The complex is transformed via a four-center-like transition state to the product, $H_2(OH)Ge\text{-}CH_3$. A Mulliken population analysis reveals that the attack of water is first nucleophilic and becomes electrophilic as the reaction reaches the transition state. The reaction with water is calculated to be 68.1(HF/DZ+d) and 61.7(MP3/DZ) kcal/mol exothermic. Reflecting the large exothermicity, the transition state rather resembles the complex in structure and is "early", as shown in Fig.2. The calculated values for the overall barrier are 16.6 (HF/DZ+d) and 10.1(MP3/DZ) kcal/mol. These values are essentially comparable to those of 12.0(HF/DZ+d) and 8.9(MP3/DZ) kcal/mol for the silaethene reaction with water[9], suggesting that germaethene is kinetically as stable as silaethene.

Compared with the value of 68(HF/4-31G) kcal/mol for the reaction of ethene[10], the overall barriers for germaethene and silaethene are much smaller. One may consider that the high reactivity of germaethene and silaethene is simply due to their strongly polarized double bonds, as often pointed out.[1a,1b] However, an overall barrier for the $H_2Si{=}SiH_2 + H_2O$ reaction is

calculated to be as small as 3.2(HF/DZ+d) kcal/mol[11]. At this point, it is noteworthy that HOMO levels rise in the order $H_2C=CH_2$ << $H_2Si=CH_2 \leq H_2Ge=CH_2 < H_2Si=SiH_2$ while LUMO levels drop in the same way along the series[12]. This means that in Klopman's terminology[13] the reactivity of π-bonded group 4B compounds is significantly "frontier controlled", as well as "charge controlled". This finding would be useful for the design of a kinetically more stable germaethene.

Hydrogenation Energy. Finally, an attempt was made to evaluate and compare the energies released upon addition of H_2 to germaethene and silaethene. The hydrogenation energies calculated at the HF/DZ+d level are 65.6($H_2Ge=CH_2$) and 67.9($H_2Si=CH_2$) kcal/mol, while those at the MP3/DZ level are 48.7($H_2Ge=CH_2$) and 49.0($H_2Si=CH_2$) kcal/mol[14]. Obviously, these results indicate that germaethene is as stable as silaethene in a thermodynamic sense.

The present work predicts that germaethene resembles silaethene closely in stability and reactivity except the relative stability of the doubly bonded and divalent forms. It is hoped that successful schemes for the synthesis of germaethene are soon devised. We are currently studing the reactivity toward self-dimerization.

Acknowledgment

All calculations were carried out at the Computer Center of the Institute for Molecular Science, using an IMS version of the GAUSSIAN80 series of programs[15].

References and Notes

(1) For comprehensive reviews, see: (a) Gusel'nikov, L.E.; Nametkin, N.S. Chem. Rev. 1979, 79, 529-577. (b) Coleman, B.; Jones, M. Rev. Chem. Intermed. 1981, 4, 297-367. (c) Schaefer, H.F. Acc. Chem. Res. 1982, 15, 283-290.

(2) Satge, J. Adv. Organomet. Chem. 1982, 21, 241-287 and references cited therein.

(3) Kudo, T.; Nagase, S. Chem. Phys. Lett. 1981, 84, 375-379.

(4) Trinquier, G.; Barthelat, J.-C.; Satge, J. J. Am. Chem. Soc. 1982, 104, 5931-5936.

(5) (a) In the DZ basis, the 6-31G basis[5b] was used except 7s5p3d contraction of Dunning's 13s9p5d Gaussian primitive set for Ge[5c]. In the polarized DZ+d basis, the Ge basis was augmented by a set of d functions (exponent 0.25) while the 6-31G* basis[5a] was used for other atoms. (b) Hehre, W.J.; Ditchfield, R.; Pople, J.A. J. Chem. Phys. 1972, 56, 2257-2261. Hariharan, P.C.; Pople, J.A. Theor. Chim. Acta 1973, 28, 213-222. Francl, M.M.; Pietro, W.J.; Hehre, W.J.; Binkley, J.S.; Gordon, M.S.; DeFrees, D.J.; Pople, J.A. J. Chem. Phys. 1982, 77, 3654-3665. (c) Olbrich, G. Chem. Phys. Lett. 1980, 73, 110-113.

(6) Pople, J.A.; Binkley, J.S.; Seeger, R. Int. J. Quantum Chem., Quantum Chem. Symp. 1976, 10, 1-19. The MP3 calculations were carried out with all orbitals included except the core-like orbitals (1s,2s,2p,3s,3p,3d for Ge, and 1s for C and O in character).

(7) Note that the geometrical parameters for germaethene and methylgermylene in Fig.1 differ little from our previous values[3] obtained with a less flexible DZ basis.

(8) (a) Gordon, M.S. Chem. Phys. Lett. 1978, 54, 9-13. Gordon, M.S. J. Am. Chem. Soc. 1982, 104, 4352-4357. (b) Goddard, J.D.; Yoshioka, Y.; Schaefer, H.F. J. Am. Chem. Soc. 1980, 102, 7644-7650. Yoshioka, Y.; Schaefer, H.F. J. Am. Chem. Soc. 1981, 103, 7366-7367. (c) Trinquier, G.; Malrieu, J.-P. J. Am. Chem. Soc. 1981, 103, 6313-6319. (d) Köhler, H.J.; Lischka, H. J. Am. Chem. Soc. 1982, 104, 5884-5889.

(9) Hanamura, M.; Nagase, S.; Morokuma, K., to be submitted.

(10) Koizumi, M.; Yamashita, K.; Yamabe, T.; Fukui, K. Abstract of Sym. on Mol. Struct. held at Kyoto in Japan, 1981, pp768-769.

(11) The subject will be discussed in detail in a future publication by Nagase, S.; Kudo, T.

(12) Nagase, S.; Kudo, T.: J. Mol. Struct., a special issue of THEOCHEM in honor of Prof. Fukui and his Nobel prize awarded in chemistry, 1983, 103, 35-44.

(13) Klopman, G. J. Am. Chem. Soc. 1968, 90, 223-237. Klopman, G. "Chemical Reactivity and Reaction Paths"; John Wiley: New York, 1974; pp55-165.

(14) The optimized geometries and energies for $H_3Ge\text{-}CH_3$ and $H_3Si\text{-}CH_3$ are available from the authors on request.

(15) Binkley, J.S.; Whiteside, R.A.; Krishnan, R.; Seeger, R.; DeFrees, D.J.; Schlegel, H.B.; Topiol, S.; Kahn, L.R.; Pople, J.A. QCPE 1981, 10, 406.

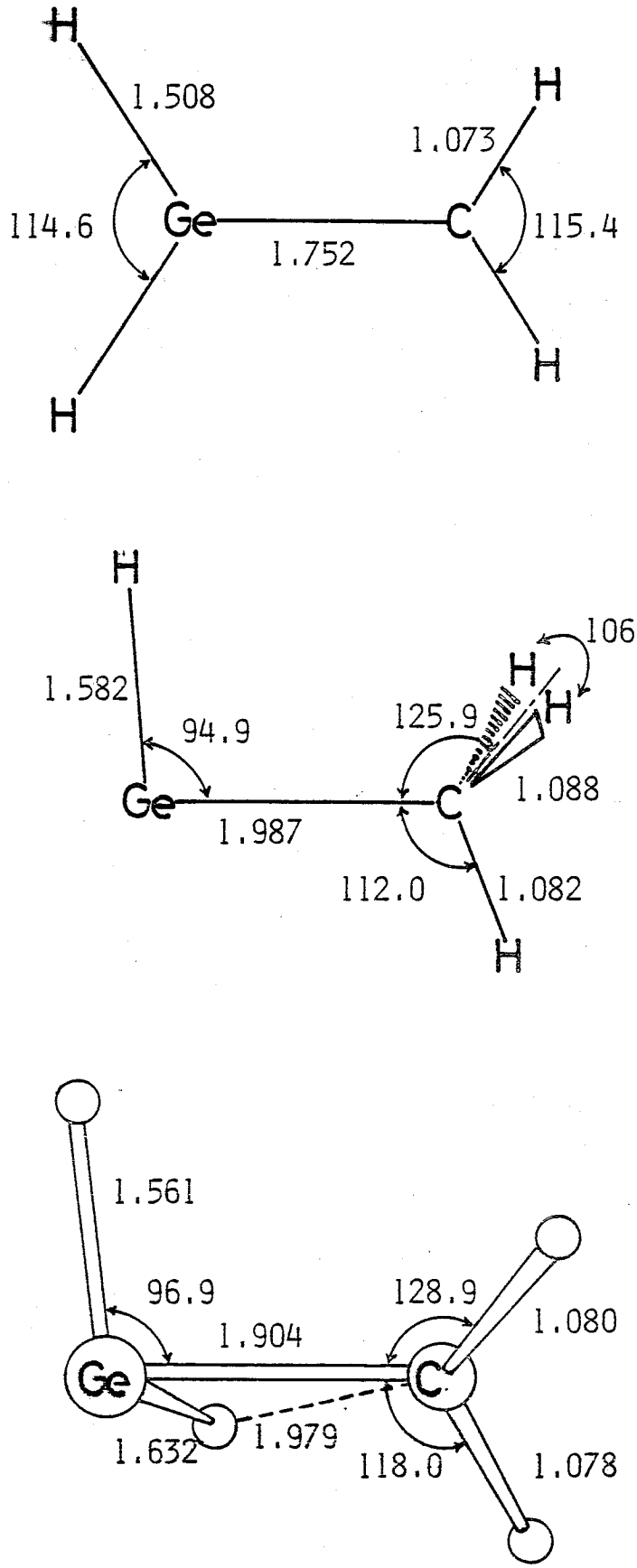

Figure 1.

Optimized geometries for germaethene, methylgermylene, and the transition state connecting them, obtained at the HF/DZ level.

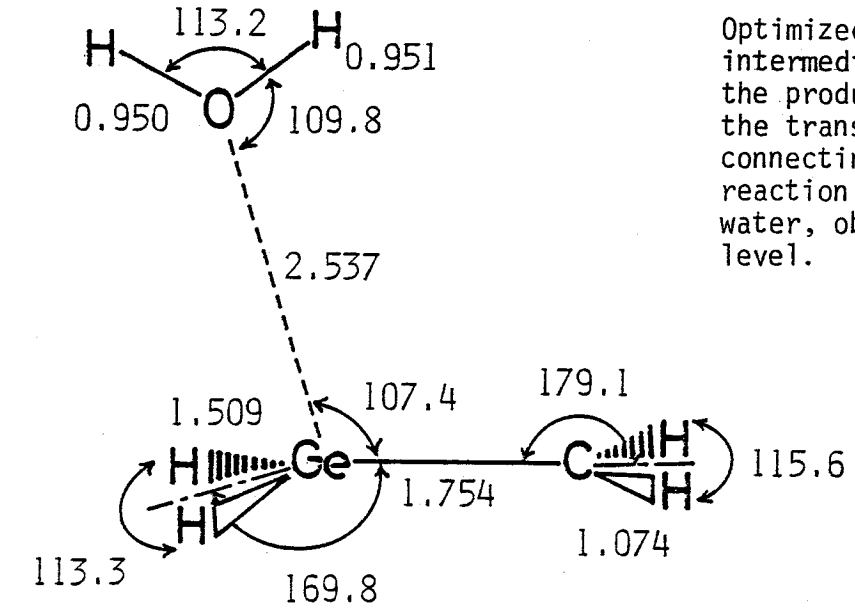

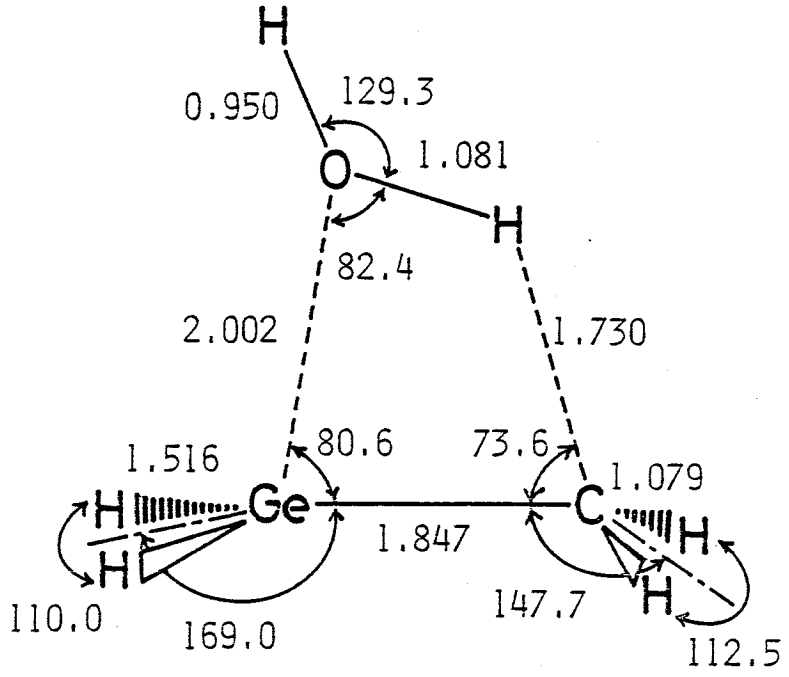

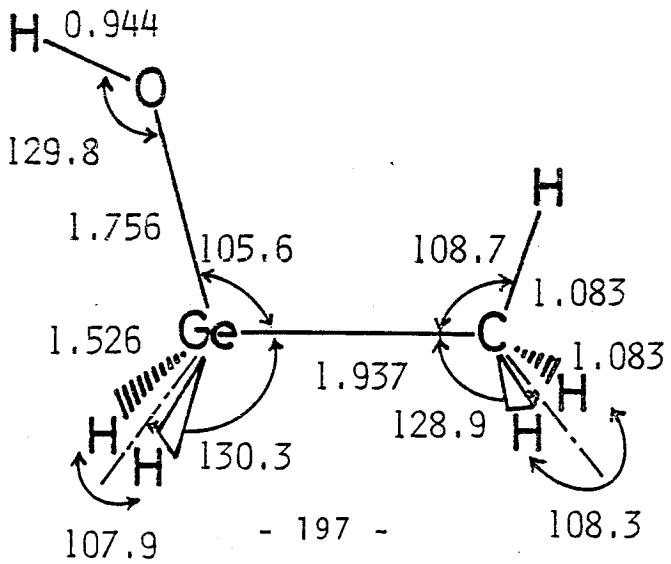

Figure 2.

Optimized geometries of an intermediate complex(top), the product(bottom), and the transition state(middle) connecting them in the reaction of germaethene with water, obtained at the HF/DZ level.

CHAPTER 3

Comparison
in
the Properties of Digermene
with
Ethene, Silaethene, Disilene, and Germaethene

In an attempt to characterize germanium doubly bonding, several properties of digermene, $H_2Ge=GeH_2$, were investigated with the ab initio SCF method. The thermodynamic and kinetic stabilities are discussed in comparison with data on $H_2C=CH_2$, $H_2Si=CH_2$, $H_2Si=SiH_2$, and $H_2Ge=CH_2$. A considerable increase in kinetic stability is found to be important for isolating a germanium doubly-bonded compound.

Introduction

There has been a great deal of interest in the generation and characterization of unstable intermediates containing multiple p_π-p_π bonded group 4B metals Si and Ge, in view of innumberable, stable counterparts of the first row elements.[1] During the past several years, multiple bonds to silicon have been substantially explored in both experimental and theoretical fields, and stable compounds containing Si=C[2a] or Si=Si[2b] π bonds have been now synthesized and isolated at room temparature. By contrast, germanium-containing multiple bonds seem to be less common and the detailed study is still in early stages. Although there is active work going on into double bonds of germanium with carbon,[3] nitrogen,[4] oxygen,[4c,5] sulfur,[5c,5d,6] and phosphorus,[7] up to now only indirect evidence is available which suggests the transient existence.

In an effort to extend knowledge of germanium doubly bonding, the present work follows our recent theoretical study on a germanium-carbon double bond.[8] We here undertake the stability and nature of a germanium-germanium double bond through ab initio SCF MO calculations of the parent compound, digermene ($H_2Ge=GeH_2$). To our knowledge, only one report[9] is available in which >Ġe-Ġe< biradicals have been considered as limit forms of germanium doubly bonded compounds >Ge=Ge< . In order to sketch a general feature of germanium doubly bonding, our primary concern is in comparison with data on carbon and silicon analogues at similar levels of calculations. Such a comparative study is expected to minimize correlation corrections

and to be useful for further experimental considerations. To this end, it is shown that the properties of germanium in the double bond formation resemble those of silicon, but differ considerably from those of carbon.

Computational Method

All calculations were carried out for closed-shell singlets and within the framework of the RHF-LCAO-SCF approximation. The basis sets used were the previously described bases A and B.[8] In brief, basis A is a contracted double zeta(DZ) set, while basis B is a less contracted DZ set augmented by a set of 4d functions (exponent 0.25) on Ge and a set of 2p functions (exponent 1.1) on H. All geometries were fully optimized with basis A using the analytical energy gradient routines in the HONDO program developed by King and Dupuis.[10] The geometries of digermene and digermane were also optimized by basis A augmented by a set of 4d functions on Ge. To obtain more reliable energies and electron densities, the geometry optimizations by basis A were followed by single-point calculations with basis B using the IMSPAC program developed by Morokuma et al..[11] Such single-point calculations were denoted by basis B//basis A.

For comparison purpose, full geometry optimizations of some silicon compounds were performed with the 3-21G basis set,[12] which were followed by the 6-31G**[13] single-point calculations.

Results and Discussion

The Equilibrium Geometry of Digermene. By analogy with the geometry of ethylene, we initially optimized the geometry of digermene

with D_{2h} symmetry constraint. The resultant geometry is shown in fig.1A. To see if the planar geometry is located on a true energy minimum, the normal vibrational frequencies were calculated by diagonalizing the force constant matrix obtained with numerical differentiation of energy gradients. The planar form was found to possess a single imaginary frequency of 281i cm^{-1} and to be a saddle point (not a equilibrium). The normal coordinate for a imaginary frequency corresponded to molecular deformation from the planar D_{2h} to the trans-bent C_{2h} form.

Shown in fig.1B is the geometry optimized without the constraint of planarity, which is calculated to be somewhat more stable by 1.8 (basis A//basis A) and 1.7(basis B//basis A) kcal/mol. As expected, the GeH_2 groups are bent up and down, respectively, by the angle of 36.2° from the molecular plane. The bent angle is considerably larger than those of 12.9[14] and 9.6°[15] found for disilene, though stabilization due to trans-bending is not very large for both molecules. Upon going from the planar to the trans-bent form, the HGeH angle decreases by 6.2°, while the GeGe and GeH bond lengths increase by 0.071 and 0.012 Å, respectively. The calculated GeGe double bond length of 2.297 Å is shorter by 0.218 Å than the calculated GeGe single bond length of digermane shown in fig.1C. This shortening is comparable with the corresponding one of 0.213 Å[16] by the 4-31G calculations from ethane to ethylene, indicating a certain strength of the p_π-p_π bonding between germanium atoms.

To examine the possible participation of germanium vacant 4d orbitals, the geometries of digermene as well as digermane were

again optimized with basis A augmented by a set of 4d functions (exponent 0.25) on Ge. These results are shown in fig.2 where digermene is again calculated to be 1.6 kcal/mol more stable in the trans-bent form than in the planar form. With the 4d orbital participation, the GeGe single bond and double bond lengths decrease by 0.047 and 0.025 Å, respectively. This is not surprising since it is considered to be a general role of polarization functions. The decreases would be compensated to some extent by the contribution of electron correlation. An important point to be noted is that the degree of the decreasing caused by 4d orbital participation is rather larger for the single bond than for the double bond. It may be reasonable to conclude from these results that vacant 4d orbitals on Ge neither have any significant effect on the strength of p_π-p_π bonding nor on the energy difference favoring the trans-bent over the planar digermene.

For comparison, the double bond lengths of the molecules of interest[8,14-20] calculated at double zeta quality are summarized in Table 1. Upon replacement of carbon by group 4B metals, the double bond lengths increase, and the longest is the double bond of digermene.

The Thermodynamic Stability to Isomerization. We examined the stability for isomerization to germylgermylene, $H\dot{G}\ddot{e}$-GeH_3. The optimized geometry of the divalent species is shown in fig.3. In Table 2 are summarized the energies relative to planar digermene together with the corresponding ones[14,15] of the silicon analogues.

As Table 2 shows, digermene is calculated to be less stable than

germylgermylene by 9.5(basis A//basis A) and 9.2(basis B//basis A) kcal/mol. Interestingly, the polarization functions on Ge and H have little effect on the energy difference between the doubly bonded and the divalent species. The energy difference favoring $H\ddot{G}\ddot{e}\text{-}GeH_3$ over $H_2Ge{=}GeH_2$ is larger than that of $H\ddot{S}\ddot{i}\text{-}SiH_3$ and $H_2Si{=}SiH_2$, this leading to the fact that germanium is more reluctant to form doubly bonded compounds than silicon, as was previously pointed out.[8] It is to be noted, however, that the energy difference between $H\ddot{G}\ddot{e}\text{-}GeH_3$ and $H_2Ge{=}GeH_2$ is considerably smaller as compared with those of 27.4(basis A//basis A) and 22.7(basis B//basis A) kcal/mol between $H\ddot{G}\ddot{e}\text{-}CH_3$ and $H_2Ge{=}CH_2$.[8] This suggests that the formation of a 'homogeneous' double bond is more preferable than that of a 'heterogeneous' one.

Here, two points are worth mentioning. First, the effect of electron correlation may be more significant for the doubly bonded species than for the divalent species, as was noted by several authors.[15,21-23] Second, even if the doubly bonded species remains thermodynamically less stable, its existence is likely to be observed in the absence of trapping reagents, since it would be separated from the more stable divalent species by a significant barrier. In fact, we calculated the transition state for the reaction of $H_2Si{=}SiH_2 \rightarrow H\ddot{S}\ddot{i}\text{-}SiH_3$ and found a barrier height of 22.3(3-21G//3-21G) and 19.8(6-31G**//3-21G) kcal/mol.[24,25]

Hydrogenation Energies. To assess further the stability of digermene, an attempt was made to evaluate and compare the energies released upon the addition of H_2 in the reaction,

$$H_2X{=}XH_2 + H_2 \rightarrow H_3X\text{-}XH_3 \qquad (X{=}\ Ge \text{ or } C).$$

As is listed in Table 3, the calculated hydrogenation energies are increased by including polarization functions. This effect is larger in the case of digermene. An important point is that the hydrogenation energy of digermene is not too different from that of ethylene. This suggests that the germanium-germanium double bond is not particularly unstable in a thermodynamic sense as compared with the carbon-carbon double bond.

Frontier Orbital Energies. The frontier orbital energies for digermene as well as ethylene, silene, germene, and disilene are displayed in fig.4. In going from ethylene to molecules containing the group 4B metals, the HOMO energy levels rise and the LUMO energy levels drop to a considerable extent. In other words, the double bonds with the group 4B metals are much more reactive towards both electrophiles and nucleophiles and thereby more unstable in a kinetical sense. This is a reason why the intermediates containing the doubly bonded group 4B metals are difficult to detect experimentally.

The HOMO and LUMO levels of silene is very similar to those of germene. The same similarity holds well between disilene and digermene. It is of interest to note that the HOMO (LUMO) levels of disilene and digermene are higher (lower) than those of silene and germene. It may be concluded that a 'homogeneous' double bond is kinetically less stable than a 'heterogeneous' double bond. It should be

recognized, however, that the conclusion is modified by the predominance of the electrostatic over the charge transfer interaction especially in ionic reactions. Strong dipolar character of a 'heterogeneous' double bond is clear from the electron-density distributions in fig.5, resulting in a decrease in its kinetic stability. In addition, the strongly polarized frontier orbitals of silene and germene lower the orbital symmetry restrictions to cycloaddition; a typical example is seen in their high reactivities toward self-dimerization.[1,19]

Proton Affinities. We also calculated protonated digermene to estimate the proton affinity. The optimized geometry of the $Ge_2H_5^+$ ion in the classical form is shown in fig.6. In Table 4 are collected the calculated proton affinities together with the values[8,26] of the molecules of interest.

As Table 4 shows, the introduction of polarization functions tends to increase the calculated values of proton affinities, though its effect is the smallest for ethylene. As expected from the abovementioned HOMO energy levels, the proton affinity of ethylene is considerably smaller than those of molecules with the group 4B metals. The calculated proton affinities increase in the order $H_2C{=}CH_2 \ll H_2Si{=}SiH_2 \leq H_2Ge{=}GeH_2 < H_2Si{=}CH_2 \leq H_2Ge{=}CH_2$. The proton affinities of the heterogeneous double bonds are larger than those of the homogeneous double bonds, this being in disagreement with the prediction simply based on their HOMO levels. The larger proton affinities of the heterogeneous double bonds should be rationalized by considering the higher polarity of their bonds.

Concluding Remarks

Germanium is somewhat more reluctant to form doubly bonded compounds than silicon. Nevertheless, in several respects the germanium double bond is analogous to the silicon double bond, while it is much less analogous to the carbon double bond. The germanium-germanium double bond is expected to be not particularly unstable to isomerization and hydrogenation, and to be formed less reluctantly than is the germanium-carbon double bond. In view of the interest in isolating a germanium doubly bonded compound, it is important to reduce its high reactivity. This would be realized with a proper choice of substituents.[27] A study along this line has been initiated in our laboratory.

Acknowledgment

All calculations were carried out at the Computer Center of the Institute for Molecular Science, using the computer center library programs HONDOG[10] and IMSPAC.[11] One of the authors (S.N.) thanks Prof. Gordon for the ref.(12) prior to its publication. This work was supported in part by a Grant-in-Aid for Scientific Research from the Ministry of Education, Science, and Culture in Japan.

References

(1) L.E. Gusel'nikov and N.S. Nametkin, Chem. Rev., 79,529(1979).

(2) (a) A.G. Brook, F. Abdesaken, B. Gutekunst, G. Gutekunst, and R.K. Kallury, Chem. Commun., 191(1981); (b) R. West, M.J. Fink, J. Michl, Science, 214,1343(1981).

(3) (a) T.J. Barton, E.A. Kline and P.M. Garvey, J. Am. Chem. Soc., 95,3078(1973); (b) T.J. Barton and S.K. Hoekman,ibid., 102,1584 (1980); (c) P. Riviere, A. Castel and J. Satge, ibid., 102,5413 (1980); (d) W.P. Neumann and M. Schriewer, Tetrahedron Lett., 21,3273(1980); (e) N.N. Zemlyanskii, I.V. Borisova, Yu.N. Luzikov, N.D. Kolosova, Yu.A. Ustynyuk and I.P. Beletskaya, Izv. Akad. Nauk SSSR, Ser. Khim., 11,2668(1980); (f) J. Dzarnoski, H.E. O'Neal, and M.A. Ring, J. Am. Chem. Soc., 103,5740(1981).

(4) (a) M. Riviere-Baudet, P. Riviere and J. Satge, J. Organomet. Chem., 154,C23(1978); (b) P. Riviere, A. Cazes, A. Castel, M. Riviere-Baudet and J. Satge, ibid., 155,C58(1978); (c) P. Riviere, J. Satge, A. Castel and A. Cazes, ibid., 177, 171(1979); (d) A. Baceiredo, G. Bertrand and P. Mazerolles, Tetrahedron Lett., 22,2553(1981).

(5) (a) H. Lavayssiere, J. Barrau, G. Dousse, J. Satge and M. Bouchaut, J. Organomet. Chem., 154,C9(1978); (b) J. Barrau, M. Bouchaut, A. Castel, A. Cazes, G. Dousse, H. Lavayssiere, P. Riviere and J. Satge, Synth. React. Inorg. Met.-Org. Chem., 9,273(1979); (c) G. Trinquier, M. Pelissier, B. Saint-Roch and H. Lavayssiere, J. Organomet. Chem., 214,169(1981); (d) J. Barrau, H. Lavayssiere, G. Dousse, C. Couret and J. Satge, ibid., 221, 271(1981).

(6) (a) H. Lavayssiere, G. Dousse, J. Barrau, J. Satge and M. Bouchaut J. Organomet. Chem., 161,C59(1978); (b) J. Barrau, M. Bouchaut, H. Lavayssiere, G. Dousse and J. Satge, Synth. React. Inorg. Metalorg. Chem., 10,515(1980).

(7) C. Couret, J. Satge, J.D. Andriamizaka and J. Escudie, J. Organomet. Chem., 157,C35(1978).

(8) T. Kudo and S. Nagase, Chem. Phys. Lett., 84,375(1981).

(9) P. Riviere, A. Castel and J. Satge, J. Organomet. Chem., 212, 351(1981).

(10) (a) H.F. King and M. Dupuis, J. Comput. Phys., 21,144(1976); (b) M. Dupuis and H.F. King, Int. J. Quantum. Chem., II,613(1977); (c) M. Dupuis and H.F. King, J. Chem. Phys., 68,3998(1978); (d) IMS Computer Center Library Program (WF10-004).

(11) K. Morokuma, S. Kato, K. Kitaura, I. Ohmine, S. Sakai and S. Obara, IMS Computer Center Library Program (WF10-007).

(12) M.S. Gordon, J.S. Binkley, J.A. Pople, W.J. Pietro, and W.J. Hehre, J. Am. Chem. Soc., in press.

(13) M.S. Gordon, Chem. Phys. Lett., 76,163(1980).

(14) L.C. Synder and Z.R. Wasserman, J. Am. Chem. Soc., 101,5222(1979).

(15) R.A. Poirier and J.D. Goddard, Chem. Phys. Lett., 80,37(1981).

(16) W.A. Lathan, W.J. Hehre, and J.A. Pople, J. Am. Chem. Soc., 93, 808(1971).

(17) M.S. Gordon and R.D. Koob, J. Am. Chem. Soc., 103,2939(1981).

(18) D.M. Hood and H.F. Schaefer III, J. Chem. Phys., 68,2985(1978).

(19) R. Ahlrichs and R. Heinzmann, J. Am. Chem. Soc., 99,7452(1977).

(20) G. Trinquier and J.P. Malrieu, J. Am. Chem. Soc., 103,6313(1981).

(21) M.S. Gordon, Chem. Phys. Lett., 54,9(1978).

(22) J.D. Goddard, Y. Yoshioka, and H.F. Schaefer III, J. Am. Chem. Soc., 102,7644(1980).

(23) H. Hanamura, S. Nagase and K. Morokuma, Tetrahedron Lett., 1813(1981).

(24) T. Kudo and S. Nagase, to be published.

(25) For the reaction of $H_2Si=CH_2 \rightarrow H\ddot{S}i\text{-}CH_3$, a barrier height of 40.6 kcal/mol is predicted by Y. Yoshioka and H.F. Schaefer III, J. Am. Chem. Soc., 103,7366(1981). Fortunately, correlation corrections are found to be not very large.

(26) P.C. Hariharan, W.A. Lathan and J.A. Pople, Chem. Phys. Lett., 14,385(1972).

(27) For an attempt to make doubly bonded isomers thermodynamically more stable than divalent isomers, see ref.(23). It should be mentioned, however, that substituents which are effective for the thermodynamic stability do not always increase the kinetic stability.

Table 1 Summary of double bond lengths(Å) calculated at double zeta SCF levels

Molecule	Length	Basis set	Reference
$H_2C=CH_2$	1.316	4-31G	16
$H_2Si=CH_2$	1.717	3-21G	17
	1.715	DZ	18
	1.69	DZ	19
	1.698	DZ	20
$H_2Ge=CH_2$	1.756	Basis A	8
$H_2Si=SiH_2$	2.140(2.150)[a]	3-21G	15
	2.083(2.102)[a]	4-31G	14
$H_2Ge=GeH_2$	2.226(2.297)[a]	Basis A	this work

a) The values in parentheses are for more stable trans-bent forms.

Table 2 Relative energies(kcal/mol) of Ge_2H_4 and Si_2H_4 isomers

	$H_2X{=}XH_2$		$H\ddot{X}{-}XH_3$	Basis set
	planar	trans-bent		
X=Ge	0.0	-1.84	-11.35	Basis A//Basis A
	0.0	-1.67	-10.88	Basis B//Basis A
X=Si	0.0	-0.38	-8.60	4-31G//4-31G[a]
	0.0	-0.05	-0.11	3-21G//3-21G[b]
	0.0	———	-2.14	6-31G*//3-21G[b]
	0.0	-0.004	-1.76	6-31G**//3-21G

a) Ref.(14). b) Ref.(15).

Table 3 Calculated hydrogenation energies

Molecule	kcal/mol	Basis set
$H_2C=CH_2$	-42.0	4-31G//4-31G[a]
	-42.7	6-31G**//4-31G
$H_2Ge=GeH_2$	-45.1	Basis A//Basis A
	-51.9	Basis B//Basis A

a) Ref.(16).

Table 4 Calculated proton affinities

Molecule	kcal/mol	Basis set
$H_2C=CH_2$	173.4	4-31G//4-31G[a]
	174.5	6-31G**//4-31G[a]
$H_2Si=CH_2$	224.9	3-21G//3-21G
	228.0	6-31G**//3-21G
$H_2Ge=CH_2$	229.7	Basis A//Basis A[b]
	233.2	Basis B//Basis A[b]
$H_2Si=SiH_2$	208.9	3-21G//3-21G
	222.8	6-31G**//3-21G
$H_2Ge=GeH_2$	209.8	Basis A//Basis A
	217.8	Basis B//Basis A

a) Ref.(26). b) Ref.(8).

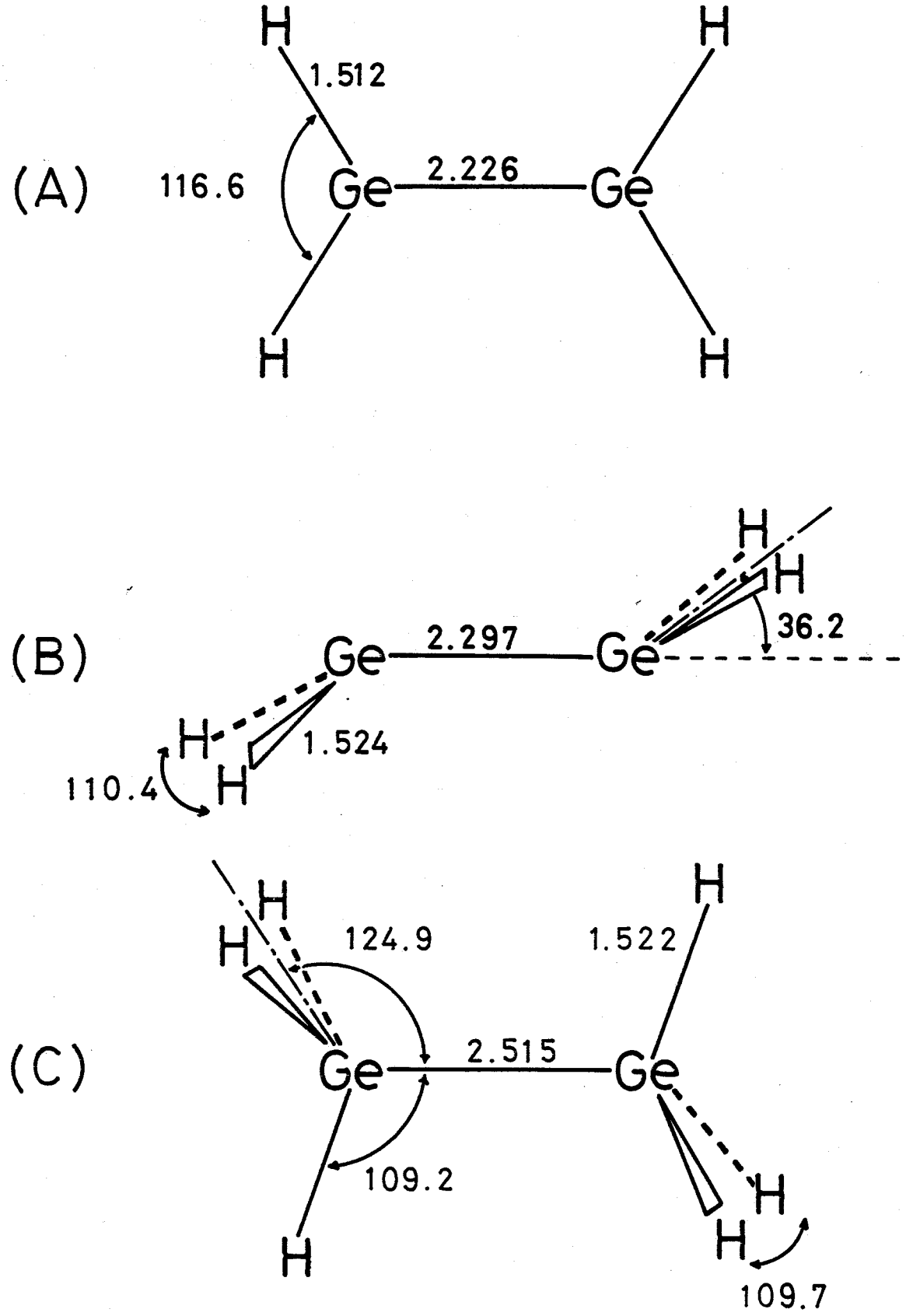

Figure 1. Optimized geometries of planar digermene(A), trans-bent digermene(B), and digermane(C). Basis A.

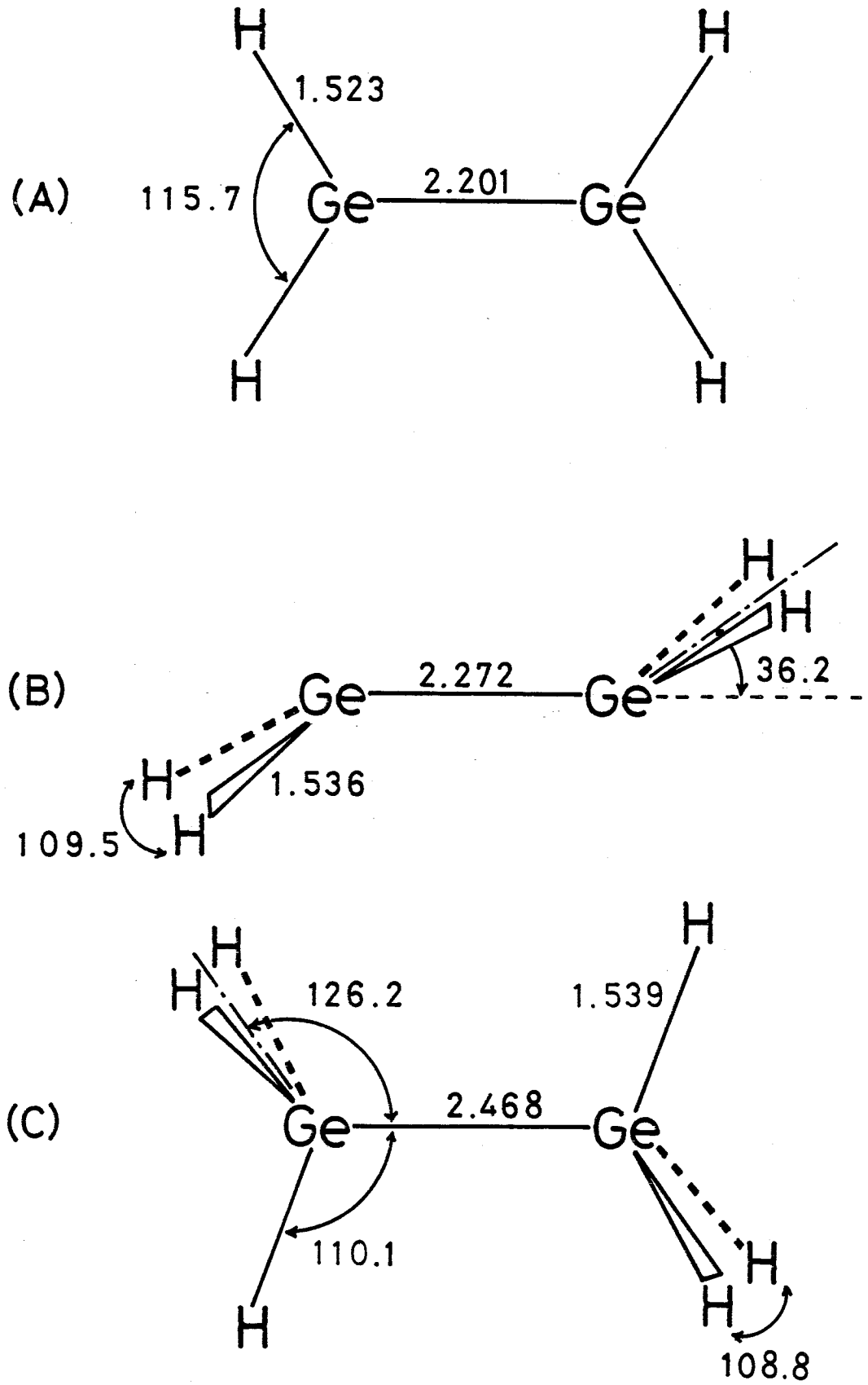

Figure 2. Geometries optimized with basis A augmented by 4d orbitals on Ge. From top to bottom, planar digermene(A), trans-bent digermene(B), and digermane(C), respectively.

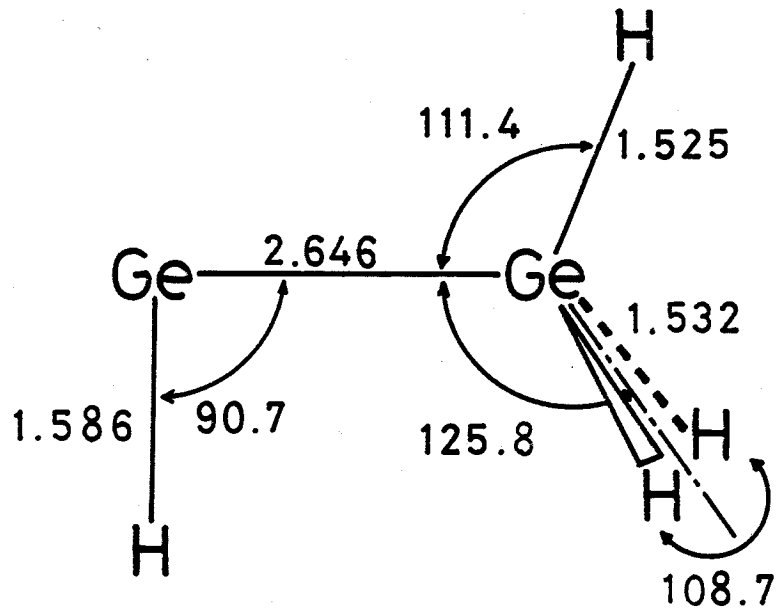

Figure 3. Optimized geometry of germylgermylene. Basis A.

Figure 4. Frontier orbital energies(eV) calculated with 6-31G**//4-31G for ethene, 6-31G**//3-21G for silicon compounds, and basis B//basis A for germanium compounds.

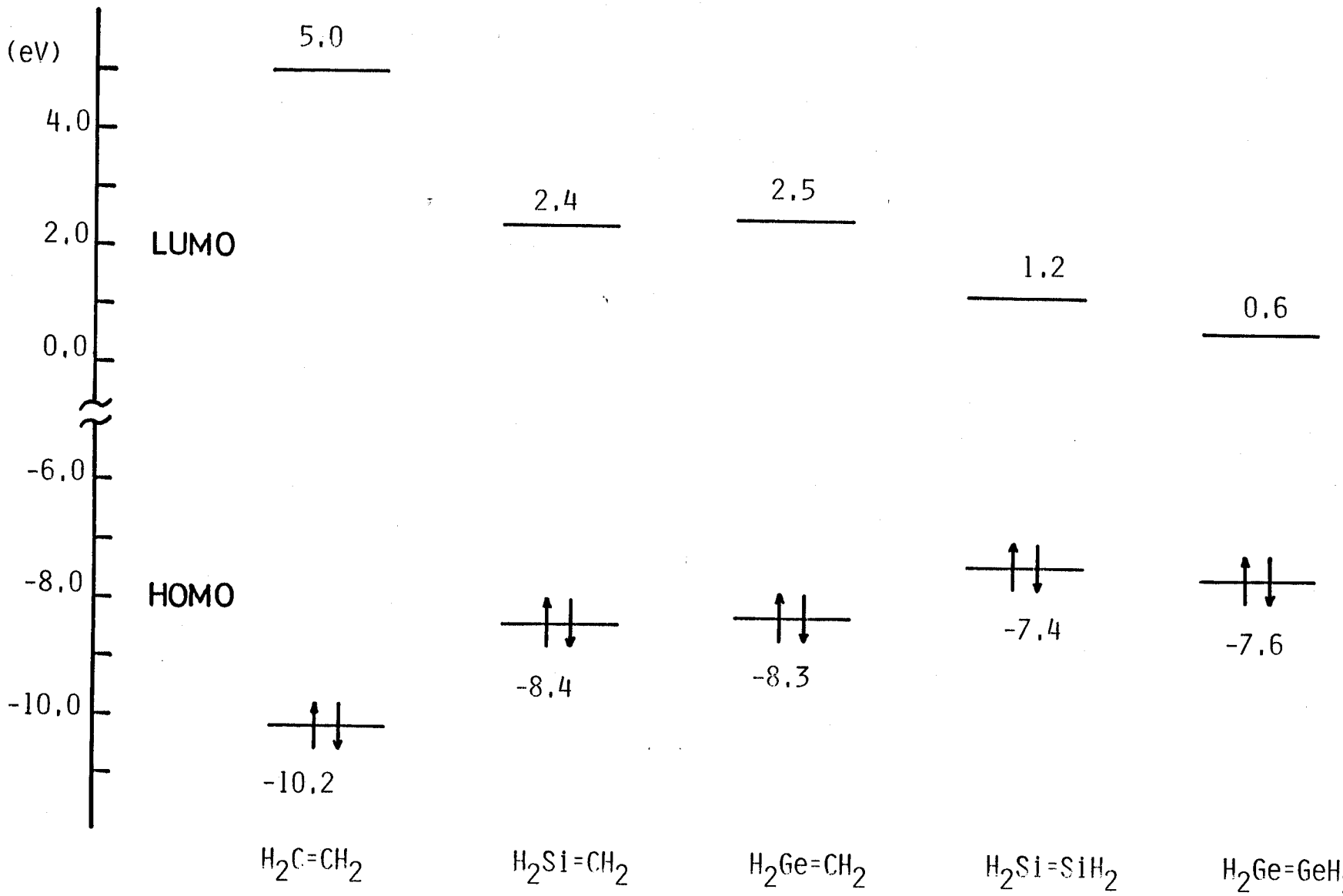

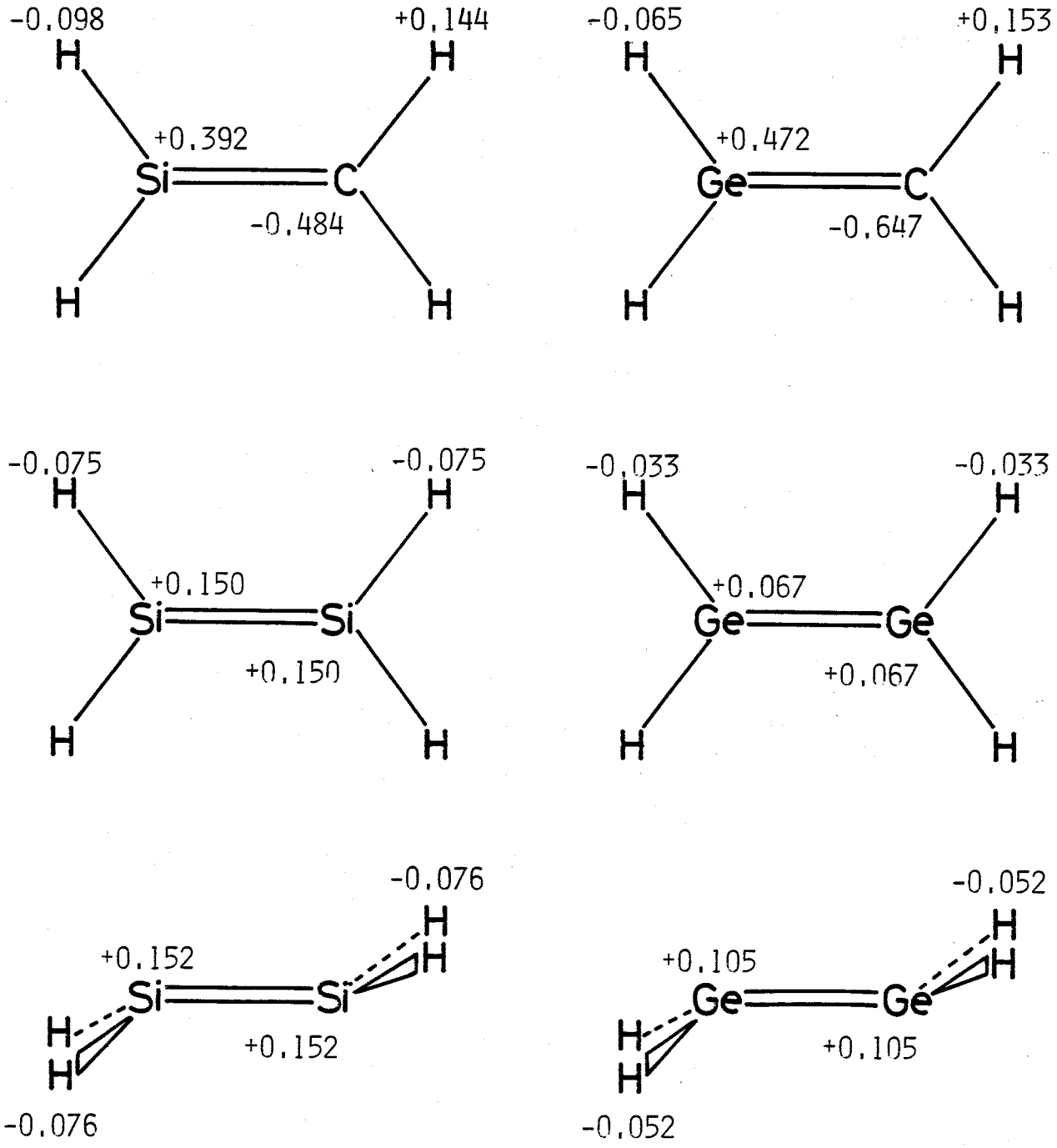

Figure 5. Net atomic charge densities calculated with 6-31G**//3-21G for silicon compounds and basis B//basis A for germanium compounds.

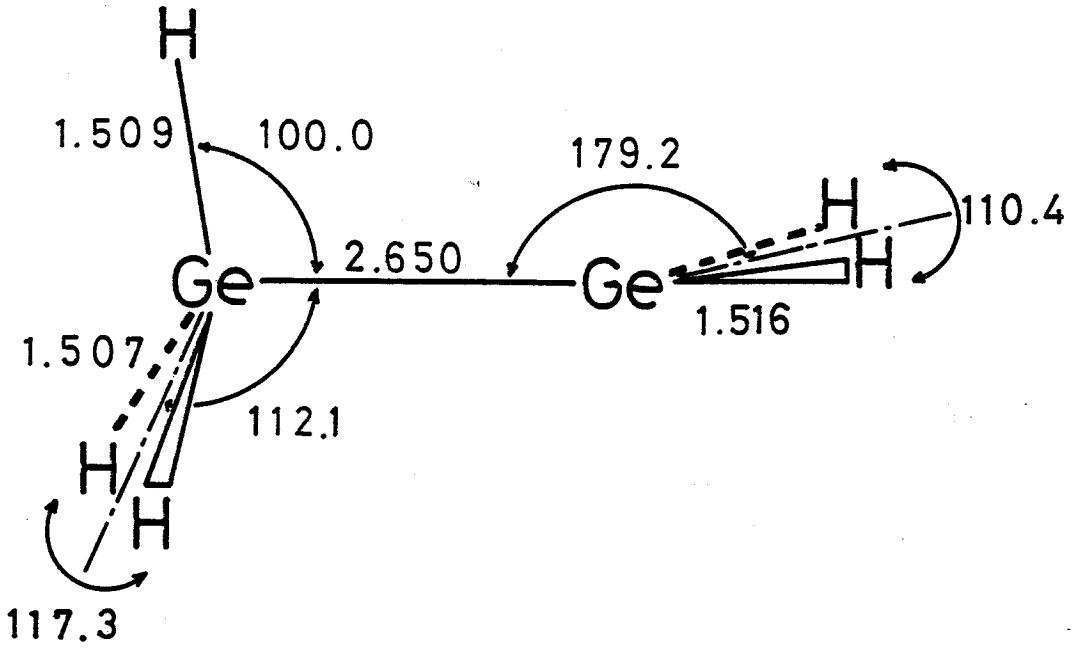

Figure 6. Optimized geometry of germylgermyl ion. Basis A.